2014

Landscape evolution and preservation of ice over one million years old quantified with cosmogenic nuclides 26Al, 10Be, and 21Ne, Ong Valley, Antarctica

Theodore C. Bibby
University of North Dakota

LANDSCAPE EVOLUTION AND PRESERVATION OF ICE OVER ONE MILLION YEARS OLD QUANTIFIED WITH COSMOGENIC NUCLIDES ^{26}AL, ^{10}BE, AND ^{21}NE, ONG VALLEY, ANTARCTICA

by

Theodore C. Bibby
Bachelor of Science, Florida State University, 2009

A Dissertation

Submitted to the Graduate Faculty

of the

University of North Dakota

in partial fulfillment of the requirements

for the degree of

Doctor of Philosophy

Grand Forks, North Dakota

December
2014

This dissertation, submitted by Theodore C. Bibby in partial fulfillment of the requirements for the Degree of Doctor of Philosophy from the University of North Dakota, has been read by the Faculty Advisory Committee under whom the work has been done and is hereby approved.

Jaakko Putkonen

_____
Ronald Matheney

_____
Gregory Vandeberg

_____
Alena Kubátová

_____
Dongmei Wang

This dissertation is being submitted by the appointed advisory committee as having met all of the requirements of the School of Graduate Studies at the University of North Dakota and is hereby approved.

_____
Dr. Wayne Swisher
Dean of the School of Graduate Studies

_____
Date

PERMISSION

Title Landscape Evolution and Preservation of Ice Over One Million Years Old Quantified with Cosmogenic Nuclides ^{26}Al, ^{10}Be, and ^{21}Ne, Ong Valley, Antarctica

Department Harold Hamm School of Geology and Geological Engineering

Degree Doctor of Philosophy

In presenting this dissertation in partial fulfillment of the requirements for a graduate degree from the University of North Dakota, I agree that the library of this University shall make it freely available for inspection. I further agree that permission for extensive copying for scholarly purposes may be granted by the professor who supervised my dissertation work or, in his absence, by the Chairperson of the department or the dean of the School of Graduate Studies. It is understood that any copying or publication or other use of this dissertation or part thereof for financial gain shall not be allowed without my written permission. It is also understood that due recognition shall be given to me and to the University of North Dakota in any scholarly use which may be made of any material in my dissertation.

Theodore C. Bibby
10/10/2014

TABLE OF CONTENTS

Page

LIST OF FIGURES

LIST OF TABLES

Table Page

ACKNOWLEDGEMENTS

I wish to express my sincere gratitude to my advisor, Dr. Jaakko Putkonen, who has provided guidance, inspiration, support, and a great example to follow throughout my academic career. I cannot thank Dr. Putkonen enough for his patience as I worked my way through this project, navigating setbacks and rough spots along the way. He has been a positive influence over the course of this work and I am extremely appreciative to have had the opportunity to work with him.

I would like to thank all the faculty members in the Harold Hamm School of Geology and Geological Engineering. Dr. Ronald Matheney deserves special recognition and I thank him for his constructive and sarcastic comments throughout the years and giving me adequate laboratory space for the cosmogenic lab. Considerable supplies were required to outfit the cosmogenic laboratory. My sincerest gratitude is extended to Dr. Hartman, Dr. Gosnold, Dr. Wang, Dr. Gerla, Dr. Korom, and Dr. LeFever for contributing to the materials and equipment (whether they knew it or not) required to build a working facility; from scales, to pipettes, fume hoods, beakers, sonic baths, and bulbs for the FAAS. Dr. Perkins reminded me that there is always life outside of Leonard Hall, and Dr. Forsman always kept me guessing about everything. Thank you to the members of my dissertation faculty committee. Dr. Vandeberg, and Dr. Kubátová for their feedback, support, and instruction over the years, and to Dr. Hou for managing to keep the FAAS running. I would also like to extend my deepest gratitude to former

director of E.A.R.L, Dr. Hanying Xu who taught me the value of quality analytical chemistry procedures, maintaining humor and a gentle nature amidst his battle with cancer.

The staff that works in the spot light but also behind the scenes at HHSGGE deserves special recognition. Darin Buri has been a close friend, was one of my first contacts in the department, and is always a resource for conversation, coffee, creativity and humor. Katie Sagstuen has made my life at GGE very pleasant and I am forever thankful for all her time, effort, and help. Thank you to Dr. Burton-Kelly, Mr. Christenson, and Mr. Buer for their friendship. I am extremely lucky to have met them during my study.

Lastly, I would like to thank Dr. Daniel Morgan, and Dr. Greg Balco for extensive comment, critique, and guidance. I am very thankful for the many hours of phone conversations and code revisions over the years, and grateful to have had the opportunity to work with them both in the field and in the laboratory.

For my mother, father, and family,
to whom I owe everything.

ABSTRACT

Antarctica has been glaciated for the past 35-40 million years (Denton et al., 1991) and evidence of periodic fluctuations of the Antarctic ice sheet (AIS) during the Cenozoic are recorded in the ice sheet itself, deep sea sediments, and glacial deposits on the continent (Ingólfsson, 2004). Quaternary continental records of AIS extent is limited to few locations along the Transantarctic Mountains (TAM) and coastal continental boundaries (Denton et al., 1984; Denton et al., 1989). Records of atmospheric variation over time, glacial extents, and ice sheet responses to environmental changes are required to understand modern day forces on climate and the environment and provide a context in which to relate modern observations to the past. In this framework, this paper evaluates the geomorphic stability of Ong Valley within the Central Transantarctic Mountains (CTM) and the preservation of Pleistocene aged ice underneath an insulating lag deposit.

Ong Valley in the Central Transantarctic Mountains (CTM) contains ancient buried glacier ice derived from past flow of the adjacent Argosy Glacier. The valley floor is covered with patterned ground and has three distinct glacial tills. Geomorphic and stratigraphic evidence shows that these deposits originate from sublimation of debris-laden glacier ice. Buried glacier ice is still present beneath the youngest two drifts, one of which is older than one million years. The tills above the ice record the repeated advances and stagnations of the Argosy Glacier. Cosmogenic exposure age dating of these tills provides ages, ice sublimation rates and regolith erosion rates that support the antiquity of the ice below.

The oldest ice on Earth has an undisputed age of 800 Kya and is at the bottom of large ice sheets (Fischer et al., 2013). Access to it requires extensive drilling through kilometers of ice. Conversely, the ice in Ong valley is preserved beneath only 1 m of till and is over 1 million years old. Geomorphically similar ice was found in Beacon Valley, but its age (~8.1 Mya) was inferred from dating of volcanic ash above the ice (Sugden et al., 1995). Subsequent analysis from other investigators suggest that the age of the ash may not be a good indicator for the age of the ice below it (Hindmarsh et al., 1998; Ng et al., 2005; Stone et al., 2000).

Concentrations of cosmogenic ^{10}Be, ^{26}Al, and ^{21}Ne were measured in regolith samples collected every ~10 cm in 1 m deep vertical transects through three tills in Ong Valley. Transects reach the buried ice surface in the two younger tills. Cosmogenic-nuclide concentrations in these transects are functions of: i) the age of the till and ice below it; ii) the rate of formation of the till by sublimation of underlying ice; and iii) the rate of surface erosion of the till. In general, a young till unit will have ^{26}Al and ^{10}Be concentrations that are primarily a function of till age; however, over time, ^{26}Al and ^{10}Be concentrations reach equilibrium with erosion, sublimation rates, and radioactive decay; thus, ^{26}Al and ^{10}Be concentrations in older tills primarily provide information about those rates. Conversely, stable nuclide ^{21}Ne only accumulates over time which makes it useful in determining the age of older tills where as ^{26}Al and ^{10}Be provide minimum limiting ages.

^{26}Al, ^{10}Be, and ^{21}Ne measurements in Ong Valley are consistent with a scenario in which tills are derived from progressive sublimation of glacial ice containing 10% by volume englacial debris. ^{26}Al and ^{10}Be concentrations in the youngest till constrain its emplacement age at 18.4 Kya. ^{21}Ne nuclide concentrations in the two oldest tills are best explained by ice sublimation rates on the order of tens of m/Mya and surface erosion rates of the till on the order of m/Mya for

at least 0.9 Mya to 1.5 Mya. Concentrations of nuclides in the bottom of the second drift suggest that local sublimation rates have increased slightly in the past 40-150 Kya. These observations imply that the ice below the middle drift is the oldest undisturbed glacier ice currently known on Earth and should provide ancient atmospheric records within one meter of Earth's surface.

CHAPTER I

INTRODUCTION

Annual accumulation of glacier ice creates a natural archive of gases, particles, and other substances. As such, ice cores from glaciers and ice sheets are a mainstay of paleoclimate research and significant effort in the last several decades has been devoted towards obtaining the longest possible ice core records of past climate. As ice becomes plastic under sufficient weight, all ice bodies thicker than ~10 m flow from areas of net accumulation to areas where melting or calving occurs (Hooke, 2005). Glaciers are dynamic systems that reflect a balance between snow accumulation, ice flow, and basal melting. Generally, the older glacier ice is, the less likely it is to be preserved (because it is continuously removed by ice flow and basal melting) and the more difficult it is to access (because it is located at the base of thick continental ice sheets).

Together these processes dictate that the oldest ice is at the bottom and that flow and basal melting continuously eliminate the oldest ice. For these reasons, the oldest glacial ice is difficult to access and is generally found at the bottom of the largest continental ice sheets. Conversely, ice at the Earth's surface is easier to access, but much less likely to survive for long periods of time as it melts and/or sublimates under normal ambient conditions. Presently, the oldest, definitively dated recovered ice was found at the bottom of the Dome C ice core on the East Antarctic ice sheet. The basal ice is dated to 800 Kya before present, yet Greenland and Antarctica have both been glaciated much longer than this (Luthi et al., 2008; Jansen et al., 1988;

Zachos et al., 1996; Zachos and Kump, 2005; Lear et al., 2000; Fischer et al., 2013). In this context it is highly unexpected to locate ancient ice close to the surface.

Background

A possible exception to the principle that older glacier ice is at the bottom of large ice sheets and is inherently more difficult to access is provided by relatively thin bodies of glacier ice covered by sedimentary deposits in polar regions. These resemble rock glaciers in that they are covered by sublimation till, a sedimentary deposit derived from englacial rock debris that covers the ice surface as the ice sublimates. In a polar climate, once the debris layer builds up to an insulating thickness, sublimation rates may be slow enough to permit the survival of ice for millions of years (Marchant et al., 2002; Kowalewski et al., 2011).

Commonly the presence of massive ice or ice cemented soils will form patterned ground polygons and the observance of these in the field usually indicate buried ice or ice cemented soil. These polygons form from thermal expansion and contraction of the underlying ice. As cracks form within the ice, sediment from the surface becomes entrained in the crack and the outline of the polygon becomes more apparent (Marchant et al., 2002). The width of the crack is then increased through positive feedback with the sediment and thermal expansion contraction. This general geomorphic formed is more specifically termed a sand wedge polygon. Previous work in the McMurdo Dry Valleys has documented the formation of patterned ground polygons in Antarctica (Berg and Black, 1966) and further studies have modeled the vapor diffusivity through the substrate to confirm the ability of a thin till layer to reduce rates of ice sublimation due to insulation from the overlying regolith (McKay et al., 1998; Hagedorn et al., 2007). The morphological maturity of polygons relates to the age of their formation and has been used for comparative study application to Mars (Sletten, 2003). Much interest in these processes and their

rates relates to the observance of similar features on Martian landscapes and the implications for our understanding of paleo-climate on timescales beyond the Anthropocene.

Ice over one million years old has never been dated anywhere in the interior of Antarctica, but similar shallowly buried massive ice overlain by sediment containing volcanic ash has been dated near the coast in the McMurdo Dry Valleys (MDV). Preservation of buried ice bodies in polar latitudes has been a subject of relatively recent study and preserved ice body ages in the MDV range from 130 Kya to 8.1 Mya (Sugden et al., 1995; Swanger et al., 2010; Konrad, 2005; Cardyn et al., 2007; Lacelle et al., 2011; Lacelle et al., 2007). Volcanic ash overlying the ice in Beacon Valley was dated at 8.1 Mya, leading the authors to propose the ice was at least this old. However, subsequent cosmogenic isotope analyses at the same location challenge the antiquity and show that the ash may not be a reliable stratigraphic indicator (Ng et al., 2005; Van der Wateren and Hindmarsh, 1995). The ice in question was most likely not static, but reflected a balance between input by flow of adjacent, confluent rock glaciers and loss by sublimation through till mantle (Ng et al., 2005; Stone et al., 2000; Hindmarsh et al., 1998). Thus, the underlying till and ice may be significantly younger than the ash.

In this study, a slightly different geological situation is described in the central Transantarctic Mountains where glacier ice is overlain by sublimation till (Figure 1). However, the geomorphic situation is simpler than described above for Beacon Valley in that there is no means by which the ice could be replenished after its emplacement, so the ice and the overlying sublimation till have the same age. Measurements of cosmogenic ^{26}Al, ^{10}Be, and ^{21}Ne in sublimation till and englacial debris are used to provide minimum ages for emplacement of drift and glacier ice as well as to gain information about ice sublimation and till erosion rates in Ong Valley.

Minimum ages are assigned to three glacial drifts, herein referred to as Youngest, Middle, and Oldest (Figure 1. and Figure 2.), of which, the two youngest are underlain by massive ice. Reported ages are based on analyzed cosmogenic isotopes that were collected in a vertical profile through ~1 m thick layer of till atop massive ice. In addition to minimum ages, till erosion rates and ice sublimation rates are also reported. Collectively, these rates and ages reveal the history and evolution of the massive ice, the surface till layer, and the landscape.

There is significant interest in the stability of the East Antarctic ice sheet, its evolution since the middle Miocene, and the preservation of paleoclimate proxies in ancient ice (Sugden et al., 1995; Schaefer et al., 2000; Stone et al., 2000; Rignot et al., 2002). The International Partnerships in Ice Core Sciences (IPICS) has listed the recovery of continuous ancient ice records to 1.5 Mya as a top scientific objective, and potential locations for ancient ice in Antarctica were recently modeled (International Partnerships in Ice Core Sciences; Fischer et al., 2013). Understanding the longevity of buried ice in the CTM may also help us interpret morphologically similar features found on Mars (Holt et al., 2008; Plaut et al., 2009). The stability and preservation of buried ice has been studied in the McMurdo Dry Valleys located near the coast (Putkonen et al., 2008a; Morgan et al., 2010a), but no similar work extends into the CTM which should record events in the interior of the continent.

The objective of this research is to assign absolute minimum ages to the three drifts on the floor of Ong Valley in the CTM and to quantify ice sublimation/regolith degradation rates for each till. Ages and rates are constrained with depth profiles of cosmogenic nuclides ^{26}Al, ^{10}Be and ^{21}Ne which serve as proxies for the age of the underlying ice. This research also demonstrates the reproducibility of ^{21}Ne concentrations in regolith of separate yet adjacent pits; supporting this method's efficacy for reliable age interpretation.

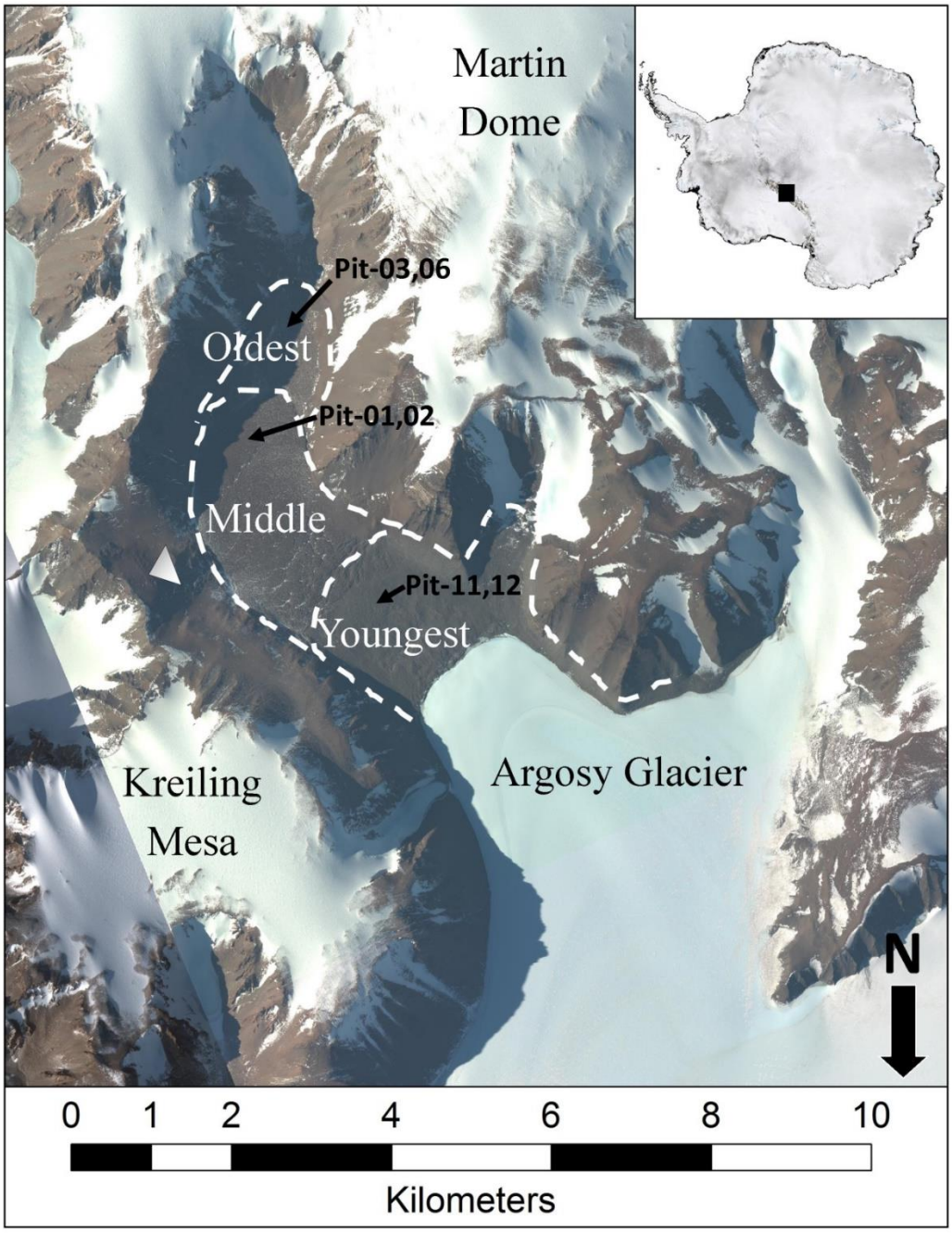

Figure 1. Ong Valley satellite image. Dashed lines designate boundaries between till units. Tills are labeled youngest to oldest, sample site locations are marked with arrow, and the triangle marks the position of panorama photograph in Fig. 2. Inset map marks relative location of valley within the Transantarctic Mountains.

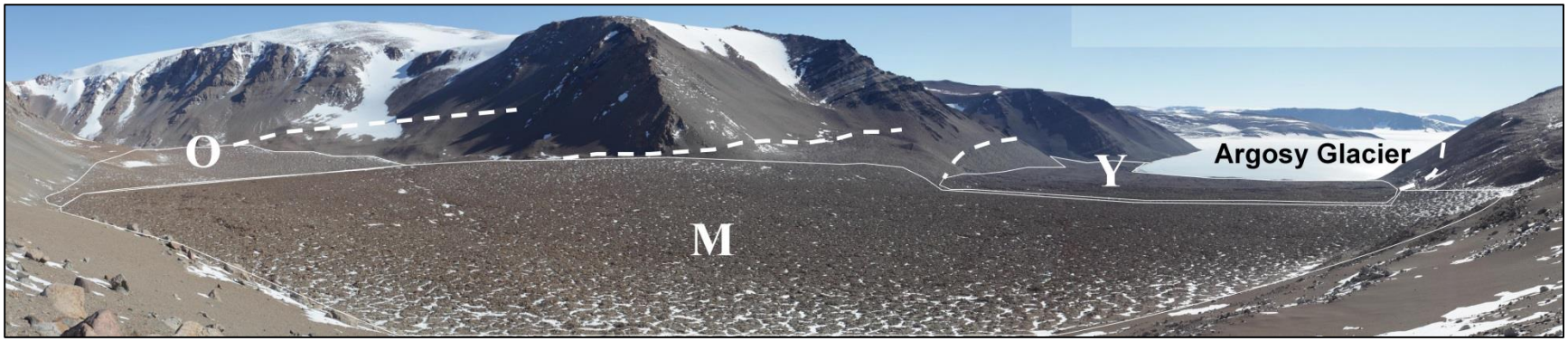

Figure 2. Panorama of Ong Valley taken from triangle in Fig. 1, Y=Youngest, M=Middle and O=Oldest drifts outlined, lateral moraines marked by dashed lines.

CHAPTER II

FIELD AREA

Location

Ong Valley (-83°14'S, 157°37'E) is a 2.5 km wide, 7.5 km long valley in the Miller Range of the Transantarctic Mountains, Antarctica (Figure 1). The head of Ong Valley has a small unnamed alpine glacier and the valley entrance is blocked by a ~2 km wide lobe of the Argosy Glacier. The mean annual air temperature recorded with data loggers for 2011 in Ong Valley was -23.9^{0}C, coldest air temperature was -49.0^{0}C and warmest was -4.0^{0}C. The valley floor gradually rises in elevation from 1500 m asl at the mouth to 1700 m asl at the head of the valley. The majority of the valley floor is covered by three lobate sedimentary deposits that are distal to the present margin of Argosy Glacier. As the greater Argosy Glacier grew thicker in the past, it advanced up valley and up elevation into Ong Valley. The advance of the Argosy into Ong Valley is interpreted as the main source of regolith into the valley, as there is no evidence that the small alpine glacier at the valley head has ever extended past the outermost boundary of Ong I and there are no other glaciers presently acting on the valley morphology based on field observations. The three tills in the valley floor were first described in 1975 with air photo analysis, and likely correspond to High, Middle, and Low moraines farther south in the Transantarctic Mountains (Grindley, 1967; Mayewski, 1975). Soil chronosequences of the tills were recently described by Scarrow et al., (2014).

Recent till provenance work suggest that the till is sourced from outside of Ong Valley and not from surrounding bedrock (Edwards et al., 2014). The valley floor contains clasts and boulders not found in surrounding local outcrops. Conversely, the valley floor and walls outside the margin of the drift sheets are covered with talus and colluvium derived from bedrock outcrops high on the valley walls. Small alpine glaciers at the head of Ong Valley and in tributary valleys display moraine sequences distal to their present termini, but in all cases these moraines are well above the margins of valley-floor drift sheets. Thus, nearby alpine glaciers were not confluent with the Argosy Glacier during past advances that deposited drift sheets. The concentric relationship of the three drifts, morphostratigraphic relationship of the moraines that form the drift boundaries, and absence of cross-cutting relationships indicate that the age of the drifts increases with distance from the present glacier margin. The surface morphology of the drifts is consistent with this age relationship.

Geology

The surfaces of the three drifts have patterned ground formation (sand wedge polygons formed from thermal expansion and contraction of ice or ice-cemented regolith) (Figure 2). The youngest drift is closest to the Argosy Glacier, has no desert varnish or desert pavement, and its regolith is dominated by fine silts/clays with interspersed cobbles and boulders. In many locations the buried ice is exposed or found within ~10 cm of the surface. The middle drift is located in the middle of Ong Valley. Desert varnish is present on surface regolith, and desert pavement exists within 1-2 cm of the surface. Its regolith is dominated by pebbles, cobbles, and boulders. The down valley profile of the middle drift is convex up as it transitions from the youngest drift to the oldest. The oldest drift is located furthest from the valley mouth, has desert varnish and development of desert pavement on patterned ground polygons. The valley

longitudinal profile is concave. The general relief from center to trough of the polygons is fairly shallow and low sloping from surface stabilization after the complete loss of massive ice, possibly due to sublimation followed by slow and persistent regolith degradation. The increasing maturity of patterned ground polygons between young to old drifts coincide with the relative age of these tills (Sletten, 2003).

The youngest and middle drifts overlie buried glacier ice at depths of 0.46-0.48 m (Youngest) and 0.68-0.80 m (middle). This can be recognized as glacier ice due to low englacial debris concentrations, bubbles within the ice, and absence of ice-cemented soils in all pits (Swanger and Marchant, 2007). No ice was found beneath the oldest drift in hand-dug pits down to 0.67-0.78 m depth. This is consistent with the topographic expression of the drift sheets; the oldest drift has little topographic expression and forms a thin layer coating the valley floor, whereas the younger drifts have significant topographic expression consistent with a buried ice body. The surfaces of all drifts lie at lower elevation than the moraines that bound each drift sheet on the valley walls. The debris content of the ice is approximately 3-10%, consisting mostly of sand-size particles with some pebbles and cobbles interspersed and similar lithology to the overlying till. Thus, stratigraphic and geomorphic information indicates that all three drifts are ablation tills composed of originally englacial debris. The englacial debris has been concentrated during steady sublimation of Argosy Glacier ice which filled the valley up to the present drift boundaries. Ice from Argosy Glacier advanced into the valley, stagnated, and gradually downwasted by sublimation, leaving the present drift units overlying, in the case of the middle and youngest drifts, the remnants of the original ice lobe. Cosmogenic nuclide concentrations in all drifts are consistent with this interpretation as shown later.

The outcrops surrounding Ong Valley, from the Macdonald Bluffs to Martin Dome (2,680 m) are composed of Granite Harbor intrusives (Figure 3). These are Cambrian to Ordovician aged Hope granite and Skelton granodiorites (Grindley, 1967). The outcrops composing Martin Dome are Precambrian Nimrod group (Grindley, 1967; Barrett et al., 1970; McDougall and Grindley, 1965). Across the Argosy Glacier is Aurora Heights which has been dated with K-Ar from muscovite (486 Mya), biotite (489 Mya), and hornblende (1011-1043 Mya) (McDougall and Grindley, 1965; Grindley and Laird, 1969).

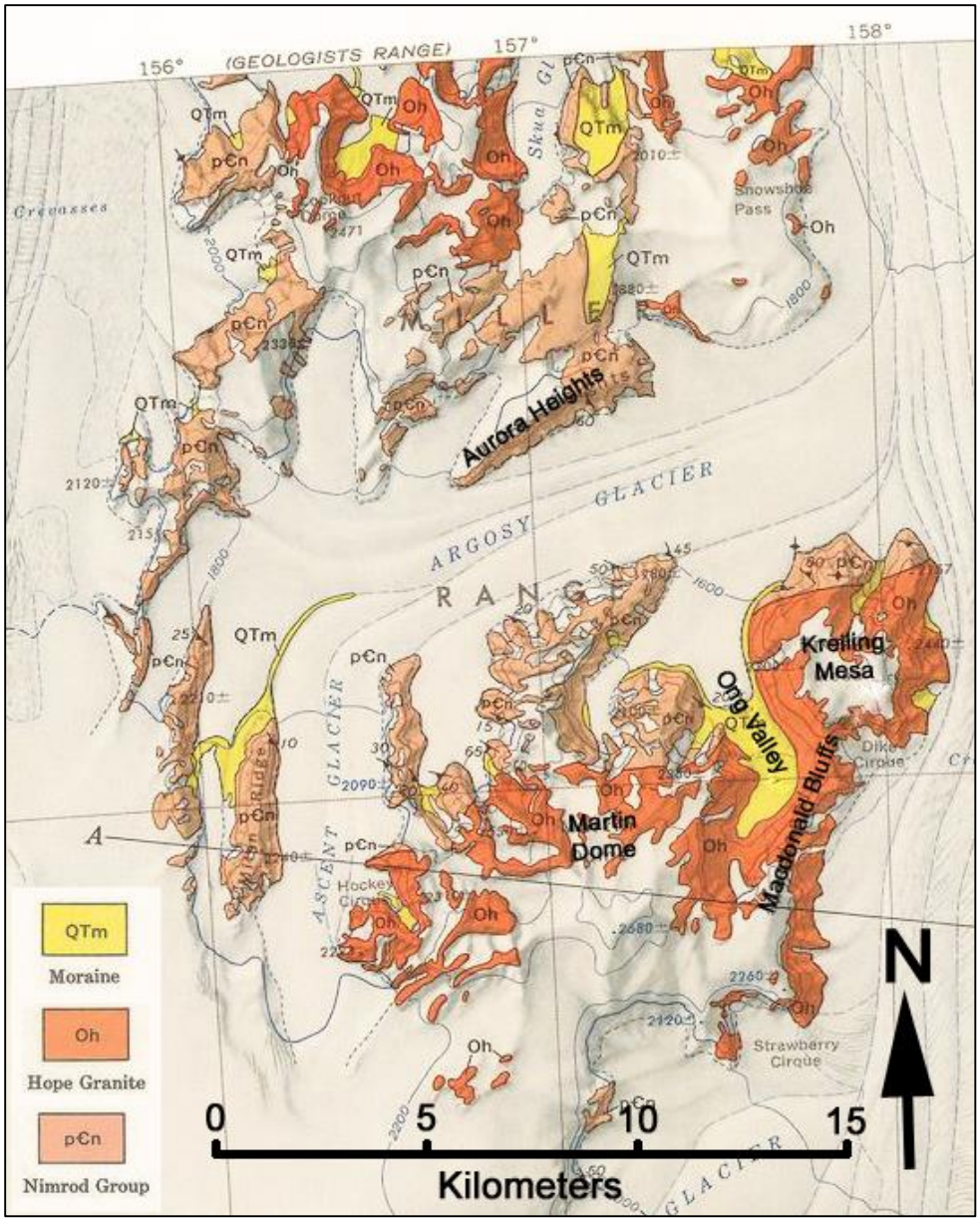

Figure 3. Geologic map of Ong Valley with surrounding outcrops. Reproduced from Reconnaissance Geologic Map of the Mount Rabot Quadrangle, Transantarctic Mountains, Antarctica, by Barret, J., Lindsay, F., and Gunner, J., 1970

CHAPTER III

METHODS

Cosmogenic Nuclides Background

Cosmogenic nuclides are created when galactic cosmic rays (GCR) interact with elements in the atmosphere and Earth. Interactions between GCR and Earth's surface are dominated by spallation in the top meter of regolith (Niedermann, 2002; Gosse and Phillips, 2001). This work focuses on nuclides produced within minerals in-situ which are at (or near) Earth's surface. Silicon and oxygen atoms are dominant target elements to form ^{26}Al and ^{10}Be from incoming GCR, while ^{21}Ne targets include magnesium, aluminum, and silicon. Quartz has common target elements for ^{26}Al, ^{10}Be, and ^{21}Ne and is useful for multiple nuclide concentration analysis (Balco and Shuster, 2009b).

The general assumptions for use with cosmogenic nuclides are: i) given no prior exposure, a rock has no cosmogenically produced nuclides in its crystal structure; ii) the production rate of nuclides is greatest at Earth's surface and decreases with depth into regolith (Figure 4); iii) increasing the exposure time to cosmic rays increases the resulting concentration of nuclides found in-situ (Figure 5); and iv) the cosmic ray flux is considered constant for the past 10 Mya (Leya et al., 2000; Dunai, 2000; Gosse and Phillips, 2001). Some nuclides produced through cosmic rays are radioactive and thus will decay spontaneously. If a surface has been exposed long enough for the production rate of the cosmogenic nuclide to match its decay rate, the system has reached secular equilibrium (Figure 5). The concentration of nuclides in a sample

is then 1) a function of the local ice sublimation rate which controls the rate of regolith aggradation to bottom of the existing till or to the surface of the existing relict ice, and/or 2) a function of the surface erosion rate of the overlying regolith (Lal, 1991; Morgan et al., 2010a).

The concentrations of cosmogenic nuclides found in the drifts of Ong Valley are expected to result from a series of events described: i) regolith was transported via Argosy Glacier into the farthest extent of the valley as englacial debris (regolith mixed with glacial ice); ii) the ice body in Ong Valley stagnated for a length of time, during which ice sublimation produced a lag deposit from the exhumed regolith; iii) the ice continued to sublimate from below the lag deposit, adding regolith to the underside and bringing regolith from ice closer to the surface; iv) the lag deposit was eroded at some rate slower than the rate of regolith aggradation; v) the thickness of the resulting lag deposit is a function of time, ice sublimation, and regolith erosion; and vi) the ice below the lag deposit is the source of the till and therefore the ages of the surficial debris layer and the ice are related (Figure 6). This series of events is the simplest explanation for the till observed today and is consistent with cosmogenic isotope analyses.

Morgan et al., (2010a) and Ng et al., (2005) considered the accumulation of cosmic-ray-produced nuclides in sublimation tills. Morgan et al., (2010a) aimed to estimate ice sublimation rates, surface erosion rates, and ages associated with sublimation tills by fitting a forward model with these parameters to depth profiles of ^{26}Al and ^{10}Be concentrations in bulk samples of till matrix. Ng et al., (2005) on the other hand, made simplifying assumptions to derive quantitative limits rather than best-fitting values for these parameters from nuclide concentrations in individual clasts. In the following sections this paper will mainly follow the approach of Morgan et al. (2010a) with brief discussion of the Ng et al. (2005) approach. In addition, this paper will

highly simplify these models to derive minimum possible ages for drifts that rely on the minimum possible number of assumptions about the geologic history of the samples.

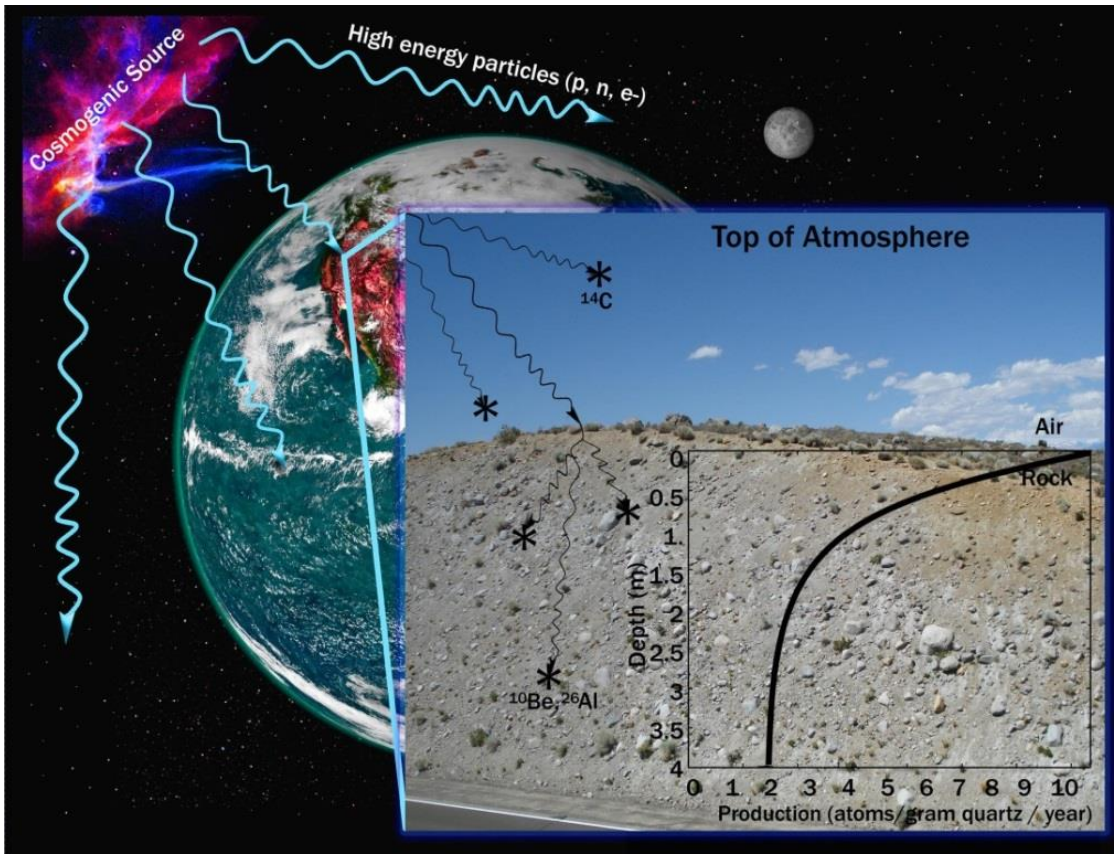

Figure 4. Conceptual schematic representation of the bombardment of Earth by cosmic rays, followed by the formation of cosmogenic isotopes in the atmosphere and top meters of Earth's surface. Inset graph shows model production rate of cosmogenic nuclides decreasing with depth, primarily as a function of decreasing energy for spallation reactions due to density. X axis units, Y axis units, and production curve are for descriptive purposes only.

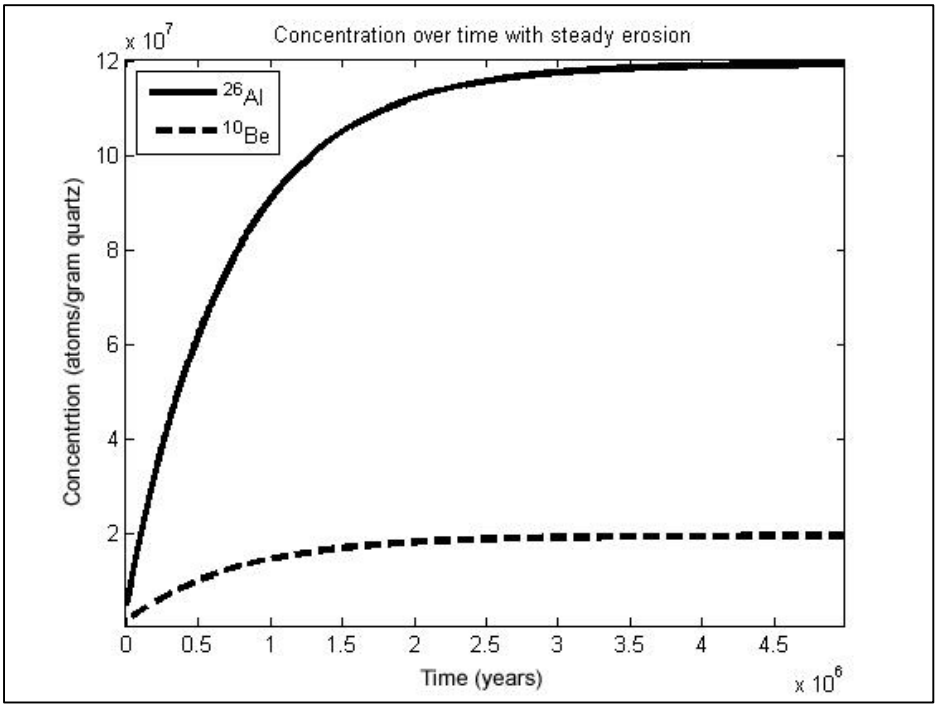

Figure 5. Accumulation of cosmogenic nuclides over time with steady state erosion. Calculated with hypothetical production rate and erosion rate typical of Antarctic surfaces. In this example secular equilibrium is reached between 1.5 and 2.5 Mya for ^{10}Be.

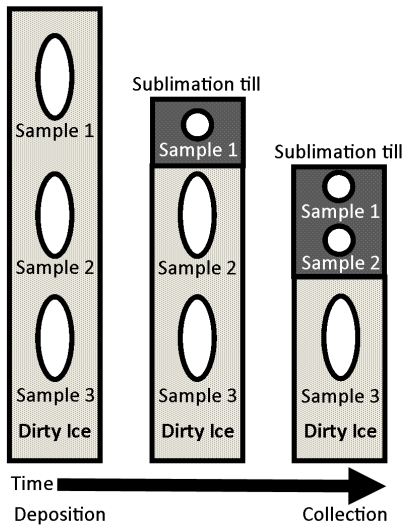

Figure 6. Cartoon depicting the formation and accumulation of sublimation till from englacial debris followed by sampling.

Field Methods

Sample sites were chosen in the middle of each drift (Figure 7), limiting the possibility that rock falls from valley walls would contribute to the measured nuclide concentrations. Sample sites were further constrained to the center of large patterned ground polygons with relatively flat tops lacking large rocks or boulders. Pits were hand dug with a shovel next to the actual sampling site and bulk regolith samples were collected with a hand trowel from the surface of the sampling site to maximum depth at approximately 10 cm increments (Figure 8).

Measurements for topographic shielding were taken using compass and clinometer and the topographic shielding factor was calculated using CRONUS-Earth Project online calculator. Topographic shielding is the physical blocking of cosmic rays to a particular location. Sites that have a completely flat horizon line (such as the ocean or the plains of the Midwest US) have zero topographic shielding and thus do not decrease nuclide production rates. Conversely, locations with nearby hills, mountains, or large boulders obstructing the skyline reduce bombardment of incoming cosmic rays and thus reduce the production rate of cosmogenic nuclides, and must be accounted for (Dunne et al., 1999) (Figure 7). Site position was obtained with a hand-held GPS and local barometric pressures were measured with a hand-held digital barometer. Site specific atmospheric pressures were normalized to a base camp logging barometer and adjusted to reflect true localized pressure (which is a function of elevation and thus affects nuclide production rates).

Samples in the middle and youngest drift consist of sand-sized till matrix. The sampling spans the thickness of the till at approx. 10-cm depth intervals. Some of the transects additionally

include sand-sized debris extracted from the buried ice. Samples from Ong I are similar except that no buried ice is present. In order to establish whether nuclide concentrations in pits were representative of each drift as a whole, samples were collected from two adjacent but separate pits dug in similar geomorphic positions in each drift.

Two depth profiles were sampled from each drift in Ong Valley (a total of 6 sample sites and 34 bulk samples) during the 2010-11 Antarctic field season. Sample sites were chosen in the middle of each drift to decrease the effect of topographic shielding of cosmic rays on the samples and limit the possibility of rock falls from valley walls to contribute to the measured nuclide concentrations. Sample sites were further constrained to the center of large patterned ground polygons with relatively flat tops lacking large rocks or boulders. Pits were dug with shovels and bulk regolith was collected at ~10 cm intervals down to ~1 m below the surface or until massive ice was reached (for exact depth in each pit, see Table 1. If ice was present, ice samples containing regolith were collected from the base of the pit using a hammer and chisel. No ice-cemented soil was found in any of the pits. Site elevations were determined by barometric pressure differences between sample sites and static GPS base stations in the valley. For cosmogenic isotope analysis, the effective topographic shielding from surrounding topography was determined with compass and clinometer for each sample site.

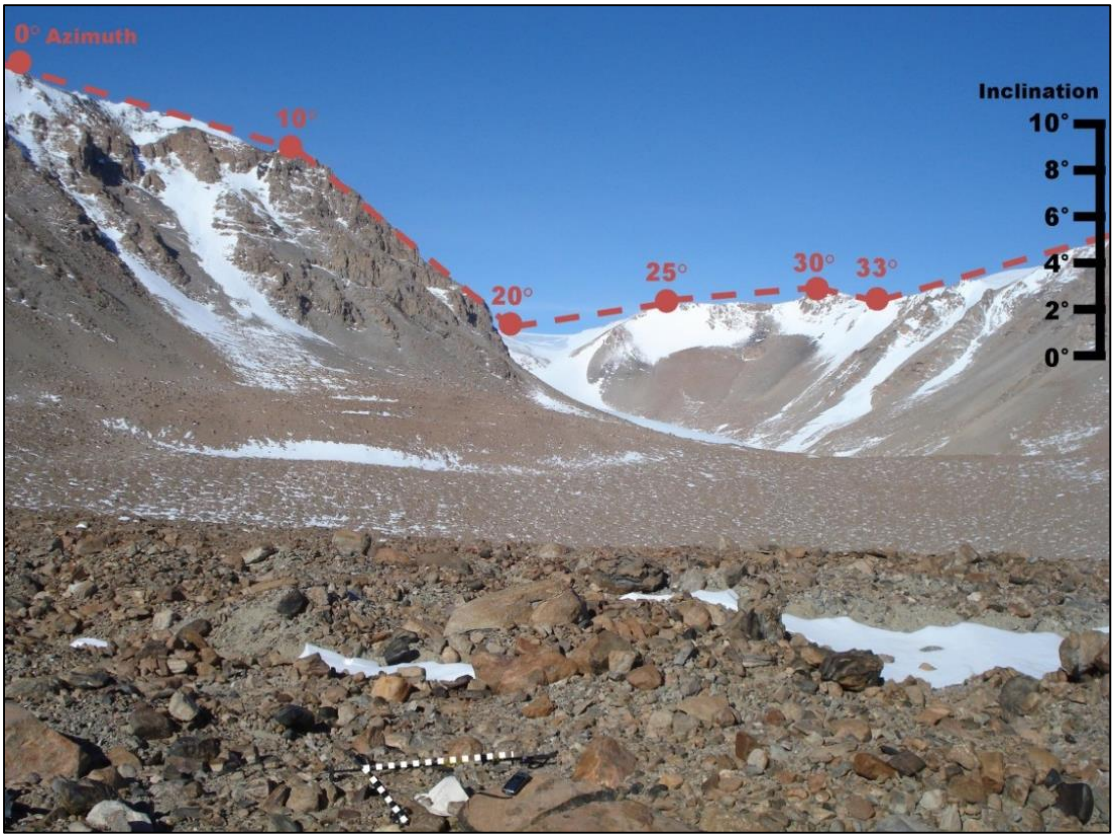

Figure 7. Sample site and topographic shielding. White dashed lines designate sample site 10-OV-Pit-01 (middle drift), red dashed lines are an example of typical measurements from compass combined with angles of inclination (black text) from clinometer used to calculate topographic shielding factor. Compass azimuths and degrees of inclination shown are for illustrative purposes only.

Figure 8. Typical field sampling procedure of bulk regolith. A pit is dug with shovel and intervals are sampled with hand trowel to depth.

Lab Methods

The preparation of bulk regolith samples for analysis by accelerator mass spectrometer (AMS) can be divided into two broad procedural steps. 1) General reduction and cleaning of regolith material to sand sized quartz, and 2) wet chemistry techniques to digest the quartz, separate aluminum and beryllium, and pack samples into cathodes for measurement with AMS. Detailed procedures used at the University of North Dakota are provided in the appendix.

Bulk densities of pit samples are required to determine the production rate of isotopes at depth and were determined by packing collected regolith into a 250 to 500 cm^3 container,

measuring the mass of the filled container, and calculating the resulting density. Ice containing regolith was weighed before and after drying, and bulk density/debris concentrations of dirty ice was calculated from remaining contents. Regolith samples were prepared and analyzed for ^{26}Al, ^{10}Be, and ^{21}Ne measurement using standard methods (Stone, 2000; Balco and Shuster, 2009a; Balco and Shuster, 2009b). Samples were sieved and separated into grain size fractions 250 to 500 μm. Quartz grains were isolated from remaining bulk sediment by cleaning in 10% hydrochloric acid, washing in water, magnetic separation, density separation using heavy liquid lithium heteropolytungstate (LST), and repeated etching in 2% hydrofluoric acid (HF). Purity of isolated quartz was tested by inductively coupled plasma atomic emission spectroscopy (ICP-AES) and/or flame atomic absorption spectroscopy (FAAS). Aluminum and beryllium were extracted from clean quartz at the University of North Dakota's cosmogenic isotope laboratory and the PRIME laboratory at Purdue University in West Lafayette, IN. Beryllium carrier spikes were used for all samples and aluminum carrier was selectively added to samples with low aluminum concentrations.

$^{10}Be/^{9}Be$ and $^{27}Al/^{26}Al$ isotope ratios were measured via (AMS) at Purdue's PRIME laboratory. Additionally, two aliquots of clean quartz from each sample depth were measured for ^{21}Ne via noble gas mass spectrometer at the Berkeley Geochronology Center (BGC). Reported concentrations are corrected for background laboratory blanks (Table 1).

Nuclide Concentration Analysis

The three drifts vary widely in age, thus two separate strategies are used to resolve absolute ages. ^{26}Al and ^{10}Be are suitable for constraining relatively young ages while ^{21}Ne is useful for constraining older ages as it does not undergo radioactive decay. The difference in

^{21}Ne concentrations between samples at depth is also used to constrain sublimation rates and exposure ages for ^{26}Al and ^{10}Be analysis (Ng et al., 2005).

Al and Be isotope ratios measured at PRIME were referenced to NIST 2000, and ^{21}Ne measurements at BGC were referenced to atmospheric standards and compared to known concentrations of ^{21}Ne found in CRONUS-A, a reference material produced from Antarctic sandstone (Vermeesch et al., 2012). This paper use a ^{10}Be half-life of 1.36 Mya with corresponding decay constant, $\lambda = 5.1 \times 10^{-7}$ yr^{-1} and ^{26}Al half-life of 0.708 Mya with $\lambda = 9.78 \times 10^{-7}$ yr^{-1} (Nishiizumi, 2004; Nishiizumi et al., 2007). ^{21}Ne is a stable isotope. Sample depths, densities, and locations were used to calculate surface production rates at high latitudes after Stone (2000) and Balco and Shuster (2009b). Site specific production rates and scaling factors are provided in Table 2.

The production rates of cosmogenic nuclides at Earth's surface are dependent on latitude and altitude (Lal, 1991), and the production rate below the surface then becomes a function of substrate density, causing nuclide production $P(z)$ to decrease exponentially with depth (Figure 4) (Dunne et al., 1999) as described by Equation 1 (Lal, 1991; Niedermann, 2002; Dunne et al., 1999). The subscript i refers to the nuclide of interest, $P(0)$ is the production rate at the surface, z is depth below surface (cm), ρ is density of sample (g cm^{-3}), and Λ is the attenuation path length of 150 g cm^{-2} which is accepted for use in Antarctica. See Gosse and Phillips, 2001 (Gosse and Phillips, 2001) for detailed discussion of Λ.

(1) $$P_i(z) = P_i(0)e^{-z\rho/\Lambda_i}$$

Given a stable, non-eroding surface, the expected radionuclide concentration C_{total} at any depth z, and time t is described by Equation 2, where C_{inh} is the inherited background nuclide

concentration from potential previous exposures (Lal, 1991; Niedermann, 2002) and can be simplified for stable nuclides (Equation 3).

(2) $$C_{total}(t,z) = C_{inh}(z)e^{-t\lambda} + \sum_i \frac{P_i(z)}{\lambda}(1 - e^{-t\lambda})$$

(3) $$C_{total}(t,z) = C_{inh}(z) + \sum_i P_i(z)t$$

Radionuclides ^{26}Al and ^{10}Be production rates will eventually reach equilibrium with their decay rate given enough time. Once the production rate matches the decay rate, only physical forces such as degradation and aggradation may affect the expected concentration of nuclides. After nuclide concentrations have reached secular equilibrium, then concentrations of the nuclides provide only minimum ages (but do not provide any older age constraints). This time is known as the effective half-life ($\tau_{1/2,e}$) and can then be determined after Morgan et al. (2010a) via Equation 4, where ε_2 is the degradation rate of the regolith (g cm^{-2} yr^{-1}). Degradation and sublimation rates are calculated after a few effective half-lives have passed.

(4) $$\tau_{1/2,e} = \frac{\ln(2)}{\left(\lambda_i + \frac{\varepsilon_2}{\Lambda}\right)}$$

As stated above, the concentration of nuclides at depth after a few effective half-lives may then only be affected by degradation (erosion) or aggradation. Here, aggradation is interpreted as a sublimation rate where the addition of material to the underside of sublimation till is a function of the local sublimation rate. The expected concentration $C_{i,j}$ of nuclides in a surface undergoing erosion is described by Equation 5 (Lal, 1991; Niedermann, 2002), and modified for erosion concurrently with sublimation acting on a body of ice by Equation 6 (Morgan et al., 2010a). Both equations can be modified for stable nuclides by removing terms with decay constants.

(5) $$C_{i,j}(\varepsilon_2, t) = C_{i,inh} + \frac{P_i \cdot e^{-z_j/\Lambda}}{\lambda_i + \varepsilon_2/\Lambda} \cdot (1 - e^{-(\lambda_i + \varepsilon_2/\Lambda)\cdot t})$$

(6) $$C_{i,j}(\varepsilon_1, \varepsilon_2, t_{ice}, t_{till}) = C_{i,inh} + \frac{P_i \cdot e^{\frac{-z_j}{\Lambda}}}{\lambda_i + (\varepsilon_1 + \varepsilon_2)/\Lambda} \cdot \left(1 - e^{-\left(\lambda_i + \frac{\varepsilon_1 + \varepsilon_2}{\Lambda}\right)\cdot t_{ice}}\right) \cdot e^{-\lambda_i \cdot t_{till}} + \frac{P_i \cdot e^{\frac{-z_j}{\Lambda}}}{\lambda_i + \frac{\varepsilon_2}{\Lambda}} \cdot \left(1 - e^{-\left(\lambda_i + \frac{\varepsilon_2}{\Lambda}\right)\cdot t_{till}}\right)$$

The subscript i is the nuclide of interest, j is the individual sample at each site, ε_1 is the sublimation rate (g cm^{-2} yr^{-1}), t_{ice} and t_{till} are the time the sample spent in ice and till respectively and is resolved independently, see Morgan et al. (2010a) for detailed discussion of t_{ice} and t_{till}. These must sum to equal the age of the deposit. P_i is the production rate of the nuclide of interest at the surface in atom g^{-1} yr^{-1}. The model used in this paper is further constrained by acceptable ranges of combinations of ε_1 and ε_2 throughout time to produce the observed till thickness if buried ice is found. The permissible combinations can be described by Equation 7, where z is the depth to ice, T_n is time from present, $C0$ is concentration of debris in ice (percent by volume), and ε_1, ε_2 represent the ice sublimation rates and regolith erosion rates respectively. Specifying unique and valid solutions for erosion and sublimation rates as a function of time, related to till thickness is challenging. Solutions for time are highly variable, especially if the concentration of a nuclides suggests it has reached secular equilibrium. Thus, the model allows for a range of acceptable combinations of ε_1 and ε_2, since solutions for time are variable and the age of the surface will increase with greater ε_1, ε_2 rates.

(7) $$z = T_n * [(\varepsilon_1 * C0) - \varepsilon_2]$$

Standard chi squared (χ^2) minimization techniques are used to resolve erosion rates, sublimation rates, inheritance, and time (Braucher et al., 2009; Morgan et al., 2010b) where χ^2 is calculated via Equation 8. O is the observed concentration, E is the modeled result, and σ is the

standard deviation of the measurement. Whole pit, χ^2 minimized modeled results use samples from ice free regolith only; they do not include concentrations from the debris in ice. Expected nuclide concentrations are calculated from starting scenarios, the best fit is determined by minimizing the resulting difference of the final χ^2 value. The smaller the resulting χ^2, the better the model fit to the observed data. The current model uses an internal minimizing function in Matlab (MATLAB 2013a), *fminsearchcon( )* (D'Errico, 2012), to modify unknowns until the lowest value for χ^2 is reached. The function *fminsearchcon( )*allows for upper (max) and lower (min) boundary conditions to be set for acceptable multi-variable solutions. Allowable boundary conditions for ^{26}Al and ^{10}Be inheritance are set with min = 0, and max = nuclide saturation, which is a function of the production rate and decay rate of the nuclide of interest. No min or max is set for stable ^{21}Ne. Acceptable erosion rate and sublimation rates are boundless between 0 and infinity with the condition that the solution for sublimation must always be greater than the erosion rate. No condition set for sublimation and erosion rate combinations as a function of englacial debris concentration to produce the observed till thickness, but this does not affect results where time dominates the solution and/or the thickness of till is unknown. In all cases, the local erosion rate dominates the modeled sublimation rate, and thus controls the resulting till thickness/ nuclide concentrations at depth. Further, max and min boundaries for time are set at 0 and 10 Mya, where Earth's cosmic-ray flux considered constant for the past 10 Mya (Leya et al., 2000).

(8) $$\chi^2 = \sum(O - E)^2/(\sigma^2)$$

The resulting accumulation rate (ε_3) of regolith from a sublimating ice body using any combination of sublimation and erosion rate is calculated with Equation 0, where ε_1 must be greater than ε_2 and $C0$ is the concentration of debris by volume entrained in ice.

(9) $$\varepsilon_3 = (\varepsilon_1 * C0) - \varepsilon_2$$

The exposure age of the surface may be calculated from modeled surface concentrations fit to nuclide profiles or to a single sample at depth following Equation 10 after (Lal, 1991; Niedermann, 2002). T_{exp} is the minimum time of exposure, C_{cos} is the concentration of cosmogenically derived nuclides in the sample, which can be further modified to account for concentrations of inherited nuclides if able to be determined independently ($C_{cos} = C_{total} - C_{inh}$). This equation assumes zero erosion, but the effect of erosion on the exposure age of the sample may be factored in using Equation 11. Here, a scaling factor is calculated (f_e) and multiplied by T_{exp} from Equation 10 to determine a corrected exposure age where ($T_{exp,\varepsilon-corr} = f_e T_{exp}$).

(10) $$T_{exp} = -\frac{1}{\lambda}\ln\left(1 - \frac{C_{cos}(z,T_{exp})\lambda}{\sum_i P_i(z) * e^{-\frac{\rho z}{\Delta_i}}}\right)$$

(11) $$f_e = 1 + \frac{\varepsilon T_{exp}\rho/\Delta}{2}$$

Error Distribution

The distribution and propagation of errors within calculations and modeled results is challenging. Equations 5 and 6 are non-linear and asymptotic over long periods of time. Local minima are avoided by selecting appropriate starting values for parameters used for optimization. A 10,000 run Monte Carlo simulation was used to determine uncertainties within modeled

results. This method assumes that measured cosmogenic nuclide concentrations follow a Gaussian distribution that is within the measured standard deviation of concentration results (Balco et al., 2005; Morgan et al., 2010b). A random concentration within the standard measurement error is taken for each sample and the best fit parameters are determined for each of the 10,000 runs. A cumulative distribution function is generated to visualize the probability distributions of the unknowns. Standard 1σ (68%) confidence intervals are used as the error of the best-fit parameters.

CHAPTER IV

RESULTS

Typically concentrations of ^{26}Al and ^{10}Be are modeled together to determine a single solution for age, inheritance, erosion rate, and/or sublimation rate. The concentrations of each nuclide are solved for independently and those results are reported here. Two scenarios were proposed in the previous chapter to describe the observed nuclide concentrations in these drifts. 1) nuclide concentration as a function of sublimation and subsequent erosion as described by Equation 6; and 2) nuclide concentration as a function of only the local erosion rate as described by Equation 5. This results in two scenarios with two nuclide solutions, reported below. Further, the concentration of ^{21}Ne in pits between sample pairs after Ng et al., (2005) is reported in Table 3. Interpretation for the Ng et al., (2005) method uses the deepest sample in each pit whether it is from ice or regolith.

Youngest Drift

The concentration of ^{21}Ne was measured in 10-OV-Pit-11 and 10-OV-Pit-12. ^{26}Al and ^{10}Be were also measured in 10-OV-Pit-12 (Table 1). Ice was found in the bottom of both pits at 46 cm and 48 cm respectively. Average whole pit ^{21}Ne concentrations in this drift were 11.38 M atoms/g and have no systematic relationship with depth and imply an older age of 0.22 Mya (Figure 10). This suggest that the majority of the present ^{21}Ne concentration is inherited from prior exposure. The variation in concentration with depth suggests that this drift is relatively young and has not been stable long enough for the production of new in-situ ^{21}Ne to overcome

any signature from previous exposure. ^{21}Ne is a stable nuclide and is retained permanently in-situ rather than undergoing radioactive decay. The maximum measured ^{21}Ne concentration gives an absolute maximum exposure age of 0.36 Mya assuming zero ^{21}Ne from previous exposure.

^{26}Al and ^{10}Be depth profiles in Pit-12 are consistent with a stable (non-mixed) till profile (Figure 10) and concentration are too low to effectively resolve erosion rates (Figure 10). The modeled best fit scenario for a sublimation based profile is solved via Equation 6 and error bounds are modeled with a 10,000 run MCS. Scenario 1) ^{10}Be and ^{26}Al concentrations give a sublimation rate = 573.23 m/Mya, +44.17 m/Mya, -49.03 m/Mya, erosion rate = 30.53 m/Mya, +1.924 m/Mya, -1.95 m/Mya, $^{10}Be_{inh}$ = 2.15 x 10^4 atoms/g quartz, +0.94 x 10^4 atoms/g quartz, -1.06 x 10^4 atoms/g quartz, $^{26}Al_{inh}$ = 5.62 x 10^4 atoms/g quartz, +6.78 x 10^4 atoms/g quartz, -5.62 x 10^4 atoms/g quartz, and χ^2_{Al+Be}=28, +9.4, -10.2, time = 18.4 Kya, +0.11 Kya, -0.11 Kya (Figure 11). Concentrations of nuclides in this drift are too low to have reached secular equilibrium, thus the concentration of nuclides in this drift are mainly a function of time and inheritance (Figure 10). A solution is generated for a representative erosion rate and sublimation rate but it is not the best suited to reflect the true surface process rates occurring in the past ~20 Kya. Figure 10 reinforces the control of time in the concentration of nuclides solved for by Equation 6 since the concentration ratios of ^{26}Al to ^{10}Be vs. ^{10}Be for all samples plots in the upper extreme of the graph.

The erosion rate and age for the youngest drift may similarly be solved for using Equation 5 where the variable of sublimation does not contribute to the calculated concentration of nuclides. Assuming a simpler situation where erosion is the only surface process contributing to observed nuclide concentrations, then a separate solution may be modeled for inheritance, the erosion rate and time. The results from this model again are dominated by time and the reported

results are mainly giving an answer to the time of exposure. Scenario 2) The ^{10}Be and ^{26}Al concentrations within samples result in a modeled erosion rate of 0.13 m/Mya, +0.005 m/Mya, -0.005 m/Mya, $^{10}Be_{inh}$ = 0 atoms/g quartz, $^{26}Al_{inh}$ = 3.13 x 10^4 atoms/g quartz, +4.84 x 10^4 atoms/g quartz, -0 atoms/g quartz, and χ^2_{Al+Be}=104.9, +20.3, -20.1, time = 8.5 Kya, +0.21 Kya, -0.21 Kya (Figure 12).

In comparison to the modeled age of the youngest drift, the apparent exposure age ($T_{exp(i,inh,e)}$) may be calculated for surface samples using Equation 10 and modified for erosion with Equation 11. Here, T_{exp} is time of exposure, *i* designates the nuclide of interest, *inh* is the modeled or independently known inheritance of the nuclide of interest, and *e* is the modeled or independently known erosion rate. For 10-OV-Pit-12, $T_{exp(Al)}$ = 13.1 Kya, $T_{exp(Be)}$ =14.8 Kya, $T_{exp(Al,inh)}$ = 12.9 Kya, $T_{exp(Be,inh)}$ = 14.8 Kya, $T_{exp(Al,inh,e=0.13)}$ = 12.8 Kya, $T_{exp(Be,inh,e=0.13)}$ = 14.8 Kya.

The interpretation between clast pairs after Ng et al., (2005) is reported in Table 3, but only the average results are accepted as loosely representative of this drift. The concentrations of ^{21}Ne at depth do not follow the decreasing concentrations vs. depth profile required by this method to resolve rates and ages between individual clast pairs, yet calculations are reported for reference and serve as loose guides for interpreting the concentrations of ^{21}Ne in this drift. The Ng et al., (2005) model gives a maximum accretion age of the deposit around 150 Kya, which is well above the apparent ages from ^{26}Al and ^{10}Be. Other maximum and minimum rate constraints provided by this model fit our chi-squared results but since inheritance is the dominant control on ^{21}Ne concentrations, the Ng et al., model should serve only as general reference for this drift. Further calculations of all exposure age variations for nuclides are reported in Table 4 and Table 5.

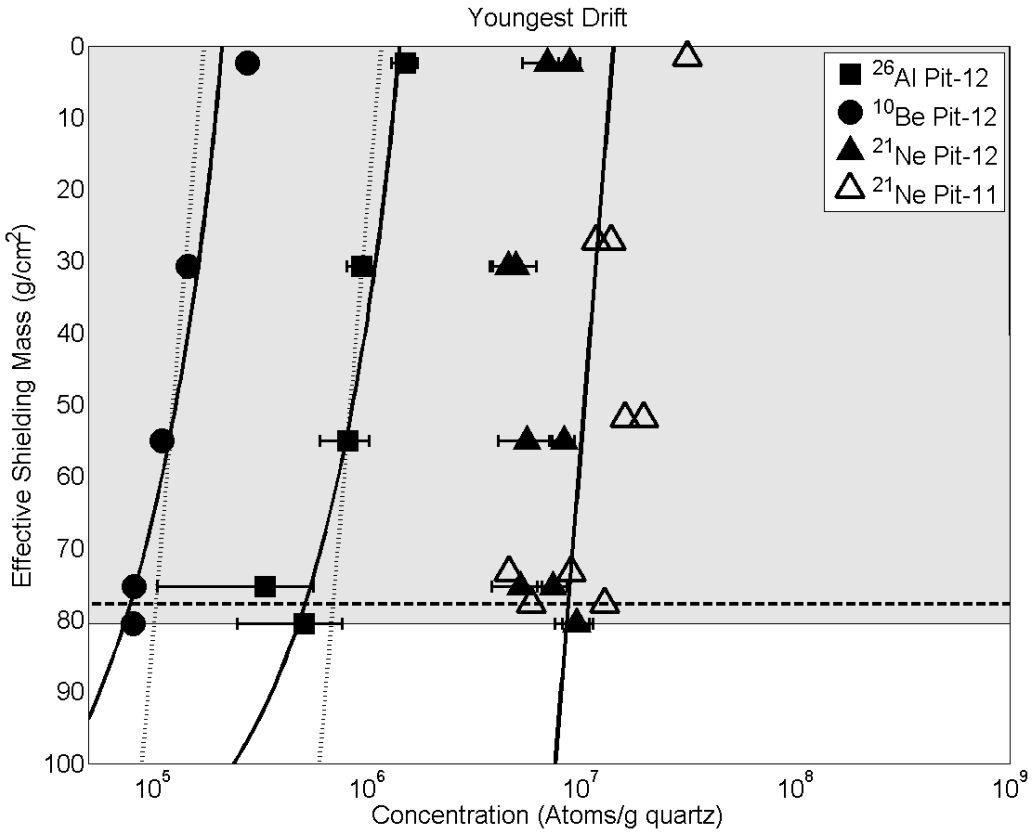

Figure 9. Youngest Drift: Concentration vs. effective shielding mass of measured nuclides. Best fit dotted lines are for erosion based model, best fit solid lines are for sublimation based model, gray shading is till, white shading is ice, horizontal dashed line is ice level in complimentary Neon pit. Best fit line for ^{21}Ne is averaged between all ^{21}Ne samples due to wide variety of concentrations with depth. Error bars are displayed but in some cases are smaller than symbol. Large error bars on the two lowest ^{26}Al samples are from low AMS beam currents during sample runs (Hunt et al., 2008).

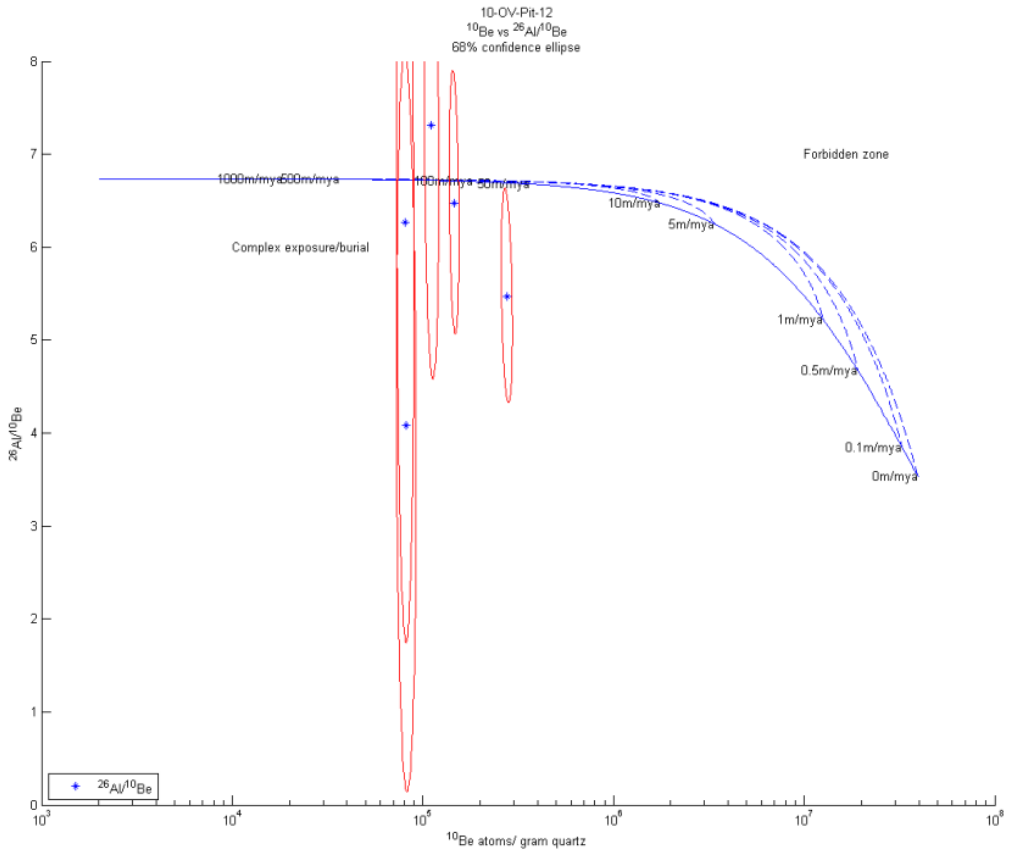

Figure 10. Youngest Drift: Plot of ^{10}Be vs. (^{26}Al/^{10}Be). Red ellipses are 68% (1σ) confidence intervals based on AMS measurement error. Blue lines are hypothetical steady state erosion profiles. Concentrations, and thus ratios of nuclides are too low to fit a steady state erosion profile and do not plot within the zone of steady state erosion suggesting concentrations in this drift are representative of the exposure age.

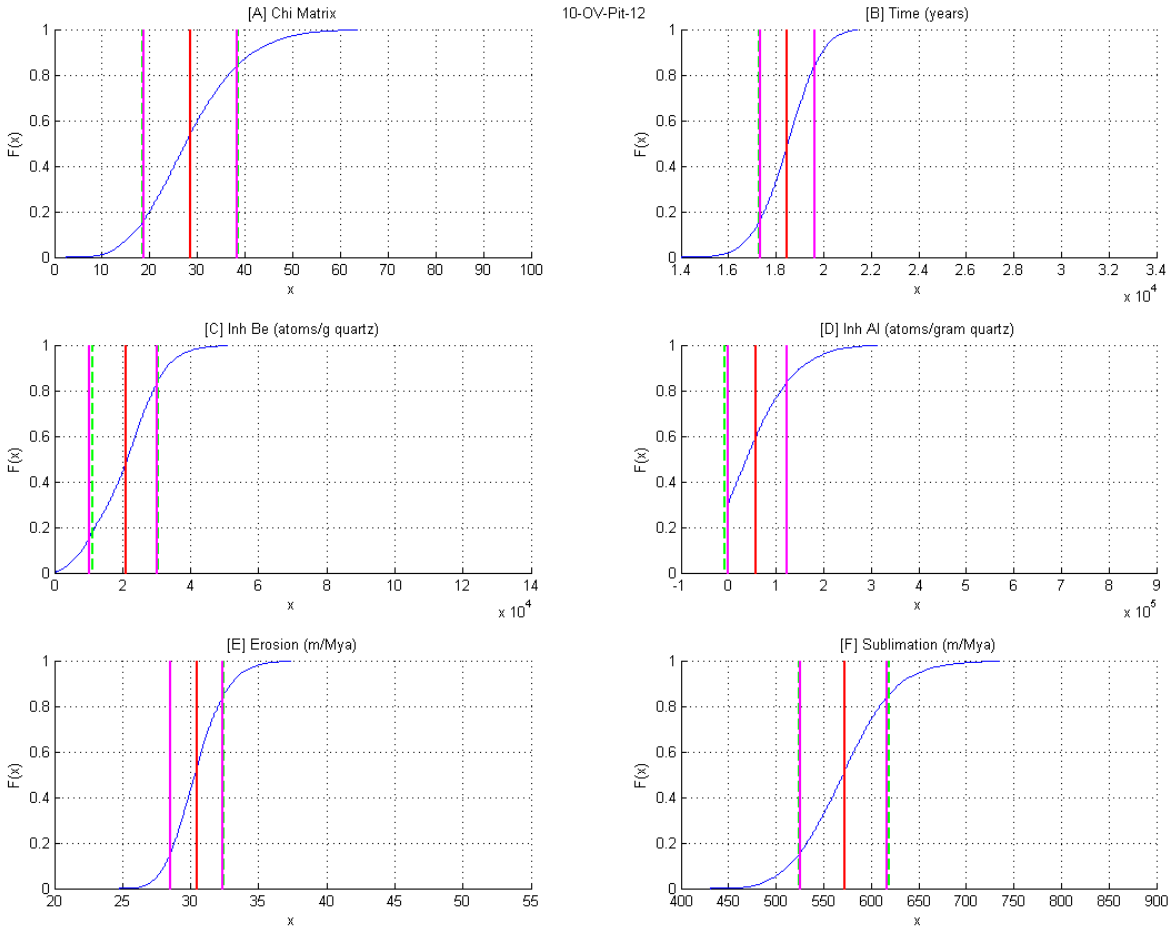

Figure 11. Youngest Drift: Sublimation based Monte Carlo Simulation (MCS) 10,000 modeled run results. [A] χ^2, [B] time, [C] ^{10}Be inheritance, [D] ^{26}Al inheritance, [E] erosion rate, [F] sublimation rate. Blue line is the cumulative distribution of the resulting solutions from MCS, red line is the mean value, pink lines are 1σ (68%) confidence intervals of modeled results, and stippled green lines are +/- standard deviations of MCS, x-axis of all plots represents the units of the variable reported, and y-axis of all plots is the relative distribution of modeled solutions.

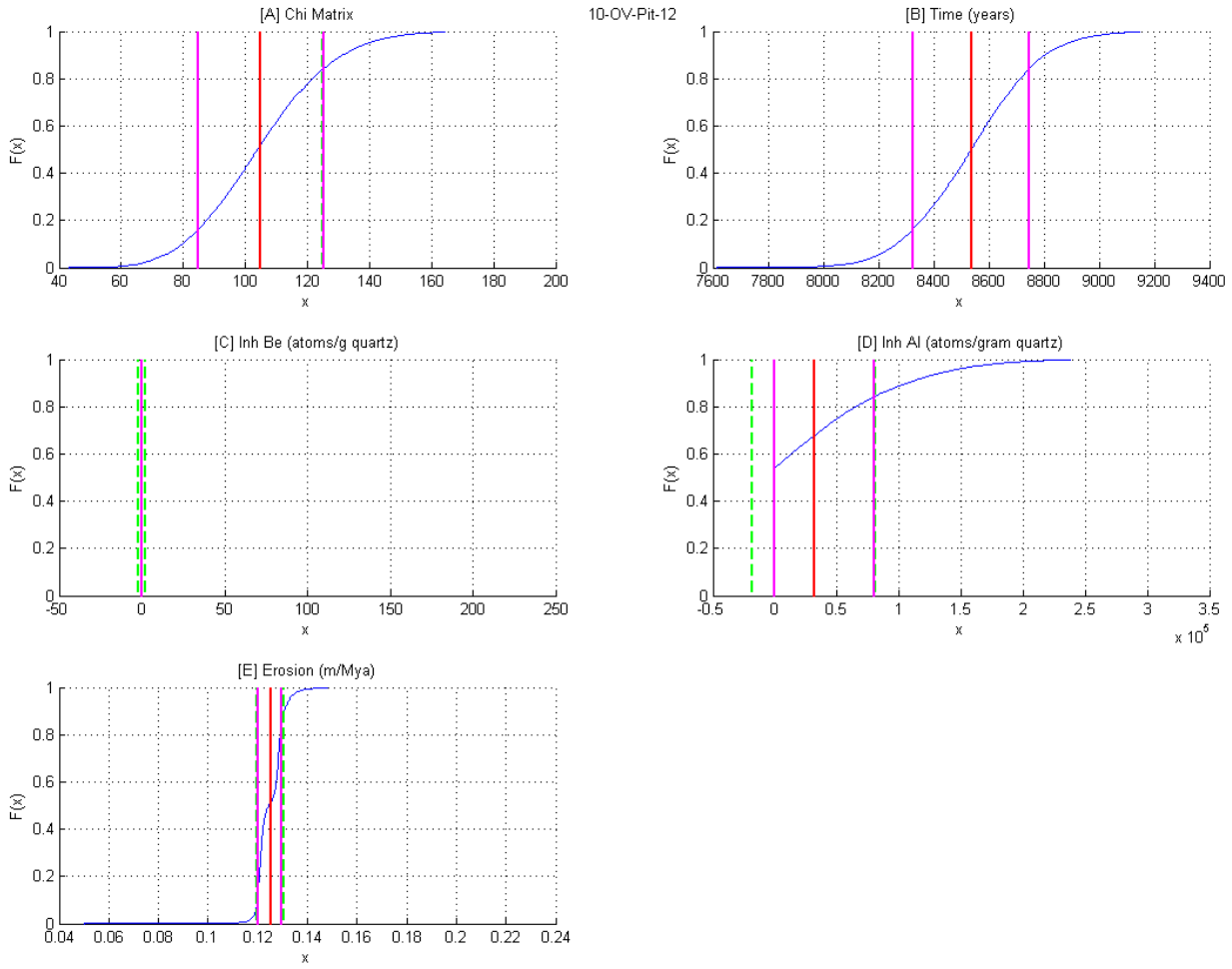

Figure 12: Youngest Drift: Erosion based Monte Carlo Simulation (MCS) 10,000 modeled run results. [A] χ^2, [B] time, [C] ^{10}Be inheritance, [D] ^{26}Al inheritance, [E] erosion rate. Blue line is the cumulative distribution of the resulting solutions from MCS, red line is the mean value, pink lines are 1σ (68%) confidence intervals of modeled results, and stippled green lines are +/- standard deviations of MCS, x-axis of all plots represents the units of the variable reported, and y-axis of all plots is the relative distribution of modeled solutions.

Middle Drift

The degree of patterned ground development, the presence of desert varnish, and the stratigraphic relationship within Ong Valley all indicate that the middle drift is older than the youngest drift. The thickness of the till is also greater in the middle drift when compared to average till thickness of the youngest drift. This matches the general expectation that the middle drift has had much more time to sublimate and produce a thicker lag deposit. The concentrations

of ^{10}Be and ^{21}Ne are also greater than those from the younger drift (Figure 13). Based on the above general geologic criteria we interpret the middle drift as a sublimation till and solve for erosion rates and ice sublimation rates after Morgan et al. (2010a) using Equation 6.

^{21}Ne was measured in 10-OV-Pit-01 and 10-OV-Pit-02. ^{10}Be was further measured in 10-OV-Pit-01 (Table 1). ^{26}Al measurements are absent due to analytical equipment failure. Ice was found in the bottom of both pits at 68 cm and 80 cm respectively. The average whole pit ^{21}Ne concentration in this drift is 136 M atoms/g, the individual concentrations decrease consistently with depth, with a resulting average age of 1.37 +/- 0.05 Mya. If zero inheritance of ^{21}Ne is assumed, the average surface exposure age for the middle drift is 1.91 +/- 0.05 Mya. The absolute minimum possible average surface exposure age is 0.90+/- 0.05 Mya, assuming the deepest sample from both pits represents the maximum allowable inheritance (Table 4).

Comparatively, the surface exposure age for 10-OV-Pit-01 may be calculated using the concentration of ^{10}Be in the top-most sample. Assuming zero erosion and zero inheritance, $T_{exp(Be)}$ =0.92 Mya. This age can be corrected for modeled inheritance (~5.1 x 10^6 atoms/g quartz and discussed below) which gives $T_{exp(Be,inh)}$ = 0.61 Mya, and corrected for erosion $T_{exp(Be,inh,e=0.9)}$ = 0.81 Mya (Table 5).

In addition to the samples collected within the till, an additional sample was collected and analyzed from the massive ice beneath the till. The ^{10}Be depth profile in 10-OV-Pit-01 is consistent with a stable (non-mixed) till profile, and concentrations of nuclides are high enough to have reached secular equilibrium to resolve an erosion rate and sublimation rate described above. Using χ^2minimization, the best fit model parameters for ^{10}Be concentrations can be determined independently. Two scenarios were again modeled: 1) sublimation of bulk ice to produce the till with additional erosion of the regolith; and 2) bulk deposition of the till with only

erosion acting on the surface. Scenario 1) ^{10}Be concentrations give a sublimation rate = 22.65 m/Mya, +11.4 m/Mya, -11.26 m/Mya, erosion rate = 0.89 m/Mya, +0.04 m/Mya, -0.07 m/Mya, $^{10}Be_{inh}$ = 3.307 x 10^6 atoms/g quartz, +1.7 x 10^6 atoms/g quartz, - 1.6 x 10^6 atoms/g quartz, and χ^2_{Be}=32, +7.6, -7.6, ^{26}Al modeled results are not reported, C0= 0.07, +0.02, -0.04. time = 6.684 Mya, +2.6 Mya, -2.5 Mya (Figure 14). The resulting accumulation rate for this model solution is approximately 0.7 m/Mya. Scenario 2) ^{10}Be concentrations result in an erosion rate = 0.58 m/Mya, -0.04 m/Mya, +0.01 m/Mya, $^{10}Be_{inh}$ = 1.48 x 10^6 atoms/g quartz,+0.3 x 10^6 atoms/g quartz, -0.3 x 10^6 atoms/g quartz, and χ^2_{Be}=33.4, +7.7, -7.8, and time = 1.87 Mya, +0.14 Mya, -0.21 Mya (Figure 15).

The ^{10}Be concentration of debris from within the ice is significantly lower than ice free debris above the ice. The isotope concentrations from the englacial debris do not conform to the model of simple steady-state sublimation and/or surface erosion. If included in the model, the englacial samples result in a very poor fit with a very high χ^2. Ice samples are excluded from basic interpretation and the concentration measured in the ice is discussed in a later section.

Concentrations of ^{21}Ne are further examined from two sample sites, 10-OV-Pit-01 and 10-OV-Pit-02 in the top center of patterned ground polygons approximately 20 m apart. ^{21}Ne results are in agreement with ^{10}Be concentrations to show a stable till layer that is not undergoing vertical mixing. To determine the absolute minimum exposure age of the surface, the inheritance is systematically removed by subtracting the concentration of ^{21}Ne in the ice from the surface concentration. The age could be older if the true nuclide inheritance is less than that of the lowest bulk sample. Doing this gives an age that does not include an erosion rate and is based only on nuclide concentration and the local production rate. The surface of 10-OV-Pit-01 then has a minimum exposure age 0.93 +/- 0.05 Mya and the surface of 10-OV-Pit-02 has an exposure age

of 0.86 +/- 0.04 Mya and both pits average to 0.90 +/- 0.05 Mya as reported above. It is unlikely that these surfaces are younger than reported here, but they could be older. If there is zero nuclide inheritance of ^{21}Ne then the surface of 10-OV-Pit-01 has a maximum exposure age 1.95 +/- 0.05 Mya and the surface of 10-OV-Pit-02 has a maximum exposure age of 1.87 +/- 0.04 Mya and both pits average to 1.91 Mya as reported above.

Expected concentrations vs. depth for all the samples in the pit are modeled, and a minimum average exposure age using the best fit line to the model is calculated. ^{21}Ne inheritance is maximized by setting the maximum allowable nuclide inheritance to equal that of the lower-most sample from the ice with zero erosion. The best model fit for the absolute minimum average exposure age of 10-OV-Pit-01 is 0.84 +/- 0.05 Mya and 0.59 +/- 0.05 Mya for 10-OV-Pit-02. Again, these are absolute minimums since nuclide inheritance was likely less than the observed concentration in ice and sublimation/erosion rates are not considered.

Conversely, ^{21}Ne is used to place bounds on the maximum accretion age of upper clast pairs (Table 3) (Ng et al., 2005). This model utilizes the concentration differences between sample pairs relative to a base concentration at the lowest depth. The lowest bulk sample is chosen as the lowest sample measured from debris in ice. See Ng et al., (2005) for a detailed description on calculating age and minimum sublimation rates. The concentration vs. depth pairs of ^{21}Ne in 10-OV-Pit-01 and 10-OV-Pit-02 gives a minimum mean interclast sublimation rate (S_{min}) of 0.11 and 0.15 m/Mya respectively within the past 2.00 to 1.98 Mya (Table 3). The minimum original interclast ice thickness ($\Delta_{i,min}$) is then calculated as 22.1 and 29.7 m.

The results using the clast pair model produces some inconsistencies within these pits due to the greater ^{21}Ne concentration in the ice as compared to some select samples at depth (Figure 13), but values at the pit surface still provide valuable constraints on exposure history and

sublimation rates and support previously reported rates from ^{10}Be analysis. When the debris concentration of original massive ice is constrained to 3% and 10%, minimum total sublimed ice thickness ($\Delta_{i,min}^{R}$) is largest at 15 to 17.6 m and minimum sublimation rates of interclast ice (S_{min}^{R}) range from <1 m/Mya to ~9 m/Mya (Table 3). Further calculations of all exposure age variations are reported in Table 4 and Table 5.

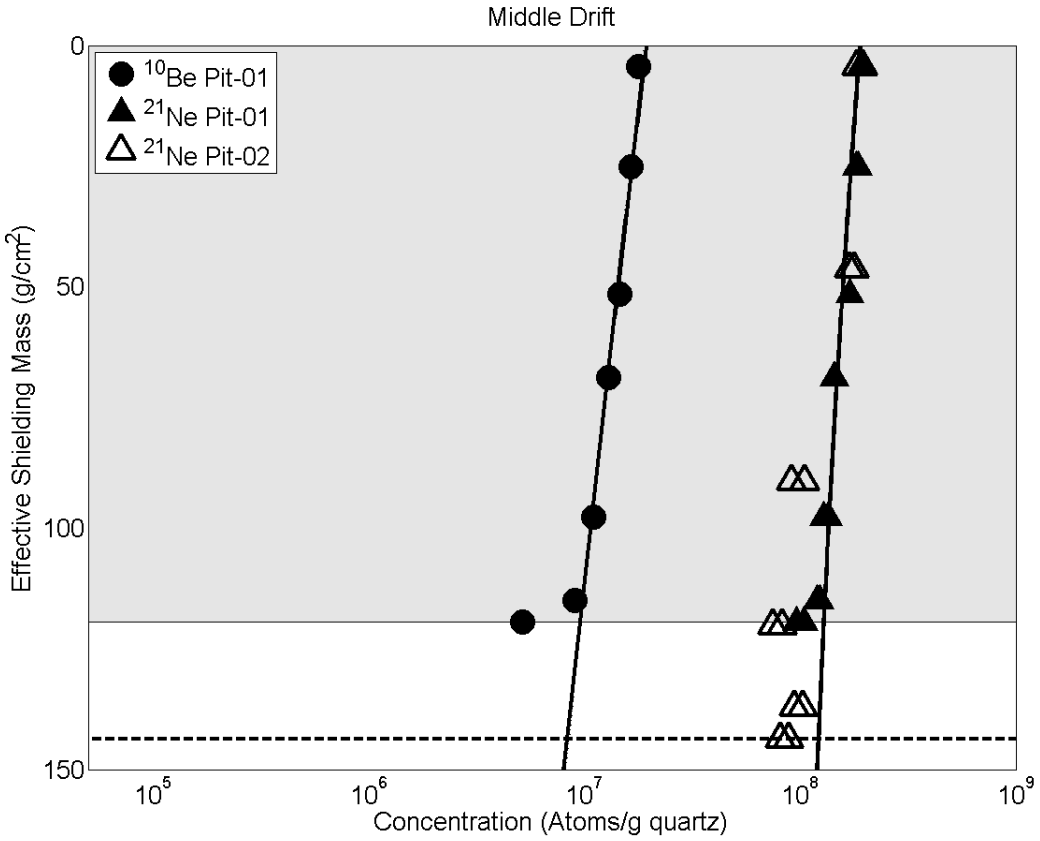

Figure 13. Middle Drift: Concentration vs. effective shielding mass of measured nuclides. Best fit solid lines are for sublimation based model (erosion based model matches sublimation profile), gray shading is till, white shading is ice, horizontal dashed line is ice level in complimentary Neon pit. Best fit line for ^{21}Ne is averaged between all ^{21}Ne. Error bars are displayed but in some cases are smaller than symbol.

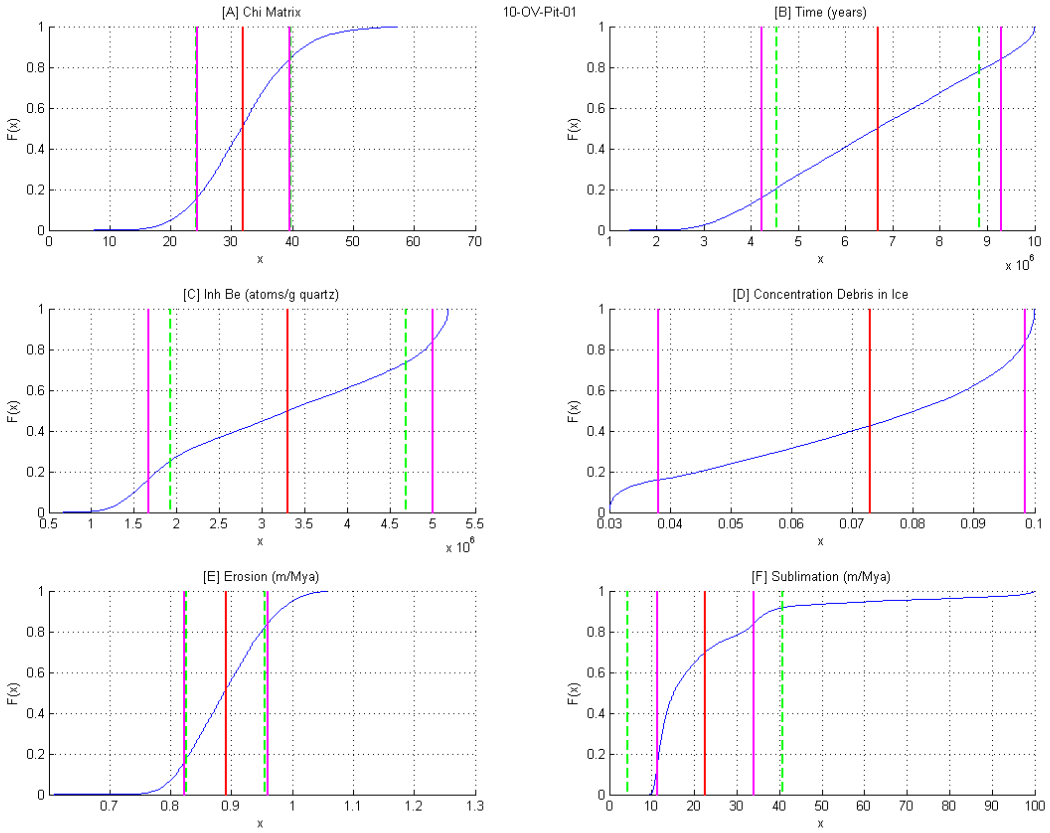

Figure 14. Middle Drift: Sublimation based Monte Carlo Simulation (MCS) 10,000 model run results. [A] χ^2, [B] time, [C] ^{10}Be inheritance, [D] concentration of englacial debris by volume, [E] erosion rate, [F] sublimation rate. Blue line is the cumulative distribution of the resulting solutions from MCS, red line is the mean value, pink lines are 1σ (68%) confidence intervals of modeled results, and stippled green lines are +/- standard deviations of MCS, x-axis of all plots represents the units of the variable reported, and y-axis of all plots is the relative distribution of modeled solutions.

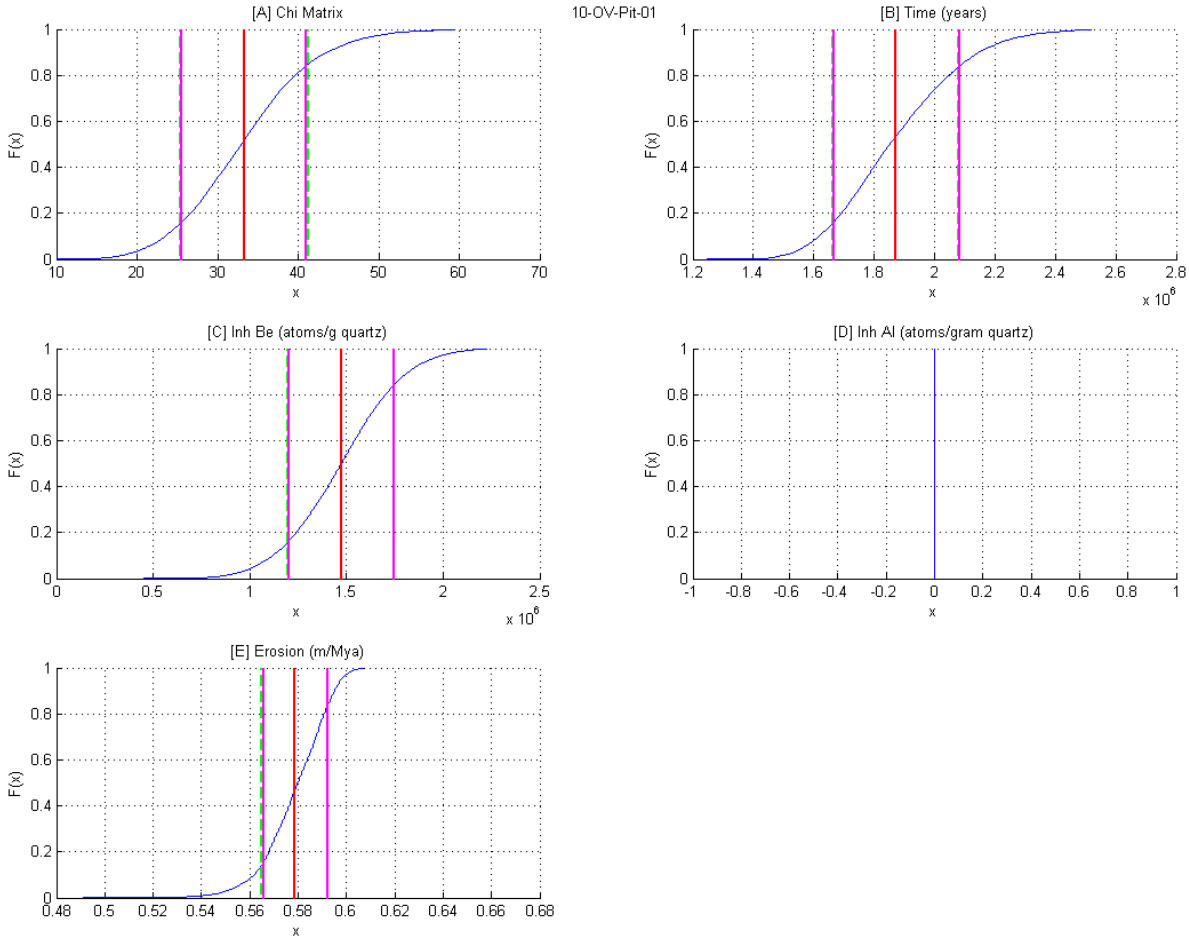

Figure 15. Middle Drift: Erosion based Monte Carlo Simulation (MCS) 10,000 model run results. [A] χ^2, [B] time, [C] ^{10}Be inheritance, [D] ^{26}Al inheritance (not reported), [E] erosion rate. Blue line is the cumulative distribution of the resulting solutions from MCS, red line is the mean value, pink lines are 1σ (68%) confidence intervals of modeled results, and stippled green lines are +/- standard deviations of MCS, x-axis of all plots represents the units of the variable reported, and y-axis of all plots is the relative distribution of modeled solutions.

Oldest Drift

The oldest drift is farthest from the Argosy Glacier and in general, patterned ground polygons have less topographic relief than the middle drift. The maximum extent of the oldest drift is delineated with an end moraine that abuts a small unnamed alpine glacier coming down from the Macdonald Bluffs and continues along the valley walls. The small alpine glacier at the

head of Ong Valley does not cross this end moraine. The surface of this drift is covered with patterned ground and desert pavement, but the topographic relief between polygons is much less than in the previous drift and appears more weathered. The general profile of the oldest drift is concave up from the boundary of the middle drift to the end moraine. Surface concentrations of cosmogenic nuclides in the oldest drift pits are similar but generally greater than those measured in the middle drift (Figure 16) due to the older age of the till.

^{21}Ne was measured in 10-OV-Pit-03 and 10-OV-Pit-06. ^{26}Al and ^{10}Be were further measured in 10-OV-Pit-03 (Table 1). No ice was found at the bottom of either pit. The average whole pit ^{21}Ne concentration in this drift is 155 M atoms/g, decreasing consistently with depth, with a resulting average age of 1.60 +/- 0.03 Mya (Figure 16). If zero inheritance of ^{21}Ne is assumed, the average surface exposure age for the oldest drift is 2.37 +/- 0.03 Mya. The absolute minimum possible average surface exposure age is 1.50 +/- 0.03 Mya if the deepest sample from both pits represents the maximum allowable inheritance. The surface concentrations of ^{21}Ne in Pit-03 and Pit-06 are similar but the concentrations between the two pits diverge with depth by ~100 M atoms/g and thus the greatest concentration at depth is modeled as the maximum allowable inheritance. The offset of Pit-03 vs. Pit-06 ^{21}Ne concentrations at depth (Figure 16) suggest a variation in the erosion rate between the two sites but this remains unresolved without further ^{26}Al and ^{10}Be nuclide measurements from Pit-06. The ages reported here are interpreted as minimum ages since the effect of erosion and sublimation are not modeled on the final expected ^{21}Ne concentration. The age of this drift must then be older than suggested by the minimum possible exposure age of 1.50 Mya given sublimation and erosion have occurred throughout the past exposure history of our samples.

^{26}Al and ^{10}Be depth profiles in Pit-03 are consistent with a stable (non-mixed) till profile, concentrations of nuclides are great enough to have reached secular equilibrium, and nuclide ratios plot within acceptable hypothetical ranges (Figure 17). The best fit model parameters using χ^2 minimization are determined for ^{26}Al and ^{10}Be together following the scenarios outlined above. Scenario 1) ^{26}Al and ^{10}Be concentrations give a sublimation rate = 19.03 m/Mya, +10.9 m/Mya, -7.72 m/Mya, erosion rate = 0.74 m/Mya, +0.06 m/Mya, -0.06 m/Mya, $^{26}Al_{inh}$ = 3.27 x 10^7 atoms/g quartz, +0.95 x 10^7 atoms/g quartz, -0.92 x 10^7 atoms/g quartz, $^{10}Be_{inh}$ = 8.64 x 10^6 atoms/g quartz, +1.67 x 10^6 atoms/g quartz, -1.58 x 10^6 atoms/g quartz, χ^2_{Al+Be}= 108.4, +19.9, -20.2, C0= 4.8%, +2.1%, -1.9%, and time= 8.77 Mya, +1.23 Mya, -1.4 Mya (Figure18). Scenario 2) ^{26}Al and ^{10}Be concentrations give an erosion rate = 0.49 m/Mya, +0.02 m/Mya, -0.02 m/Mya, $^{26}Al_{inh}$ = 1.3 x 10^6 atoms/g quartz, +1.8 x 10^6 atoms/g quartz, -1.3 x 10^6 atoms/g quartz, $^{10}Be_{inh}$ = 6.83 x 10^5 atoms/g quartz, +2.5 x 10^5 atoms/g quartz, -2.5 x 10^5 atoms/g quartz, χ^2_{Al+Be}= 120.8, +21.7, -21.8, and time = 9.89 Mya, +0.11 Mya, -0 Mya (Figure19). The resulting high χ^2 is due to the relatively small measurement error of ^{10}Be. The ages reported here should not be taken for absolute ages but rather serve as an indication that the concentrations of nuclides in this drift have reached secular equilibrium . In contrast to the middle drift, no ice surface was reached in the oldest drift, thus, no rate-based age may be inferred from the resulting accumulation rate and till thickness. By comparison, surface concentrations of ^{26}Al and ^{10}Be provide an apparent surface exposure age $T_{exp(Al),}$ $T_{exp(Be)}$ at 0.78 Mya to 1.02 Mya respectively, assuming zero erosion and zero prior inheritance. Taking sublimation modeled inheritance into consideration results in $T_{exp(Al,inh)}$ = 0.44 Mya, $T_{exp(Be,inh)}$ = 0.50 Mya, further calculations for apparent exposure age given the local modeled erosion rate gives $T_{exp(Al,inh,e=0.8)}$ = 0.52 Mya, $T_{exp(Be,inh,e=0.8)}$ = 0.62 Mya. Further calculations of all exposure age variations are reported in Table 4 and Table 5.

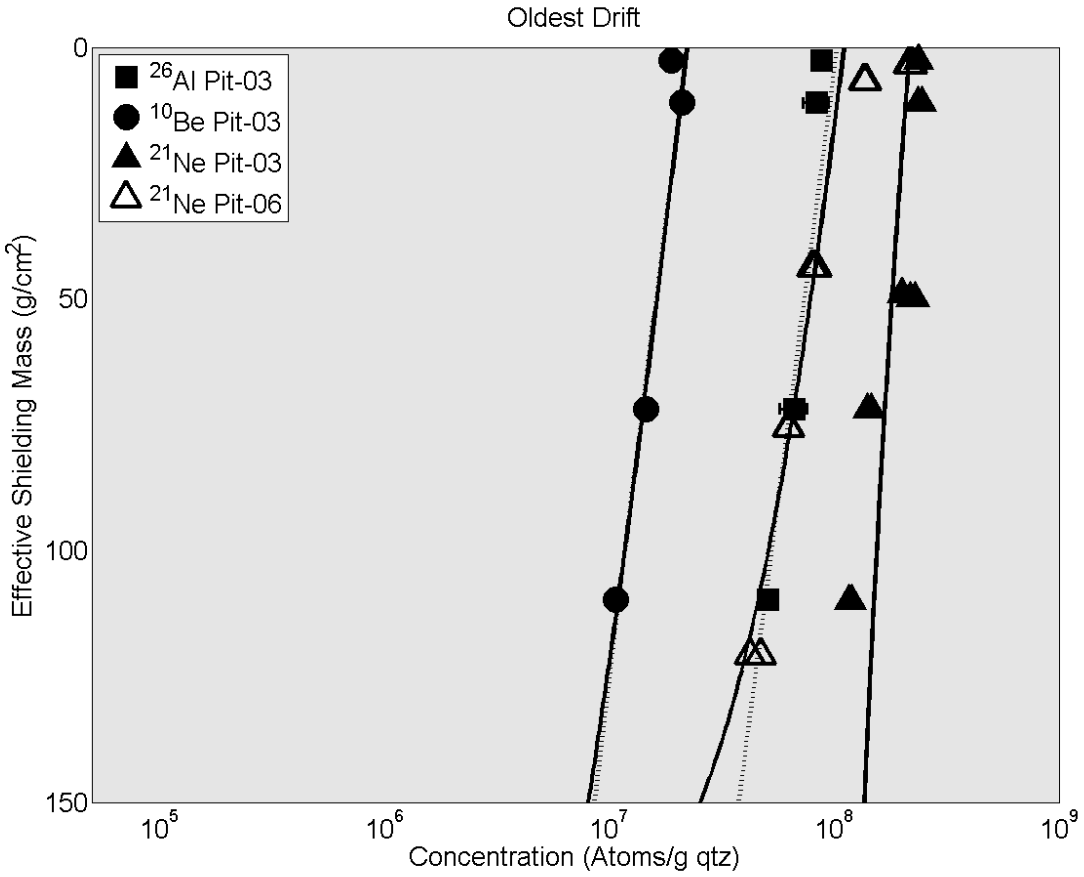

Figure 16. Oldest Drift: Concentration vs. effective shielding mass of measured nuclides. Best fit solid lines are for sublimation based model, dotted line is erosion based model solution, gray shading is till, no ice is present. Best fit line for ^{21}Ne is fit to Pit-03. Error bars are displayed but in some cases are smaller than symbol.

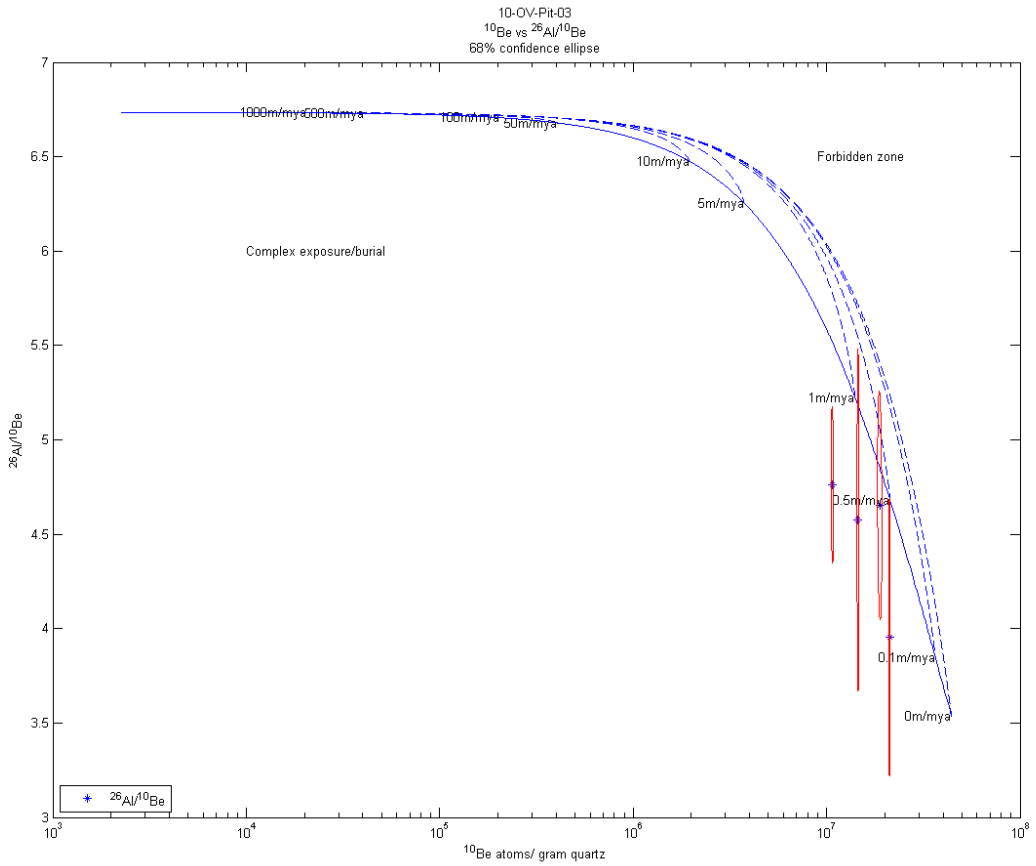

Figure 17. Oldest Drift: Plot of ^{10}Be vs. (^{26}Al/^{10}Be). Red ellipses are 68% (1σ) confidence intervals based on AMS measurement error. Blue lines are hypothetical steady state erosion profiles. Concentrations, and thus ratios of nuclides are within the complex exposure zone and plot near the steady state erosion profile as predicted by modeled best fit parameters.

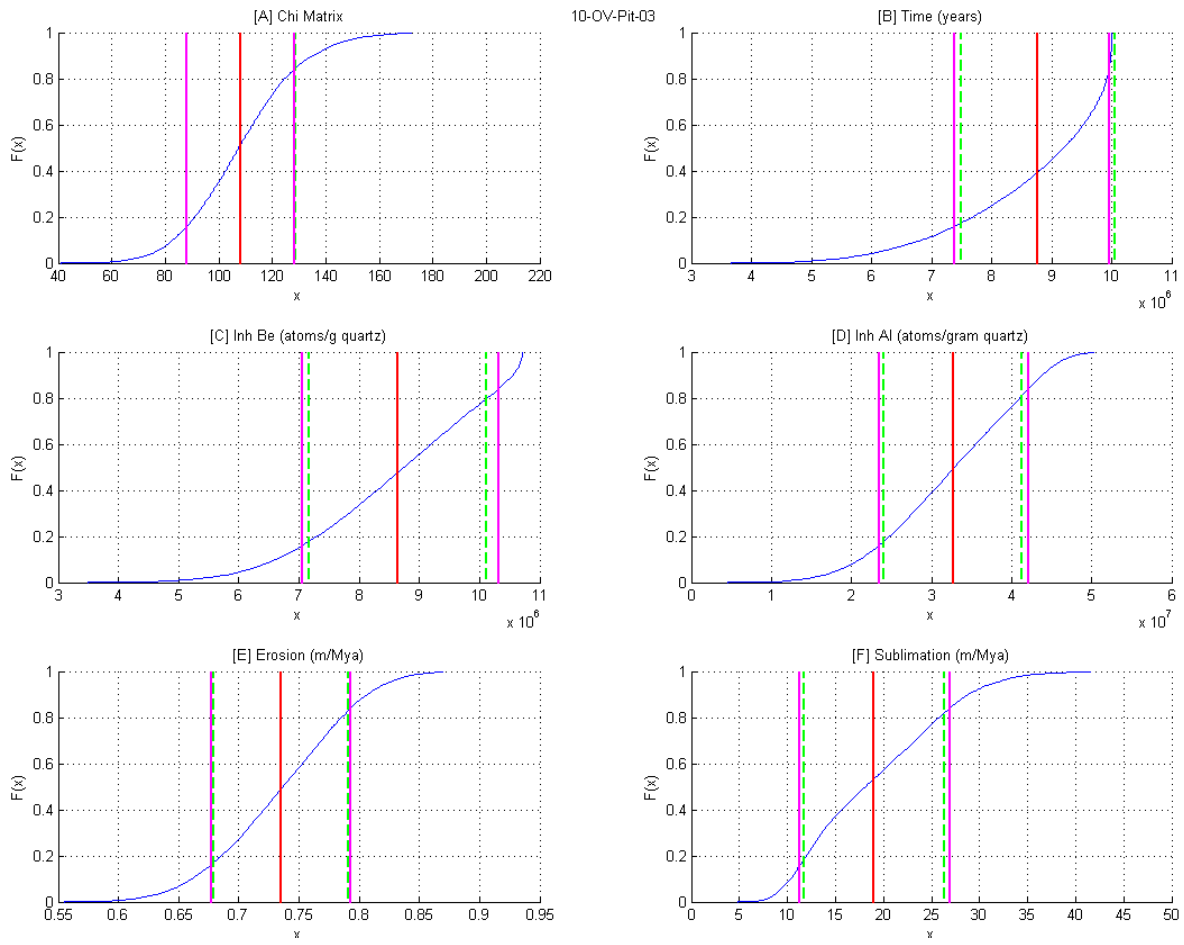

Figure 18. Oldest Drift: Sublimation based Monte Carlo Simulation (MCS) 10,000 modeled run results. [A] χ^2, [B] time, [C] ^{10}Be inheritance, [D] ^{26}Al inheritance, [E] erosion rate, [F] sublimation rate. Blue line is the cumulative distribution of the resulting solutions from MCS, red line is the mean value, pink lines are 1σ (68%) confidence intervals of modeled results, and stippled green lines are +/- standard deviations of MCS, x-axis of all plots represents the units of the variable reported, and y-axis of all plots is the relative distribution of modeled solutions.

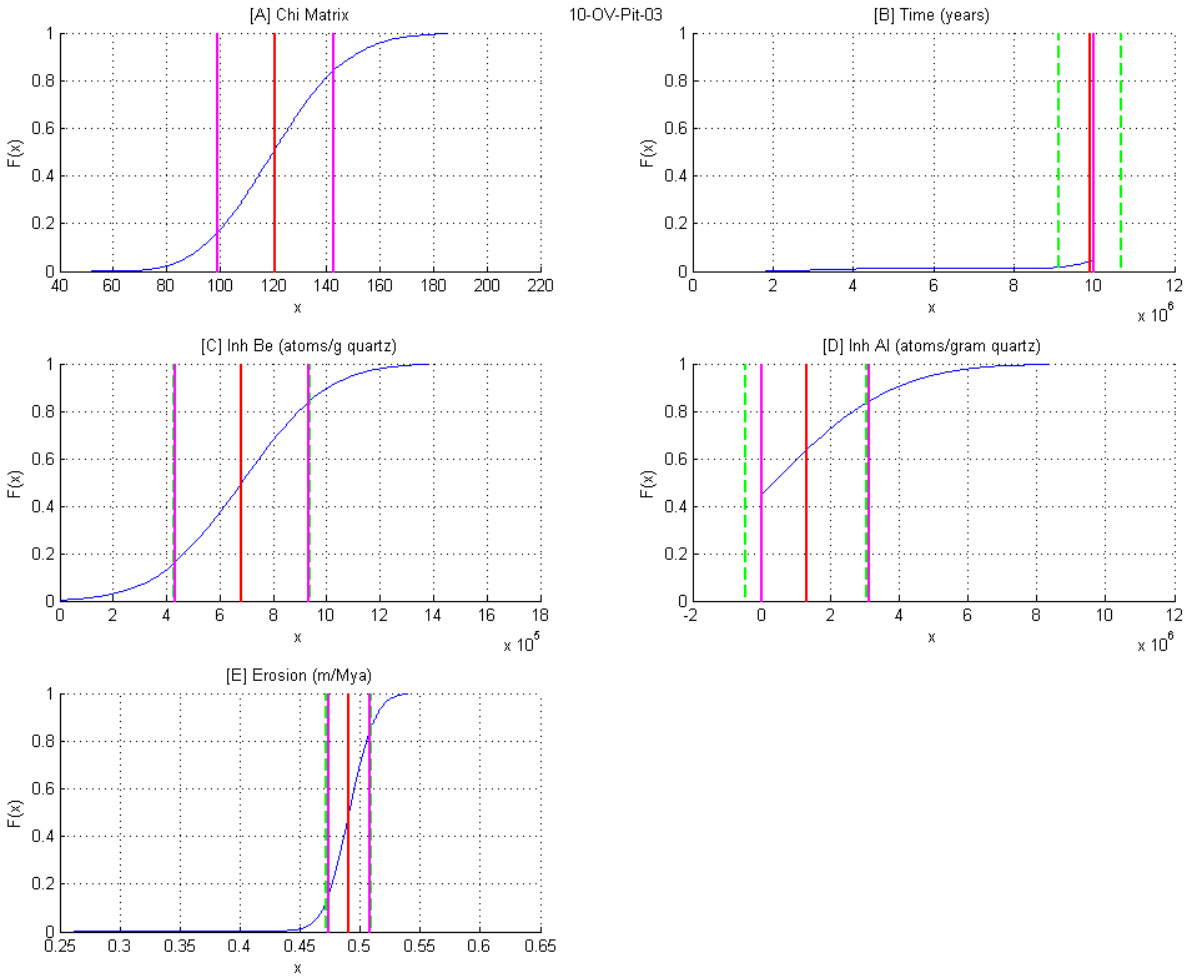

Figure 19. Oldest Drift: Erosion based Monte Carlo Simulation (MCS) 10,000 model run results. [A] χ^2, [B] time, [C] ^{10}Be inheritance, [D] ^{26}Al inheritance, [E] erosion rate. Blue line is the cumulative distribution of the resulting solutions from MCS, red line is the mean value, pink lines are 1σ (68%) confidence intervals of modeled results, and stippled green lines are +/- standard deviations of MCS, x-axis of all plots represents the units of the variable reported, and y-axis of all plots is the relative distribution of modeled solutions.

CHAPTER V

DISCUSSION

Isotope Concentrations of Debris within the Ice

Concentrations of nuclides from englacial debris below the middle drift are lower than expected and do not follow the steady state erosion or sublimation profiles as predicted from modeled best fit parameters (Figure 13). Ice was sampled from the bottom of Pit-01 and Pit-02 in the middle drift using a hammer and chisel. Regolith from the ice was separated at McMurdo Station. The concentration of debris in the ice ranged from 3% to 10% by volume and samples were measured for ^{10}Be and ^{21}Ne. The concentration of ^{10}Be in regolith from the ice is 4.3 X 10^6 atoms/g quartz. This is less than the expected concentration at depth if it underwent a similar exhumation history as other samples in the same pit. The ^{21}Ne concentration of the deepest sample in the pit (prepared and measured for noble gas mass spectrometry rather than AMS) also follows this trend, which suggests this is not an analytical or procedural error.

It is hypothesized that concentrations diverge from a steady state nuclide profile in the bottom of the middle drift due to an increased sublimation rate in the recent past. A greater sublimation rate would exhume a sample from depth and bring the ice (and the encased debris) closer to the surface in a shorter period of time than the older samples higher up in the regolith. A change in the local regolith erosion rate would be reflected in all samples including the ice sample and thus is not enough to explain the observed lower concentration. The sample above the ice/till boundary (10-OV-Pit-01-65-68) also has a slightly lower concentration relative to the

samples above it, and less than the best fit solution from the model. This sample abuts the ice surface in the bottom of the pit, and thus contains the nuclide record in the lag deposit from the sublimated ice. The rate of change and the average sublimation rate resulting in the concentration of the last samples are poorly constrained, since it is not known at what time in the past the sublimation rate changed, or rather at what depth in the till the rate change is reflected in the nuclide concentrations.

It may only be assumed when or where the rate change is reflected within the samples from the pit profile. There are two basic scenarios that may be expected to be recorded in the till. 1) The sublimation rate increased sometime after 58 cm of till was deposited. This is when the third deepest sample (55-58 cm) was accreted into the base of the lag deposit. When using the absolute minimum exposure age of drift 2 (~1 Mya) from ^{21}Ne, the resulting till thickness (10 cm in the bottom of the pit) represents a maximum time boundary of approximately 0.15 Mya. If this sample was added to the bottom of the till due to a greater sublimation rate, then the period of time it represents must be shorter. Thus, sometime in the past 0.15 Mya, the sublimation rate increased substantially enough to affect the resulting concentration of nuclides in the second deepest sample (65-68 cm). The best sublimation rate to fit Scenario 1 and explain the low concentration found in the ice is a sublimation rate of 15 m/Mya for the past 0.15 Mya or after the till was ~58 cm thick. No sample was collected between the second and third deepest samples; thus, a gap from 58 to 65 cm exists where it is not possible to resolve a potential rate change.

Scenario 2) Instead of using the bottom of the third deepest sample (58 cm) as the rate change boundary, the top of the second deepest sample (65 cm) was selected to represent the beginning period in which the sublimation rate increased. This sample, as stated earlier must

contain the lag deposit most recently sublimated from the buried ice. The resulting maximum amount of time represented by the last 3 cm in the base of the pit is approximately equal to 45 Kya. This is a maximum time boundary because the accumulation rate used to calculate time as a function of the accumulation rate is based on the slower sublimation rate calculated from all till samples. It is likely that the amount of time required to accrete this till to the bottom of the pit is less than 45 Kya. This hints at a changing local climate system sometime less than 45 Kya ago. The best sublimation rate to fit Scenario 2 and explain the low nuclide concentration found in the ice is approximately 34 m/Mya for the past 45 Kya or after the till was 65 cm thick. This is approximately 23 m/Mya (0.023 m/Kya) greater than the averaged whole pit sublimation rate.

The results for increased sublimation rates in the past 150 Kya or past 45 Kya are rough approximations. Both rate increases are plausible and within acceptable ranges as measured in the MDV (Kowalewski et al., 2011; Kowalewski et al., 2006; Hagedorn et al., 2007), any number of solutions of calculated rate changes in the bottom of the pit could be solved for depending on the local variation of englacial debris concentration, time, and/or inheritance. Additionally, as stated above, the point of marked transition from a representative whole pit sublimation rate is obscured when choosing at what depth the concentration of nuclides reflects the changing conditions. By choosing a greater period of time (150 Kya) as the portion of time to reflect the sublimation rate change, the solution nears the average whole pit estimated sublimation rate. Conversely, solving for a smaller unit of time (45 Kya) results in a greater sublimation rate that has fewer whole pit averaging effects and may more closely represent the true rate change. Interval samples from deeper within the buried ice are required to adequately resolve this uncertainty.

With the above considerations, the best geologic and isotopic scenario to produce the till in the middle drift today requires approximately 20 m of ice with 10% debris concentration to sublimate over the past 2 million years with subsequent erosion of the lag deposit at less than 1 m/Mya.

Sublimation Rates

The reported rates and ages of similar regolith generally correlate well to other locations throughout the TAM. The McMurdo Dry Valleys are more coastal than locations in the CTM, yet have only minor local climate differences between each area with reported modeled sublimation rates of ice and erosion rates similar between the two regions (Comiso, 2000; Kwok and Comiso, 2002; Wang and Hou, 2009). Morgan et al., (2010) reports cosmogenic nuclide concentrations reflecting local ice sublimation rates in Beacon valley and Arena Valley at 0.7 - 12 m/Mya and erosion rates ranging between 0.4 – 1.2 m/Mya. These sublimation rates include a variation in englacial debris concentration of 12-45% which is greater than modeled in the above analysis and a contrast of lower englacial debris concentrations of 8.5% have been reported in Beacon Valley (Marchant et al., 2002). It should be noted that a greater percent by volume of englacial debris ice content will result in a lower modeled sublimation rate than if englacial debris concentration is 3% to 10% (as is the case in the model results reported in this paper and observed in Ong Valley). Further nuclide concentration rate calculations for ice sublimation in the MDV report rates of 4 to 23 m/Mya (Ng et al., 2005; Schäfer et al., 1999) and regolith erosion rates in Arena Valley from 0.2 to 2 m/Mya (Putkonen et al., 2008a).

Non-cosmogenic modeled sublimation rates also exist from Antarctica. Kowalewski et al., (2011) reports sublimation rates at Mullins Valley of 66 m/Mya from a vapor diffusion model and meteorological observations over a four year period and suggest that local

summertime sublimation rates could drop to zero with small changes to local temperatures and relative humidity. The potential for long term survival of buried ice under current climate conditions is reinforced from similar ice bodies in Beacon Valley. Relative humidity plays a dominant role of resulting sublimation rates. The diffusivity of water vapor decreases as till thickens atop a lag deposit, slowing sublimation rates of the underlying ice (Kowalewski et al., 2006) and Liu et al., (2014) reports sublimation rates of ground ice from 50-150 m/Mya.

In stark contrast to sublimation rates from a relatively stable ancient ice body are sublimation rates of active alpine and continental scale glaciers that do not have an insulating till layer and undergo comparatively massive annual ice loss in ablation zones. Blue ice and other areas with relatively low albedo experience higher sublimation than snow surfaces due to enhanced absorption of solar radiation, and high sublimation rates occur where advection of dry air is greatest (van den Broeke, 1997). Mean annual surface snow sublimation rates range between ~930 to 1860 m/Mya (Lenaerts et al., 2010). The edges of the Antarctic continent and boundary edges of the Ross ice shelf have the greatest fraction of annual precipitation removed by sublimation annually (van den Broeke, 1997). One example of this is at Taylor Glacier which flows from the East Antarctic Plateau and terminates at several lobes in the MDV. Taylor Glacier has a reported a sublimation rate of 40 cm/year or 4×10^5 m/Mya (Bliss et al., 2011).

Erosion Rates

Bedrock and regolith long term erosion rates reported from other investigators throughout the TAM are generally similar to those reported here. Typical long term erosion rates are most commonly reported from concentrations of cosmogenic nuclides (Portenga and Bierman, 2011). Bedrock, erratic, and ground surface rates generally come from a single sample where the ratio of the concentration of two nuclide pairs is compared to the concentration of a single nuclide as

shown in Figure 17 . Multiple surface samples are generally required to effectively represent a specific outcrop, locality, or region.

Reported erosion rates in the TAM are extremely low compared to temperate locations (Portenga and Bierman, 2011). For reference, the global averaged bedrock outcrop erosion rate is 12 m/Mya, and basin wide erosion rates are two orders of magnitude greater at 218 m/Mya (Portenga and Bierman, 2011). Bedrock and erratic erosion rates in the TAM are, on average, less than those of loose regolith and range from 0.17 - 0.20 m/Mya (Oberholzer et al., 2003), 0.26 - 1.02 m/Mya for low elevation slopes and 0.133 - 0.164 m/Mya for high elevation surfaces (Summerfield et al., 1999). Regolith erosion rates inferred from similar model methods as used in this paper from the McMurdo Dry Valleys range from 0.19 - 2.6 m/Mya for the past 4 Mya (Morgan et al., 2010b; Putkonen et al., 2008a). The rates reported here are not unusual but are important none the less due to the sparseness of records of such rates in Antarctica. In the case of the preservation of near surface ancient ice, accurate erosion rates are necessary to constrain the true age of the deposits and thus the ice below them.

CHAPTER VI

CONCLUSIONS

Cosmogenic nuclides ^{21}Ne, ^{26}Al, and ^{10}Be were measured from three glacial drifts in the floor of Ong Valley, Antarctica. These drifts were formed from the sublimation of massive debris-laden glacial ice from the Argosy Glacier as it advanced into the valley in the past. Massive ice is still present beneath the youngest drift, and the middle drift. No ice was found beneath the oldest drift, although the existence of patterned ground sand-wedge polygons suggests previous presence of either massive ice or ice-cemented soil. Concentrations of ^{26}Al and ^{10}Be were sufficient to constrain the exposure age of the youngest drift and mark the most recent stagnation and sublimation of the Argosy Glacier within the past 18.4 Kya. The youngest drift is too young to confidently resolve erosion and sublimation rates with ^{26}Al and ^{10}Be.

The inferred ages of the three drifts from concentrations of cosmogenic nuclides agree with the relative ages of the deposits. The cosmogenic nuclide system used for this work relies on three separate nuclides (^{26}Al, ^{10}Be, and ^{21}Ne). Each nuclide has a different production rate, a different radioactive decay rate (if at all), and multiple sites were sampled comparatively for nuclide concentrations. Given the multiple sample sites and variation amongst individual nuclides, all results are generally correlated with no major discrepancies. This alone should serve as a robust marker of the reliability and usability of the methods and results reported here.

The depositional ages of the three tills, reported here broadly conform to observations from other locations along the TAM. The youngest drift's apparent age agrees with other Holocene age deposits in the TAM ~7 to 17 Kya (Di Nicola et al., 2009; Todd et al., 2010; Ackert and Kurz, 2004) with the last glacial maximum at Reedy glacier dated at 14-17 Kya. In the Dry Valleys region a number of similar drifts fall generally within the same time frame as those in Ong Valley, including Taylor II-IV, and Alpine A-D (Marchant et al., 1993), along with Alpine I, Trilogy drift, Onyx drift, and Wright drift (Hall and Denton, 2005). The oldest tills conform to progressive thinning of the peripheral lobe of Ferrar Glacier over the last ~4 Mya (Staiger et al., 2006) although, in the Dry Valleys region there is a prominent glacial expansion at around 150-200 Kya which is not seen in CTM (Di Nicola et al., 2009).

Concentrations of ^{26}Al and ^{10}Be in depth profiles from the middle drift result in a regolith erosion rate of 0.89 m/Mya and ice sublimation rate of 22.7 m/Mya. ^{26}Al and ^{10}Be in the oldest drift results in a regolith erosion rate of 0.74 m/Mya and ice sublimation rate of 19.03 m/Mya. These are consistent with regolith erosion and ice sublimation rates reported in the McMurdo Dry Valleys, and support the notion of landscape stability in a polar arid desert (Marchant et al., 2002; Morgan et al., 2010b; Morgan et al., 2010a; Putkonen et al., 2008b; Sugden et al., 1999). The debris encased in ice below the middle drift has lower than expected nuclide concentrations suggesting a change in the sublimation rate within the recent past, potentially reflecting a local climate shift in the past 45 Kya. This is a particularly unusual scenario where the proposed sublimation rate may have increased though it was insulated by what was most likely the maximum thickness of the till above it. At current, there is no proposed mechanism other than enhanced warming and local climate variability within the past 40-150 Kya. This signature of the proposed increased sublimation rate at the bottom of the pit should be a point of future research

to quantify this mechanism of rate change and the relationship to local climate variation in the recent past.

The exposure age of the oldest drift is 1.20 – 1.79 +/- 0.05 Mya. The middle drift must have formed after the oldest drift and ^{21}Ne concentrations in this drift record a younger exposure age of 0.86 – 0.93 +/- 0.05 Mya. The variability in age is due to the uncertainty in the amount of inherited ^{21}Ne in the samples from previous exposure. The effect of erosion on the resulting apparent nuclide concentrations would increase the minimum age of these deposits by almost 2.4 Mya.

Buried ice found below the middle drift and its age is constrained by the age of the overlying till. Cosmogenic isotope depth profiles confirm the existence of ancient ice within 1 m of the surface and support a slow but recently accelerating rate of sublimation accompanied by regolith erosion on timescales of 10^6 years. Basic assumptions have been applied to derive the absolute youngest possible exposure age of the middle and oldest drifts with concentrations of cosmogenic nuclides. This suggest that the ice below the middle drift must be at least one million years old, which potentially represents the oldest archive of atmospheric conditions currently found on Earth.

In the context of Antarctic earth science, the observation and argument of preserved ice below an insulating till layer is not a new one, but the ages reported from work therein generally refers to the MDV where local climate and processes are slightly different than the interior of the continent. Many reliable ages of buried ice bodies have used a variety of isotopic and physical model based techniques to confirm ages and antiquity. Typically, ages of buried ice in the MDV are limited to roughly the past 100 Kya and the acceptance of ~8 Mya in Beacon Valley ice is still debated. The limited age of preserved ice bodies is generally due to mechanisms of ice

recharge and complex geologic settings in a coastal area where humidity and temperature are greater, liquid water is more prevalent (though limited) and buried ice is affected by active glacial processes from debris covered and debris-free glaciers.

Ong Valley is unique in this context in that there is no evidence of subsurface saturation of soils (which acts as an ice recharge mechanism) and the geologic setting is relatively simple with no active glaciers through the valley. These complications are seen at other locations in Antarctica that have sources of buried ice such as Beacon Valley and University Valley.

Annual climate records in Ong Valley are limited to field measurements from the 2011-12 field season, and there is not enough information to report from direct observation alone, that the climate in the valley is distinctly different than MDV, but the proximity to the South Pole and distance from the Ross Sea suggest that relative humidity on the time scale of millions of years should be less in the Central Transantarctic Mountains.

This research demonstrates that the age of the till overlying ice in Ong Valley is representative of the age of the buried ice and the surface process rates are similar to other regions in the MDV. This is done with cosmogenic nuclide profiles of bulk regolith samples at depth. The analysis of these nuclides is compared across three drifts in Ong Valley, and the reliability of concentrations vs. depth is confirmed with duplication of pit sampling sites within 10-20 meters of each other. In this context it is proposed that two relatively old deposits reflect Quaternary recessions and the youngest deposit marks the most recent period since the last glacial maximum.

The results herein fill a void in our scientific understanding of Central Transantarctic ice sheet fluctuations with absolute ages relating to the positions of the Argosy glacier and modeled results further constrain local rates of ice sublimation and regolith degradation in a single site of

the Central Transantarctic Mountains. The greater than million year old ice in the middle drift of Ong Valley should contain some of the oldest atmospheric records currently found on Earth. Concentrations of gasses trapped in the ice serve as an invaluable archive of the role of Antarctica for reconstructions of Earth's global climate cycles. Significant age control is required to appropriately apply this information to current records and further sampling of the ice itself along with a diversified geochemical analytical approach should resolve better age controls for application to global paleo-climate reconstructions.

Table 1. Depth, Density, Effective Shielding Mass and Isotope Data.

Sample ID	Depth in soil (cm)	Soil density (g cm^{-3})	Effective shielding mass (g cm^{-2})	^{21}Ne X 10^6 ± 1 standard deviation (atm g^{-1}_{quartz})	^{26}Al X 10^6 ± 1 standard deviation (atm g^{-1}_{quartz})	^{10}Be X 10^6 ± 1 standard deviation (atm g^{-1}_{quartz})
Youngest Drift		*1.64*				
10-OV-Pit-11-0-2a	0-2	1.6	1.65	31.37 ± 1.79	- -	- -
10-OV-Pit-11-0-2b	0-2	1.6	1.65	31.31 ± 2.58		
10-OV-Pit-11-15-18a	15-18	1.59	27.22	13.91 ± 1.65	- -	- -
10-OV-Pit-11-15-18b	15-18	1.59	27.22	11.78 ± 1.71		
10-OV-Pit-11-30-33a	30-33	1.69	51.97	19.67 ± 2.13	- -	- -
10-OV-Pit-11-30-33b	30-33	1.69	51.97	16.16 ± 2.52		
10-OV-Pit-11-43-46a	43-46	1.69	73.42	4.61 ± 1.25	- -	- -
10-OV-Pit-11-43-46b	43-46	1.69	73.42	9.03 ± 1.38		
10-OV-Pit-11-46-50*I*a	46-50	0.93	77.75	5.85 ± 2.42	- -	- -
10-OV-Pit-11-46-50*I*b	46-50	0.93	77.75	12.91 ± 2.11		
Youngest Drift		*1.65*				
10-OV-Pit-12-0-3a	0-3	1.62	2.42	7.00 ± 1.70	1.509 ± 0.21	0.276 ± 0.013
10-OV-Pit-12-0-3b	0-3	1.62	2.42	8.84 ± 1.01		
10-OV-Pit-12-17-21a	17-21	1.57	30.77	4.96 ± 1.21	0.945 ± 0.14	0.146 ± 0.006
10-OV-Pit-12-17-21b	17-21	1.57	30.77	4.56 ± 0.70		
10-OV-Pit-12-32-36a	32-36	1.77	55.07	5.62 ± 1.51	0.812 ± 0.21	0.111 ± 0.007
10-OV-Pit-12-32.36b	32-36	1.77	55.07	8.31 ± 0.97		
10-OV-Pit-12-45-48a	45-48	1.64	75.32	5.19 ± 1.38	0.335 ± 0.23	0.082 ± 0.007
10-OV-Pit-12-45-48b	45-48	1.64	75.32	7.41 ± 1.17		
10-OV-Pit-12-48-54*I*a	48-54	0.93	80.53	9.47 ± 1.91	0.508 ± 0.26	0.081 ± 0.006
10-OV-Pit-12-48-54*I*b	48-54	0.93	80.53	9.57 ± 1.36		

Table 1 cont.

Sample ID	Depth in soil (cm)	Soil density (g cm^{-3})	Effective shielding mass (g cm^{-2})	^{21}Ne X 10^6 ± 1 standard deviation (atm g^{-1}_{quartz})	^{26}Al X 10^6 ± 1 standard deviation (atm g^{-1}_{quartz})	^{10}Be X 10^6 ± 1 standard deviation (atm g^{-1}_{quartz})
Middle Drift		*1.73*				
10-OV-Pit-01-1-4a	1-4	1.9	4.32	192.07 ± 4.19	- -	17.80 ± 0.39
10-OV-Pit-01-1-4b	1-4	1.9	4.32	191.71 ± 4.62		
10-OV-Pit-01-13-16a	13-16	1.66	25.08	186.74 ± 4.20	- -	16.39 ± 0.21
10-OV-Pit-01-13-16b	13-16	1.66	25.08	181.48 ± 5.11		
10-OV-Pit-01-28-31.5a	28-31.5	1.69	51.46	170.14 ± 4.29	- -	14.60 ± 0.20
10-OV-Pit-01-28-31.5b	28-31.5	1.69	51.46	169.86 ± 4.05		
10-OV-Pit-01-38-41.5a	38-41.5	1.67	68.76	145.61 ± 3.17	- -	12.96 ± 0.19
10-OV-Pit-01-38-41.5b	38-41.5	1.67	68.76	143.66 ± 3.75		
10-OV-Pit-01-55-58a	55-58	1.80	97.74	128.09 ± 3.04	- -	11.05 ± 0.18
10-OV-Pit-01-55-58b	55-58	1.80	97.74	135.43 ± 3.81		
10-OV-Pit-01-65-68a	65-68	1.68	115.04	119.52 ± 3.29	- -	9.053 ± 0.20
10-OV-Pit-01-65-68b	65-68	1.68	115.04	123.64 ± 2.90		
10-OV-Pit-01-68-72*I*a	68-72	0.93	119.49	103.78 ± 2.89	- -	5.184 ± 0.05
10-OV-Pit-01-68-72*I*b	68-72	0.93	119.49	96.21 ± 2.90		
Middle Drift		*1.78*				
10-OV-Pit-02-1-4a	1-4	1.62	4.44	184.62 ± 3.72	- -	- -
10-OV-Pit-02-1-4b	1-4	1.62	4.44	195.41 ± 4.60		
10-OV-Pit-02-24-28a	24-28	1.68	46.27	169.94 ± 3.28	- -	- -
10-OV-Pit-02-24-28b	24-28	1.68	46.27	179.03 ± 3.83		
10-OV-Pit-02-48-53.5a	48-53.5	1.78	90.31	91.12 ± 2.11	- -	- -
10-OV-Pit-02-48-53.5b	48-53.5	1.78	90.31	105.39 ± 2.61		
10-OV-Pit-02-66-69a	66-69	1.83	120.14	74.72 ± 2.63	- -	- -
10-OV-Pit-02-66-69b	66-69	1.83	120.14	82.93 ± 2.68		
10-OV-Pit-02-74-80a	74-80	1.99	137.03	93.95 ± 3.17	- -	- -

Table 1 cont.

Sample ID	Depth in soil (cm)	Soil density (g cm^{-3})	Effective shielding mass (g cm^{-2})	^{21}Ne X 10^6 ± 1 standard deviation (atm g^{-1}_{quartz})	^{26}Al X 10^6 ± 1 standard deviation (atm g^{-1}_{quartz})	^{10}Be X 10^6 ± 1 standard deviation (atm g^{-1}_{quartz})
Middle Drift						
10-OV-Pit-02-74-80b	74-80	1.99	137.03	103.09 ± 3.56		
10-OV-Pit-02-80-83*I*a	80-83	0.93	143.79	81.25 ± 2.86	- -	- -
10-OV-Pit-02-80-83*I*b	80-83	0.93	143.79	88.95 ± 2.98		
Oldest Drift		*1.69*				
10-OV-Pit-03-0-3a	0-3	1.66	2.53	235.81 ± 5.24	87.53 ± 7.93	18.82 ± 0.35
10-OV-Pit-03-0-3b	0-3	1.66	2.53	239.05 ± 3.93		
10-OV-Pit-03-4-9a	4-9	1.57	10.97	236.50 ± 4.90	83.55 ± 11.1	21.14 ± 0.15
10-OV-Pit-03-4-9b	4-9	1.57	10.97	245.76 ± 3.82		
10-OV-Pit-03-27-31Aa	27-31	1.75	49.00	202.30 ± 4.63	- -	- -
10-OV-Pit-03-27-31Ab	27-31	1.75	49.00	200.38 ± 4.21		
10-OV-Pit-03-27-32Ba	27-32	1.71	49.84	218.03 ± 4.71	- -	- -
10-OV-Pit-03-27-32Bb	27-32	1.71	49.84	229.16 ± 4.08		
10-OV-Pit-03-41-44a	41-44	1.66	71.82	141.12 ± 3.40	66.52 ± 9.41	14.54 ± 0.12
10-OV-Pit-03-41-44b	41-44	1.66	71.82	146.82 ± 3.18		
10-OV-Pit-03-63-67a	63-67	1.76	109.84	116.82 ± 2.89	50.99 ± 3.12	10.71 ± 0.11
10-OV-Pit-03-63-67b	63-67	1.76	109.84	119.92 ± 2.73		
Oldest Drift		*1.68*				
10-OV-Pit-06-1-3a	1-3	1.73	3.36	215.45 ± 4.80	- -	- -
10-OV-Pit-06-1-3b	1-3	1.73	3.36	222.62 ± 4.51		
10-OV-Pit-06-3-5a	3-5	1.64	6.72	135.89 ± 3.64	- -	- -
10-OV-Pit-06-3-5b	3-5	1.64	6.72	139.26 ± 4.16		
10-OV-Pit-06-24-28a	24-28	1.65	43.67	83.79 ± 2.53	- -	- -
10-OV-Pit-06-24-28b	24-28	1.65	43.67	80.36 ± 3.53		
10-OV-Pit-06-42-48a	42-48	1.68	75.57	62.99 ± 1.96	- -	- -

Table 1 cont.

Sample ID	Depth in soil (cm)	Soil density (g cm^{-3})	Effective shielding mass (g cm^{-2})	^{21}Ne X 10^6 ± 1 standard deviation (atm g^{-1}_{quartz})	^{26}Al X 10^6 ± 1 standard deviation (atm g^{-1}_{quartz})	^{10}Be X 10^6 ± 1 standard deviation (atm g^{-1}_{quartz})
Oldest Drift						
10-OV-Pit-06-42-48b	42-48	1.68	75.57	62.94 ± 2.63		
10-OV-Pit-06-66-78a	66-78	1.68	120.85	42.53 ± 2.11	- -	- -
10-OV-Pit-06-66-78b	66-78	1.68	120.85	47.43 ± 2.49		

I = sample from within ice

Table 2. Nuclide Production Values at Each Sample Site.

Sample Site	Latitude (°S)	Longitude (°E)	Pressure (hpa)	Shielding correction	P_{10}(atm g^{-1} y^{-1})	P_{26}(atm g^{-1} y^{-1})	P_{21}(atm g^{-1} y^{-1})
Youngest Drift							
10-OV-Pit-11	83.23022	157.66171	811.9	0.992	21.92	147.89	89.43
10-OV-Pit-12	83.23020	157.66443	811.9	0.992	21.92	147.89	89.43
Middle Drift							
10-OV-Pit-01	83.25420	157.69177	790.6	0.990	25.64	173.00	104.61
10-OV-Pit-02	83.25420	157.69241	790.6	0.990	25.64	173.00	104.61
Oldest Drift							
10-OV-Pit-03	83.26945	157.62112	795.3	0.983	24.52	165.45	100.04
10-OV-Pit-06	83.26902	157.62193	797.5	0.982	24.52	162.80	98.45

Table 3. Cosmogenic ^{21}Ne Samples in Till Clast Separation Model Results.

ID	(cm)			Δ_s (cm)	$\Delta_{i,min}$ (cm)	$T_{A,max}$ (Mya)	S_{min} (m/mya)	C_{max} (%)	$\Delta_{I,min}{}^R$ (m)		$S_{min}{}^R$ (m/mya)	
Youngest Drift									*3%*	*10%*	*3%*	*10%*
10-OV-Pit-11-0-2	1.0	-	48.0	47.0	143.82	0.38	3.82	21.79	10.44	3.13	27.73	8.32
10-OV-Pit-11-15-18	16.5	-	48.0	31.5	13.42	0.17	0.71	-2123	7.00	2.10	40.78	12.23
10-OV-Pit-11-30-33	31.5	-	48.0	16.5	86.91	0.27	3.20	13.12	3.67	1.10	13.76	4.13
10-OV-Pit-11-43-46	44.5	-	48.0	3.5	-66.59	0.11	-8.40	-11.99	0.78	0.23	7.71	2.31
10-OV-Pit-11-46-50I	48.0	-	48.0	-	-	0.16	-	-	-	-	-	-
10-OV-Pit-12-0-3	1.5	-	51.0	49.5	-92.29	0.10	-10.03	-37.42	11.00	3.30	116.7	35.01
10-OV-Pit-12-17-21	19.0	-	51.0	32.0	154.95	0.07	-23.85	-13.80	7.11	2.13	109.2	32.77
10-OV-Pit-12-32-36	34.0	-	51.0	17.0	-76.13	0.11	-8.04	-18.24	3.78	1.13	36.83	11.05
10-OV-Pit-12-45-48	46.5	-	51.0	4.5	-77.02	0.11	-8.04	-4.58	1.00	0.30	9.77	2.93
10-OV-Pit-12-48-54I	51.0	-	51.0	-	-	0.17	-	-	-	-	-	-
Middle Drift												
10-OV-Pit-01-1-4	2.5	-	70.0	67.5	22.13	2.00	0.11	203.31	15.00	4.50	7.51	2.25
10-OV-Pit-01-13-16	14.5	-	70.0	55.5	30.60	2.10	0.15	121.66	12.33	3.70	5.87	1.76
10-OV-Pit-01-28-31.5	29.8	-	70.0	40.3	36.87	2.18	0.17	72.78	8.94	2.68	4.10	1.23
10-OV-Pit-01-38-41.5	39.8	-	70.0	30.3	22.75	2.01	0.11	88.86	6.72	2.02	3.35	1.01
10-OV-Pit-01-55-58	56.5	-	70.0	13.5	28.62	2.08	0.14	32.30	3.00	0.90	1.44	0.43

Table 3 cont.

ID	(cm)			Δ_s (cm)	$\Delta_{i,min}$ (cm)	$T_{A,max}$ (Mya)	S_{min} (m/mya)	C_{max} (%)	$\Delta_{I,min}^R$ (m)		S_{min}^R (m/mya)	
Middle Drift												
10-OV-Pit-01-65-68	66.5	-	70.0	3.5	28.07	2.07	0.14	8.40	0.78	0.23	0.38	0.11
10-OV-Pit-01-68-72I	70.0	-	70.0	-	-	1.75	-	-	-	-	-	-
10-OV-Pit-02-1-4	2.5	-	81.5	79.0	29.65	1.98	0.15	182.27	17.56	5.27	8.87	2.66
10-OV-Pit-02-24-28	26.0	-	81.5	55.5	46.44	2.19	0.21	80.38	12.33	3.70	5.64	1.69
10-OV-Pit-02-48-53.5	50.8	-	81.5	30.8	-17.03	1.50	-0.12	-244.40	6.83	2.05	4.58	1.37
10-OV-Pit-02-66-69	67.5	-	81.5	14.0	-31.45	1.37	-0.23	-32.13	3.11	0.93	2.27	0.68
10-OV-Pit-02-74-80	77.0	-	81.5	4.5	18.30	1.85	0.10	19.97	1.00	0.30	0.54	0.16
10-OV-Pit-02-80-83I	81.5	-	81.5	-	-	1.66	-	-	-	-	-	-
Oldest Drift												
10-OV-Pit-03-0-3	1.5	-	65.0	63.5	36.75	2.56	0.14	115.30	14.11	4.23	5.52	1.66
10-OV-Pit-03-4-9	6.5	-	65.0	58.5	45.54	2.70	0.17	86.06	13.00	3.90	4.82	1.45
10-OV-Pit-03-27-31A	29.0	-	65.0	36.0	43.60	2.66	0.16	55.07	8.00	2.40	3.00	0.90
10-OV-Pit-03-27-32B	29.5	-	65.0	35.5	61.65	2.97	0.21	38.57	7.89	2.37	2.66	0.80
10-OV-Pit-03-41-44	42.5	-	65.0	22.5	4.52	2.11	0.02	710.73	5.00	1.50	2.37	0.71
10-OV-Pit-03-63-67	65.0	-	65.0	-	-	2.05	-	-	-	-	-	-
10-OV-Pit-06-1-3	2.0	-	72.0	70.0	176.91	2.41	0.73	26.39	15.56	4.67	6.46	1.94
10-OV-Pit-06-3-5	4.0	-	72.0	68.0	101.89	1.54	0.66	44.51	15.11	4.53	9.84	2.95

Table 3 cont.

ID	(cm)			Δ_s (cm)	$\Delta_{i,min}$ (cm)	$T_{A,max}$ (Mya)	S_{min} (m/mya)	C_{max} (%)	$\Delta_{I,min}{}^R$ (m)		$S_{min}{}^R$ (m/mya)	
Oldest Drift												
10-OV-Pit-06-24-28	26.0	-	72.0	46.0	43.09	1.08	0.40	71.63	10.22	3.07	9.47	2.84
10-OV-Pit-06-42-48	45.0	-	72.0	27.0	22.55	0.95	0.24	79.84	6.00	1.80	6.29	1.89
10-OV-Pit-06-66-78	72.0	-	72.0	-	-	0.83	-	-	-	-	-	-

Table 4. Calculated ^{21}Ne Exposure Age Matrix of Top Most Sample with and without Minimum Inheritance and Erosion Rate Values from Modified Equations 10,11.

Age (Mya)				
	E=0	E=0	E=0.13	E=0.13
	Inh=0	Inh_1=9.4E6	Inh=0	Inh_1=9.4E6
Youngest Drift	Inh=0	Inh_2=9.5E6	Inh=0	Inh_2=9.5E6
10-OV-Pit-11	0.36	0.25	0.37	0.36
10-OV-Pit-12	0.08	n/a	0.08	n/a
	+/- 0.02	+/- 0.02	+/- 0.02	+/- 0.02
	E=0	E=0	E=0.92	E=0.92
	Inh=0	Inh_1=1E8	Inh=0	Inh_1=1E8
Middle Drift	Inh=0	Inh_2=1E8	Inh=0	Inh_2=1E8
10-OV-Pit-01	1.95	0.93	3.95	2.91
10-OV-Pit-02	1.87	0.86	3.79	2.75
	+/- 0.05	+/- 0.05	+/- 0.05	+/- 0.05
	E=0	E=0	E=0.79	E=0.79
	Inh=0	Inh_3=1.2E8	Inh=0	Inh_3=1.2E8
Oldest Drift	Inh=0	Inh_6=4.7E7	Inh=0	Inh_6=4.7E7
10-OV-Pit-03	2.44	1.20	5.08	3.73
10-OV-Pit-06	2.29	1.79	4.59	4.09
	+/- 0.05	+/- 0.05	+/- 0.05	+/- 0.05

E= Erosion rate (m/mya)

Inh_i= Inherited nuclides from lowest sample with reference to the pit of interest (atoms/gram quartz)
"n/a" calculated result is not a real number when Inh_i is greater than the surface concentration

Table 5. Calculated ^{26}Al, ^{10}Be Exposure Age Matrix of Top Most Sample with and without Modeled Inheritance and Erosion Rate Values from Equations 10,11.

Ages (Mya)	**^{10}Be**				**^{26}Al**			
Youngest Drift 10-OV-Pit-12	E=0 Inh=0 0.014 +/- 0.001	E=0 Inh=0 0.014 +/- 0.001	E=0.13 Inh=0 0.014 +/- 0.001	E=0.13 Inh=0 0.014 +/- 0.001	E=0 Inh=0 0.012 +/- 0.002	E=0 Inh=3.1e4 0.012 +/- 0.002	E=0.13 Inh=0 0.012 +/- 0.002	E=0.13 Inh=3.1e4 0.012 +/- 0.002
Middle Drift 10-OV-Pit-01	E=0 Inh=0 0.92 +/- 0.03	E=0 Inh=5.1e6 0.61 +/- 0.03	E=0.92 Inh=0 1.37 +/- 0.03	E=0.92 Inh=5.1e6 0.81 +/- 0.03	E=0 Inh=0 -	E=0 Inh=n/a -	E=0.92 Inh=0 -	E=0.92 Inh=n/a -
Oldest Drift 10-OV-Pit-03	E=0 Inh=0 1.02 +/- 0.03	E=0 Inh=8.26e6 0.50 +/- 0.03	E=0.79 Inh=0 1.47 +/- 0.03	E=0.79 Inh=8.26e6 0.62 +/- 0.03	E=0 Inh=0 0.78 +/- 0.13	E=0 Inh=3.1e7 0.44 +/- 0.13	E=0.79 Inh=0 1.05 +/- 0.13	E=0.79 Inh=3.1e7 0.52 +/- 0.13

E= Erosion rate (m/Mya)

Inh= Inherited nuclides from chi-squared models (atoms/gram quartz)

APPENDIX

Detailed cosmogenic nuclide laboratory methods used at the University or North Dakota. Methods and procedures are specific for the Harold Hamm School of Geology and Geological Engineering Cosmogenic Nuclide Laboratory but may be adapted to other laboratory settings.

UND COSMOGENIC ISOTOPE LAB PROCEDURES

Guidelines for turning quartz-bearing rocks into ^{26}Al and ^{10}Be sample targets for Accelerator mass Spectrometry (AMS)

Geochemistry, Leonard 203/205

Written/ modified by: Theodore Bibby 2009 to 2014

Harold Hamm School of Geology and Geological Engineering

University of North Dakota

Introduction:

Persons are not allowed to work in the lab until they have been properly trained. Training must include demonstration and understanding of applicable lab, safety and emergency procedures. Material Safety Data Sheets (MSDS) for all hazardous chemicals used in the lab, are available on site.

The laboratory shall be posted with appropriate signs and placards as determined by EH&S and the laboratory supervisor (Dr. Ronald Matheney). Provisions must be in place for preventing custodians, maintenance staff and unauthorized personnel from entering the area at times deemed to be potentially unsafe (i.e. when HF is in use). The building manager/ department chairman must also be made aware of the hazardous operations in Leonard 203/205, including emergency procedures if alarms are activated.

This procedure is modified (if not taken directly from) lab methods of John Stone, Greg Balco, Daniel Morgan, Kohl and Nishiizumi, Bodo Bookhagen, Arjun Heimsath and Paul Bierman. The overall goals of each part are described. Safety is extremely important in dealing with this procedure, especially because of the modest amounts of hydrofluoric acid (HF) that is used. All HF is stored in the acid cabinet below the HF fume hood. Typically there is no more than 1 liter of 50% HF available at any one time. Familiarize yourself with all hazards as listed on the available MSDS's.

Other Procedural References:

(Hunt et al., 2007; Hunt et al., 2008; Hunt et al., 2006; Ivy-Ochs et al., 2007; Balco and Stone, 2003; Ditchburn and Whitehead, 1994; Ditchburn et al., 2000; Kohl and Nishiizumi, 1992; Ochs and Ivy-Ochs, 1997) and, Prime lab procedures communicated in person.

Crushing

- Crushing and Size Separation (Leonard Room 3)
- This step reduces bulk field samples, rocks or mixed sand fractions into well-sorted sand fractions, which will be used in the chemistry phase of the sample preparation.
- The crushing, and sieving in this step is done in a designated "crushing room" located in the basement of Leonard Hall (Room 3). This work produces relatively high amounts of dust compared to typical lab work. At a minimum a dust mask (NIOSH approved N95) and safety glasses and hearing protection must be worn while working in the grinding room. Hair must be tied back, and no loose articles of clothing or jewelry may be worn. You must also review safe operating procedures for the equipment (see Ted Bibby) before beginning work. The jaw crusher has a large flywheel which may cause serious personal harm if any body part or clothing is caught in it.
- Start lab data sheet and lab notebook. Photograph and weigh the sample(s) as taken from the field.
- Weigh solid samples 5 times (hanging in air and hanging in water) and record in lab book. Weigh regolith samples 5 times using designated 100 ml beaker (Leonard Room 9).
- Clean the work area in room 3 with a vacuum, wire brush and compressed air. (It is particularly important to not introduce other rock sample contaminants to each crushed sample.
- Use the mechanical jaw crusher or a hammer to reduce pieces to gravel size. Thin metal plates near the jaw crusher may be used to adjust crushing gap.
- Use the wood 2x4 to cover the jaw crusher mouth to prevent samples from being ejected (which will happen).
- Crush sample into pre-cleaned plastic tray and place in appropriately labeled Zip-Lock bags.
- We currently do not have a radial crusher which is used reduced the gravel sized fractions to sand sized fractions. This particular part is done with Dr. Daniel Morgan at Vanderbilt University.

Mineral Separation

- In room 3, sieve the crushed rock or regolith sample for fraction sizes >500um, 250-500um, 125-250um and <125um. Stack sieves in sieve shaker and run 100 – 200 ml of material for 5 minutes. Sieve enough material until the 0.25 – 0.5 mm fraction size weighs >100 grams.
- Pour the fractions into appropriately labeled plastic Zip-Lock bags. Put away the > 0.5 mm, 125-250um and < 0.250 mm fractions into storage. Bring the 0.250 – 0.500 mm fraction to the chemistry lab 203 Leonard Hall. We can re-sieve for 500-1000um if there is not enough of the smaller fraction.
- Clean the work area and machinery using the shop vacuum and pressurized air hose. Brush sieves with wire brush and bang on the countertop to dislodge sand grains. Be conscientious not to cross contaminate samples.

Cleaning Grain Fractions

This step removes adhered dust and other contaminants from our desired grain sized fractions before density and magnetic separations. All of the acids used (HCl & HF) present skin

and inhalation exposure risks, HF exhibits unique systemic toxicity and first aid requirements. Review MSDS and fact sheets posted in 203/205 Leonard Hall. For all chemical work in the lab, follow standard lab safety guidelines for handling strong acid which include:

General Requirements for work in 203/205 Leonard Hall:

- Wear splash goggles that seal around the eyes for all acid handling.
- Use a chemically resistant apron and closed toe shoes (no flip flops or sandals) for handling acid.
- Use a face shield with splash goggles for operations that might involve splashing (ex. acid disposal)
- Work inside fume hoods (6 inches in from face with the sash as low as practical) when handling volatile, concentrated or heated mixtures in open containers.
- Thin single use nitrile gloves only provide barrier protection from chemicals and acids. They must be changed when they become contaminated followed by hand washing. Heavy duty acid resistant gloves (neoprene or butyl for HF) are required when acid exposure is likely and must be kept handy for cleanup of routine spills.
- Acid boiling, digestions and heating must take place in the HF hood of Leonard 203/205.
- Keep access to the eyewash/safety shower clear at all times.
- Always have water running in a sink if handling concentrated acids.

HF exposures must be treated as medical emergencies by dialing 911 from the phone in the lab (203 Leonard Hall). Flush the area with water until EMS arrives and provide calcium gluconate gel (stored by lab safety kit) to responders and/or Emergency Room personnel. Review HF poster in lab.

Small spills must be promptly cleaned/ absorbed with Chemwipes. Contaminated absorbents or materials must be bagged for disposal as hazardous waste through *the UND Environmental Health and Safety Office (*EHS*).* Large spills or those escaping fume hoods should be handled as emergencies and reported to EHS and or the fire department by dialing 911.

- Label all hazardous waste containers (corrosives with pH <2 or >12.5) with EHS labels, and fill in the date and chemical components on the label. Liquid wastes must be stored within secondary containment bins, this is an EPA requirement.
- Always label hood with "HF in Use" to protect other lab users.
- Empty acid containers must be triple rinsed with water and labels should be defaced/crossed out prior to disposal in the trash/recycling bin. Take care not to expose the custodians to harm.
- Training – In addition to EH&S required training, all laboratory workers must review this procedure and the MSDS and fact sheets posted in the lab.
- Remember: Hope for the best and plan for the worst… Always keep work area clean and keep Chemwipes handy for spills. *If you do have an exposure to strong acid, flush affected area with water immediately and remove contaminated clothing. Call 911 and flush until EMS arrives. If HF, apply Calcium Gluconate gel to exposed area with gloved hand.* An emergency shower is located in the lab.

Remove clays and other contaminants: Leonard 203/205

- Start by pouring ~400 grams of the appropriate grain fractions into a 1L glass beaker labeled with permanent marker around the top edge.

- Use the “Dirty Sink” at the end of the lab bench to wash grains. The water will become milky from all the silt.
- Wash grains by spraying and stirring the sample and pour the milky water down the drain, making sure not to pour the rest of your sample with it!
- Repeat until water is reasonably clear.
- Once water is reasonably clear, fill the beaker ¾ of the way with tap water and place the beaker in the large sonicator. Make sure the sonicator is filled to the “fill line” with tap water and let run for the maximum amount of time (99 minutes) and heated at 50 deg. C.
- After sonication, pour off the newly acquired sludge from the grains and re-wash the sample with tap water 3 times or more.
- Repeat the water sonication step if the sample appears to be very dirty or milky

Clean with 10% HCl: Leonard 203/205

Note: Concentrated HCl is available for making 10% HCl. Please be versed is proper lab safety, protocol and training prior to acid dilution. *Always add acid* to water, never the reversed!

- After a quick sonication, you now want to remove iron oxides and organics that are still adhered to the grains. Safety tips: point spout of beaker to the back of the hood. Wipe any spills off the hotplate. Lift the watch glass away from you. Be careful of condensation drips.
- In the same 1L. beaker used from sonication wearing personal safety equipment and inside the fume hood, slowly pour ~200 ml of 10% HCl into the glass beaker or enough to cover the sample by 1 cm. It may effervesce if there is significant calcium carbonate in the sample.
- Cover the beaker with a large watch glass (with 10% HCl written on it with permanent marker).
- Place covered beaker on the large pancake griddle inside the fume hood.
- Turn the pancake griddle temperature up to 275 and allow the sample to boil for ~10 minutes. (HCl boils at 130 deg. F, but the griddle has uneven heating). Keep an eye on the beaker as it will jump around as it boils. Luckily the pancake griddle has a raised lip that keeps your sample from jumping off of it.
- After 10 or so minutes have passed, the HCl will most likely be yellow. Let it cool. Use tongs to remove from griddle if necessary. Do not place directly on the fume hood base (it's plastic), use something to insulate the hot beaker from the surface or simply keep it on the griddle to cool.
- Once cooled, pour the 10% HCl solution into the waste bucket located inside the wooden fume hood. The bucket is filled with limestone and will react with the dilute acid. Do not breathe the vapors and pay very close attention that the bucket does not bubble over, it is a very messy situation if it does.
- In the "Dirty Sink" Rinse/ wash sample with tap water 3 times and pour rinse water down drain with running water.
- Repeat with the 10% HCl boil until solution is generally clear or colorless.
- Bag dried sample or keep in glass beaker for mineral separation.

Magnetic Separation: Leonard 212

- Basic:
- Use a strong magnet, and pour the sample past the magnet with a sheet of paper or plastic between the two to remove any strongly magnetic grains
- Advanced:
- This procedure takes the cleaned mineral grains and separates quartz or other target minerals based on their magnetic susceptibilities using the Frantz Magnetic separator located in the Sedimentology lab room 206. Using the Frantz separator is fairly straightforward. You are essentially ramping up the voltage till you have separated quartz and feldspars from the more magnetic minerals. The main item to note here, is to clean the Frantz thoroughly after each separation to avoid sample contamination. Also, keep your wrist watch and other electronics away.
- After ensuring it is clean, turn on the Frantz using the furthest switch on the lower right side.
- Adjust the amperage to 0.25 amps using the black knob on the side and fill the aluminum cup ¾ of the way with your sample.
- Turn on the vibrating switch at the front of the machine.
- Repeat 4 more times, using the quartz rich fragment and increasing amps to 0.50, 0.75, 1.0 and >1.0 after each run.
- The flow should be something like 3g/min, which is fairly quick. Increasing the forward tilt of the machine can also speed up sample flow.
- Place separated fractions into labeled Zip-Lock bags

Heavy Liquid Separation: Leonard 203

- Before you start, if you haven't used the Frantz yet, use a strong magnet to remove any magnetic fractions from each sample.
- (This procedure could be reworked using the PRIME procedure of bringing our LST to 2.67 first using the hydrometer, then diluting to 15 drops with Di to drop the quartz)
- If your sample does not look like "salt" but instead contains small pink and blue hues, you need to clean it up a bit using heavy liquid separation. The whole premise is based on density. Quartz will float on a "heavy liquid" of a density > 2.65. Other denser rocks will sink, hence heavy liquid separation. We can also separate samples that are lighter than quartz, namely feldspars. We use LST for this procedure (lithium heteropolytungstates) from Central Chemical Consulting.

Items required:

- Clean paper towel
- Clean stop cocks
- 1L. Separatory funnel
- 3 small beakers
- Large mouth funnel
- Teflon stir rod
- Vacuum flask
- LST
- DI water in wash bottle
- Scale
- Chemwipes
- Permanent marker
- Optional scoop
- ~40^{+}g. of sample material

- The LST area is most likely ready to go, but if it is not… set up 2 rings stands with open rings and CAREFULLY place a separatory funnel in the open ring. Be careful with them because they are fragile. Make sure the stopcock is in the closed position. You don't want the heavy liquid to flow right thru. It's quite expensive and we can recycle it.
- Place a fresh/ clean paper towel next to the separatory funnel and place 3 small beakers on it, all labeled with the sample # and "heavy", "quartz", and "feldspar" respectively. You can use the "feldspar" beaker to hold your Teflon stir rod after it's been in LST. Make sure to weigh the glass beaker used for quartz when it is clean and empty and record the weight in your lab book.
- Carefully pour some of the LST heavy liquid into the separatory funnels to the base of the white square printed on it. This is about 250ml.
- Set up the vacuum flasks (the ones with the side-arms), Buchner funnel and filter paper. You'll need 1 flask and 1 Buchner funnel for each separatory funnel. Place the Buchner funnels into the flask with a neoprene adapter in between. They should fit snuggly. Place a coffee filter (drawer below the LST area) in the Buchner funnel, and lightly wet it with DI water so it gets an OK seal.
- Using a large mouthed cone funnel, take one sample and pour it into the sep funnel. Be very careful of scattering grains. We want a clean lab bench and do not want to risk contamination of any other samples. Notice that some grains start to sink and most of it floats. That will change shortly.
- Use a Teflon stir rod and stir up the contents. Use one stir rod for each sample; you don't want to contaminate anything. You can place the wet and contaminated stir rod in the feldspar beaker.
- Add a little DI water to get more "heavies" to settle (too much will cause the quartz to sink). Once the heavies have settled from the quartz and lighter minerals, rock the stopcock back and forth to empty the heavies into the Buchner funnel. Use the vacuum pump to help the LST through the filter paper. Using DI water, wash the "heavy" grains 3 times. Use the vacuum pump to help the water through the filter paper.
- Remove the filter paper, and with DI water, gently wet the grains off the filter paper and into their respective beaker.
- Discard the used filter paper and place a new coffee filter in the Buchner funnel to catch remaining quartz and feldspars.
- Now it's time to try and separate the quartz from the feldspars. Gently add, little by little, more DI water to the LST in the separatory funnel. Stir often. Eventually you'll notice the quartz settling to the bottom. You may have to be patient and wait for the feldspars to float as the quartz sinks.
- Once you are satisfied that your quartz is as separated as it will get, rock the stopcock back and forth and allow the quartz layer go through into the filter papered funnel. Don't fill the funnel all the way up, you can filter in increments. Use the vacuum hose attached to the side arm to help draw the heavy liquid through.
- Wash your separated quartz three times and use the vacuum to draw the rinse water through the filter paper. Make sure not to over fill the vacuum flask! Remove the filter paper and wash the quartz grains into their respective beaker. Place on a hot plate to dry.

Re-weigh the quartz beaker with dried sample and record it in your lab book. If your quartz dries and is clumpy, there's probably some LST residue in it. Rinse it again, 2 or 3 times and pour off the waste.

- You can reuse the quartz filter paper, to filter out the remaining feldspars. Wash 3 times and rinse into the feldspar beaker, place on a hot plate to dry just as before.
- Try your best to recapture all residual LST.
- Pour all waste LST/water into the large cone flask. Once the flask is 3/4 full, inside the fume hood and on a hot plate, turn on the heat to 20 (~150 deg. C) and the rpm to 20 and boil off the water. You can use the hotplate thermometer if you wish. Test the LST density with the pink quartz in the small glass beaker, on the lab bench. When it floats, the LST is back to normal density.
- Rinse the glassware with DW water. Take apart the stopcock of the separatory funnel and make sure there are no grains in there. Rinse the funnels and the Teflon stir rod. It's not necessary to rinse the vacuum flasks if you are going to use them again. If that was the last sample, rinse the flasks as well.
- Once your samples are dry, weigh them and record the mass. You can place all the separated fractions into plastic bags and/or go ahead and pour the quartz fraction in to a clean and labeled 1 L. HDPE narrow mouth Nalgene bottle for HF etching.
- It takes a few hours to reconstitute a full liter of LST, be prepared to wait!

~My LST Heavy Liquid has turned dark blue/grey/black. What causes this, is the LST Heavy Liquid damaged, and how can I get the LST Heavy Liquid back to the original state?~

- The blue coloration is a well-known chemical reaction which polytungstates can undergo when chemically reduced. The reduced compounds are sometimes called the 'heteropoly blues'. This can occur when a reducing agent comes in contact with the heavy liquid. At high temperatures, such as might occur if the heavy liquid crystallized on a hotplate, even dust/dirt can sometimes act as a reducing agent. You can also get this color if the LST Heavy Liquid is contaminated by contact with iron.
- There are two ways to get rid of the dark color. The easiest way when dealing with small quantities is to add a few drops of 30% hydrogen peroxide solution H_2O_2) to re-oxidise the LST Heavy Liquid. You don't need to overdo the addition of hydrogen peroxide. Typically you need add no more than 1 mL of 30% (H_2O_2) for every 200 mL of affected LST Heavy Liquid, but it will depend on how much reduction there is. You can then heat the discolored LST Heavy Liquid and hydrogen peroxide at about 80^{o}C to make the reaction go faster (it will fizz a little!), or if you prefer just wait overnight for the blue to disappear.

Quartz cleaning by HF etching

BEFORE PROCEEDING — WARNING: Contact with hydrofluoric acid is extremely dangerous. Burns from small amounts of concentrated HF (48-50%) can be lethal. Read the safety literature in the "HF Lab Book". Wear heavy nitrile gloves, apron, sleeve guards and face shield throughout the following procedure. Wear sturdy clothes and shoes when working with HF and around the HF process bath. Know where the calcium gluconate is kept and how to use it for any contact with HF. Know where the eyewash stand and emergency shower is located. Wipe up any drops (even suspect droplets) with Chemwipes and soak under running water for several minutes before discarding. Never dispose of HF-contaminated material in the trash. Neutralize waste solutions in the acid waste container.

- Judge the amount of sample, aiming to finish up with 20-40 g of quartz after the full clean-up procedure. If you've done a density separation, use the entire "quartz" fraction. This procedure will remove composite grains and most minerals other than quartz likely to remain in the 2.63 g/cc < r < 2.67 g/cc density fraction.
- Label a clean 1 liter high density polyethylene (HDPE) bottle twice with the sample name or number.
- Transfer the sample to the bottle using a clean plastic funnel. Slurry the last grains through with water from a DI wash bottle.
- Fill the bottle to ~ 1" below the neck with distilled water.
- Rinse the plastic funnel thoroughly before using it for the next sample.

HF addition - First treatment

- In the fume hood, use the "reagent beaker" with red tape to measure 40 ml of concentrated (48-50%) HF. The bottom of the red tape marks 40ml.
- Recap the parent HF bottle before pouring measured HF into you sample bottle
- Pour 40ml of concentrated HF into your sample bottle. The final solution strength will be ~2% HF or ~1.15 M HF/liter.
- Gently squeeze each bottle before capping. This gives the contents room to expand when the bottle heats up. Also, loss of vacuum will alert you to the possibility that the bottle has leaked or the sample is over-reacting.
- Check that the bottle is tightly sealed and holding its slight vacuum. In the fume hood, gently invert it 3-4 times to mix the contents.
- Mark the bottle to indicate how many times the sample has been processed.
- Place it in the sonic bath and process at 69°C for 99 minutes (these are the maximum temperature and time for the Branson ultrasonic baths).
- Repeat the processing for 2-3 days. Turn the heat down to 50°C and top up the bath at the end of each day. (Reset the sonic bath for a final 99 minute run at the end of each day). The sonic action compacts the grains together and, especially in the initial stages of the reaction, can produce very firm aggregates of clay and fluorides on the floor of the bottle. Re-suspend the sample to break up these aggregates by inverting the bottle several times, each time you re-start the bath.
- Clean the "reagent beaker" by filling it with water inside the fume hood. Pour the rise water down the drain funnel in the fume hood while water is running. Rinse and repeat 3 times inside the hood, then rinse with DW water, then rinse with DI water, cover with parafilm and store in the reagent ware lab drawer.

HF addition - Second treatment

- After the first 3-day process, change the HF as follows:
- Cool and dry the bottle. Uncap it in the wood fume hood and discard the contents in the acid waste bucket.
- Rinse the remaining grains thoroughly with 3 changes of distilled water (DW), pouring off the rinse water while any clay or fine, milky fluoride precipitate is still suspended, but after "fine sand"-sized grains have settled.
- Don't worry about losing some of the very fine grains, unless the sample is unusually small.
- Top up the bottle with distilled water (DW) to ~ 1" below the neck.
- Add 40 ml of HF and repeat the ultrasonic processing for a second 2-3 day period.

Sample Recovery

- After the second 3-day treatment, inspect the sample for purity. Pure quartz samples have a uniform appearance and do not cake on the floor of the bottle. Impure samples usually appear speckled and may contain a cloudy fluoride precipitate.
- If the quartz appears pure, recover the sample:
- Cool and dry the bottle. Uncap it in the fume hood and discard the contents in the acid waste bucket.
- Rinse with at least 3 changes of DI water, as above. Try to rinse away any trace of milky fluoride. The rinse water must be clear (and absolutely free of residual HF) before transferring the sample to a glass beaker.
- Label a small 500ml glass beaker.
- Now swirl the sample in the Nalgene bottle in a little DW water and tip it into the beaker. It may take 2-3 rinses to transfer all the grains.
- Rinse/ final wash the grains from the 1L. Nalgene into the "clean quartz" beakers. I found it best to fill the Nalgene with ~100ml of distilled water, shake and swirl it around to capture all the grains and then invert it, so all the quartz settles into the cap. Then, over the "clean quartz" beaker, slowly un-screw the cap from the Nalgene, letting the water trickle out of the Nalgene and into the beaker and holding carefully onto the cap. Most of your clean quartz will be caught in the cap. Use a DW squirt bottle to wash the grains from the cap, into the beaker. Pour off excess water and repeat this process 3X.
- Finish by rinsing clean quartz sample 3X in DI water.
- Place beaker/ clean quartz in oven to dry.
- Rinse 6-8 times with DW water. Be sure to mix and re-suspend all the grains during rinsing. Any fluoride or acid left among the sample grains will cause them to cake up when dried.
- Dry the sample the oven or on hot plate.
- You can use the microscope to visually inspect the cleanliness of the grains. Ca-feldspars look sort of like white laundry detergent crumbles.
- Cool the sample and transfer it to a labeled Zip-Lock bag. Label this fraction "final quartz" to indicate that it has been purified in HF.
- Place the sample in the holding bin labeled "Al check" to await for Al analysis.

Al test for quartz purity

Check the Al content of the quartz separate before dissolving it for ^{26}Al analysis. It is important to obtain the lowest possible Al concentration. High Al levels decrease the $^{26}Al/^{27}Al$ ratio and limit the number of ^{26}Al ions that can be counted, compromising the counting statistics of the measurement. Careful quartz clean-up usually results in Al concentrations of 10–100 ppm. Higher levels commonly (though not always) indicate the presence of impurities such as feldspar, muscovite or insoluble fluorides from the HF treatment.

Note : A 99.5% pure quartz separate containing ~0.5% feldspar still has an Al concentration of ~1000 ppm. ACS grade acids are OK to use in this part (don't need trace metal grade). Our samples will be processed in batches of 6 using the EARL's photospectrometer. No Blanks are needed yet, as this is just a threshold check for the samples.

Weights needed:

- Weight of empty vial, weight of quartz grains added, weight of vials with quartz grains, weight of final solution.
- You'll also need 2 plastic beakers, 2 disposable pipettes, and an empty plastic bag for lids.

Aluminum Check preparation:

- Select a batch of Aluminum-check vials, one for each sample you wish to check for quartz purity. Make sure the lids match the bottoms (they're labeled ab-1, ab-2…). If space is available, run a blank. A blank is not entirely necessary for this run. We will re-measure aluminum concentrations with FAAS later on in the Al-Be cathode procedure.
- Weigh each vial and record its weight along with the vial ID and corresponding sample # on the batch worksheet.
- Remove the static buildup around the lip of the vial with the ionizer. This encourages our sand grains to not stick to the edges.
- With a clean metal scoopula, transfer ~~~0.1 g~~ ~ 0.6 g of quartz sample into the Teflon vial. Do this using the table top ionizer and transferring directly into tarred vials, or with weighing paper. Record the weight of sample added. Screw on lid and transfer to hood.
- Note: weighing of quartz grains with weighing paper should be done with the analytical scale, but weighing of the digestion vessel (if using the heavy white vials) must be done with the 200 g top loading scale. Our digestion vessels are too robust (too heavy) to use on the delicate analytical scale. If you're using the translucent 22 ml savillex vials you can use the analytical scale.
- Place the aluminum-check vials uncapped on a hotplate in the HF hood. Lids can be put on a paper towel in front of the hotplate.
- Add 1 ml of full strength nitric acid. This should also help collect the grains in the bottom of the vial.
- Don the HF safety gear and get 1 clean plastic beaker with water and the small 50 ml reagent Teflon beaker for HF, there may also be a 50 ml test tube already prepared with HF. (see picture below).

- Carefully pour 3-4 mL of full-strength HF into the 50 ml reagent beaker for each aluminum-check you're completing (8 checks = 24 to 32 mL).
- Add 3-4 mL of this HF to each sample vial using a disposable pipette. Make sure the pipette does not contact any sample grains so you can reuse it. When finished with the pipette place it in the beaker of water.
- Carefully cap each vessel tightly, and remove any unnecessary items from the fume hood.
- Turn the hotplate to 250 and allow the samples to digest for ~1hr. Lower the sash and put a "Danger HF" sign on it. You will see the acid possibly bubbling and if there is not a good seal on the vails/lids you may see acid vapor forcing its way out. DO NOT put your hands in the hood at this point.
- After 1 hour unplug the hotplate and letting everything cool for at least 45 minutes
- Once cool, remove the lids and place them facing upwards on the hot plate, being very conscientious about droplets stuck to the lids.
- Add 1-2 ml of 8% sulfuric acid to each vial and turn the hotplate to 200.
- Turn the hotplate to ~200 degrees F and dry the vials down to a droplet of sulfuric acid. This may take a few hours, possibly overnight.
- Once a small droplet has condensed in the bottom of the vials, unplug the hotplate and cool the samples.
- Add 5 mL of 1% nitric acid to each vial for FAAS. (8-10 ml if diluting for ICP).

- If prepping for FAAS, add 0.2 ml of 5% potassium ionization buffer to each sample (200 ul) additionally.
- Cap the vials, weigh and record the solution weights of each vial.
- Using a disposable pipette, transfer the liquid from the vials to a tarred and labeled test tube. Record the weight of the liquid added.
- Vortex before measuring via FAAS in EARL (third floor)
- Note: Previously we left the vials open and kept the temperature low to prevent all the HF from evaporating before complete digestion takes place. Other's procedures only digest 0.1gram of material and stepwise heat the vial from 200 F (1 hour) then 275 F overnight. This temperature ramp is too quick if we want to limit the amount of HF required to digest our 0.6 grams of grains.
- Process samples in house or mail samples to MVTL Laboratories for Al, Ti and Fe determination. Include return address, elements to be processed via ICP and expected concentrations of 10-100ppm

Performing Al Checks in EARL using FAAS:

- General upkeep and notes about our FAAS:
- Our machine by Thermo was made ~2001-2003
- Always ensure there is DI water in flexible corrugated black hose U-trap. (Pull burner head off when cool and pour DI into spray chamber until you see water run out drain tube. Replace head)
- Ensure drain tube is always above the water level in the drainage bucket and that the drain bucket is plastic. Never glass.
- Burner head is typically at 0 deg. position, can be turned if concentrations are very high.
- 5 Things that affect/optimize the absorbance signal the most: burner head height (y), fuel flow, head angle, head depth (z), Teflon spray dispersion bulb distance (you can turn the little metal circle on the outside of the spray chamber to adjust it, best spray is usually when it is generally closer to the input jet than further away, this adjustment usually gets you the biggest "bang for the buck"
- If there is a plug in the uptake line, you can try cleaning the nebulizer head in 2% nitric
- Beryllium Standards for FAAS: 0.5, 1, 2, 5 ppm in 1% nitric
- Aluminum Standards for FAAS: 5, 10, 15, 20, 50 ppm in 1% nitric
- Other specifications based on Thermo cookbook: To run Aluminum you will need to add a 0.2% K m/V ionization buffer to all solutions (standards and samples). EARL at present has a 5% K solution available for just that purpose. Since we dilute our samples to 5 ml for Al checks, that means we need to add 0.2 ml of 5%K to our 1% nitric solution to bring the final test tube volume to 5 ml. (this was probably done in the previous step). Same goes for standards. Add 0.32 ml of 5% K ionization buffer to standard labeled test tubes, then fill test tube to 8 ml mark with the desired standard.
- Other note: Ionization buffers are sold specifically for this purpose and it is best to buy one. You could buy a Potassium standard for ICP of FAAS, but they are usually sold as either 10,000 or 1,000 mg/l bottles in 500 ml volumes. This equals ~0.1 % and 0.01% K solutions respectively (not really a good way to go).
- Prepare a Blank by adding 0.32 ml 5% K to labeled test tube and fill to 8 ml mark with 1% nitric

Using the Flame Atomic Absorption Spectrometer:

- In Leonard Hall, room 203/205, pour at least 5 ml of prepared standards into labeled test tubes. Do not cross contaminate. (Ensure you add an ionization buffer if measuring Aluminum)
- In EARL, turn on FAAS exhaust vent (head level switch between sink and refrigerator)
- Have a large beaker (~500 ml) of DI water available. Dip/wash sampling tube between every measurement to prevent cross talk.
- Turn on acetylene gas, nitrous oxide gas (40 psi), air gas/ compressor,
- Turn on the FAAS using the switch on the back right of the FAAS (behind the furnace side).
- Turn on required lamps for analysis using the lamp button.
- Open the Solaaris program, and load Al or Be method. Under the "Flame" tab, choose Acetylene-Air.
- Ensure the intake tube is in a beaker of DI water
- After optics have been set, light flame by holding in the white button. You may need to blow on the burner head to push the gas to ignite from the sparker. Once lit, allow flame to warm up for 10 minutes.
- Click "Set Optics"
- After burner head has warmed up, open the methods tab again, and change the "Flame" drop-down menu to Nitrous Oxide.
- When done, click "Set Flame". The FAAS will automatically change the gas to N2O. This flame is much more dynamic, violent, bigger... and brighter. Do not stare at it for very long unless using eye protection or viewing shield.
- Allow flame/burner head to stabilize for 5-10 minutes while sucking up DI water.
- Again, click "Set Optics"
- Under methods--> Calibration, make sure all your standards are listed, and all your sample ID information is entered as well.
- When ready you can begin your analysis.
- If you have very trace amounts to detect you may consider using the Graphite Furnace Atomic Absorbtion Spectrometer (GFAAS). Below are methods for preparing standards for GFAAS.
- We will be using the Graphite Furnace Atomic Absorbtion Spectrometer (GFAAS) for determining Al and Fe concentrations in our samples (Be will be determined in the second ICP run later on). The detection limit for this machine is in the parts per billion range (ppb) and much care is required to prevent background contamination and accurate results of samples.
- Ideal concentrations for accurate resolution on GFAAS is as follows:
- Al: 12-60ppb
- Be: 0.2-2ppb
- Fe: 0.2-20ppm
- From the 10 ml solution you previously prepared for the Al check we will make a 5ml solution with a concentration of ~40 ppb (this is the middle of our desired range for Al). Use the repeat pipette and double check via scale to ensure it delivers exactly 1 ml of solution every time.

- To dilute our samples, we are assuming that they are clean quartz and that the estimated amount of Al in clean quartz grains is something like 0.02mg Al per g quartz. This is a ballpark number calculated from previous samples.
- Just to show the math:
- 10 ml solution (nitric and digested grains) at 0.02 mg Al/g quartz X 0.1g quartz (the amount in solution) = .002mg Al in the actual solution.
- 0.002 mg Al / 10 ml (volume solution) = 0.0002 mg/ml Al or 0.2 ppm or 200 ppb (this is our initial concentration)
- So Back to our Dilution:
- In a clean labeled centrifuge tube, pipette 1ml or the original digested solution using a clean pipette tip.
- The pipette in exactly 4 ml of DI water. Vortex the sample. You should now have 5 ml at some concentration range around 40 ppb.
- Your samples are now ready for their Al check via GFAAS. Take them up to the EARL lab on the third floor.

Using the GFAAS

- We use Thermo SoLAAR AA Spectrometer with FS95 auto sampler. We use the 394.4 nm wavelength for Al determinations. Bandpass 0.2nm, lamp current 4uk, argon 0.2 L/min, working volume 20ul, peak area, D2 background correction. Al is a difficult metal to detect and commonly has high background absorbance issues. We have tried other wavelengths(309.3 nm) but our system has had the best success with 394.4 nm.
- Temperature program from Ling et al 2003 (in chinese, translated by Xiaodong Hou in EARL Lab GGE): Trace aluminum the matrix modifier graphite furnace atomic absorptiometry, Occupation and Health 2003, Volume 19, Issue 11, pages 51-52

1. Dry 80 deg C 15 sec, 10 deg C/sec
2. 120 deg C, 25 sec, 5 deg C/sec
3. Ash 500 deg C, 5 sec, 100 deg C/sec
4. 2500 deg C, 3 sec, Fast
5. 2700 deg C, 3 sec, Fast

- Calibration curve (0.0, 5.0, 10.0, 20.0, 30.0, 40.0, 50.0 ug/L)
- Before loading samples follow the startup procedure below to allow the lamp(s) warm up for at least 10 minutes.
- Turn on ventilation system
- Turn on carrier gas (must be argon NOT nitrogen), output pressure should be around 15psi
- Turn on chiller by pressing the power button. The temperature ranges/alarms should already be set with a low around 15 C and a high around 25 C. Our chiller is a bit finicky and will not maintain a constant temperature. When the alarm goes off (either high or low) you will need to quickly plug or unplug the designated cable from the circuit board to force the machine to start cooling down or heating up. It's a bit of a pain and must not be left un attended.
- Turn on AAS system and the furnace (2 large power buttons)
- Open the SoLAAR program

- Turn on lamps desired for analysis (in our case this is the Al lamp and possibly the Fe lamp)
- Allow the lamp(s) to warm up for at least 10 minutes
- At this time you can now start loading the auto sample with your samples and reagents
- Our GFAAS method calibrates, then runs a sample blank, then runs our samples 3X's.
- Using the small sample vessels pour ~0.5 ml of your samples into a labeled cup and place in order in the auto-sampler. Ensure the Sample Blank is appropriately labeled in the program to account for background concentrations.
- The reagents are as follows:
- R1: Master standard (prepared by us) at 100ppb
- R2: Matrix modifier of $Mg(NO_3)_2$ at 0.1% (the method should be auto diluting our 10g/L modifier to 0.1%
- R3: Diluent (1% Nitric trace metal grade)
- R4: Blank (1% Nitric trace metal grade)
- In the GFAAS method, turn ON the background correction using D2 quadraline (but make sure this is off when adjusting the optics)
- Turn the "Intelligent Dilution" check box ON. This will automatically re-run samples that are outside our calibration curve by diluting them and re-measuring the sample, then automatically calculating what the true higher concentration should be.
- Use peak height instead of peak area, although peak area is recommended by Rodger Starek, a senior training instructor for GFAAS
- GFASS is no longer used for Al because dilutions to ppb require too much time/care and too great a dilution (1:10,000).
- We use the HACH spectrophotometer in EARL. It can resolve concentrations up to 0.80 mg/L. We want our final quartz samples to fall within this range, and if the quartz cleanup is bad, then the sample can range higher than 0.8 and we'll know, most likely that it needs to be cleaned some more.
- Batch 2 was run with ~0.05g quartz digested as outlined above, and then diluted in 1% nitric acid. Based on expected concentrations from previous samples, we will shoot for a final Al concentration of 0.4mg/L in our sample so as to be resolved by EARL's spectrophotometer. The HACH kit requires a total of 50ml of sample (divided into 2 vials of 25ml each).

What you'll need:

- Repeat pipettor (and tips)
- 50ml volumetric flask
- 50ml conical flask for each sample
- Rubber stoppers for each conical flask
- Small beaker with DI (to clean and re-use pipette tips)
- Large beaker (for DI rinse waste)
- Trays and paper towels

- Use the 50ml volumetric flask (property of EARL) to properly dilute samples.
- Use a clean repeat pipette tip to transfer 4ml of your nitric/digested sample into the volumetric flask. The repeat pipettor should currently be calibrated to deliver precisely 1 ml of fluid. (check with an analytical scale if unsure)
- Fill the 50ml flask the remaining way with DI water, carefully adding the last few drops with a DI squirt bottle.
- Invert the flask a few times to mix the solution, then pour the sample into a clean and properly labeled 50ml conical flask and plug it with a stopper.
- Rinse the 50ml volumetric flask 3 times with DI, and discard waste into DI waste beaker.
- Repeat previous steps for all samples. Make sure you rinse all re-useable equipment with DI water thoroughly and dry in the oven.
- Take your 50ml conical flask of diluted samples and an additional 50ml beaker for each sample to EARL. You will end up pouring 25ml of your diluted sample into the empty 50ml beaker as part of the HACH kit procedures as listed below.

Calculate Al ppm in quartz:

Al $ppDI_{tz}$ = (Al ppm_{AS}) * (Solution Volume) / (Aliquot Wt.)

example: measured ppm Al of aliquot solution from ICP= 3.12 mg/L
aliquot solution volume = 4.2 mL
quartz grains aliquot = 0.18 g
Al $ppDI_{tz}$ = (3.12 mg/L) * (4.2 mL) / (0.18 g)
Al $ppDI_{tz}$ = 72.8 ppm Al

- Proceed to the sample dissolution if the 1 gram aliquot shows a favorable ^{Total}Al concentration. We're looking for something generally below 150 ppm.
- Note: Bodo pg 45/84 has another example of sample math to be used.

Cleaning of Al check vials & ICP tubes:

- Rinse with high purity DI water 3 times. Use a ChemWipe and a squirt of alcohol to clean the inside. Place the lids and vials in separate 5% nitric baths and heat on a hotplate overnight (275 degrees: don't boil). Pour cooled acid wash back into the 5% nitric acid carboy. Remove Teflonware rinse with DI water 3 times and dry in oven (dial set to 2). Match lids and store vials in AL check drawer. Nitric acid is reused and stored in the carboy labeled 5% Nitric for glass and Teflon washing.

Aliquot for ^{21}Neon

- Set aside 2 grams of clean quartz in an appropriately labeled vial for ^{21}Ne analysis at Berkeley Geochronology Center, via Greg Balco. Mail when appropriate

Pre-Column Chemistry

Sample weighing:

- Estimate the amount of sample required for the measurement. 1 mg of Al (which will make ~2 mg of Al_2O_3) is required for the AMS measurement, though larger amounts, up to a few mg, are easier to handle. For a sample containing 50 ppm Al, you will need to dissolve at least 20 g of quartz to obtain sufficient Al. Note that: (i) For "hot" samples with high levels of ^{26}Al, the necessary amount of Al can be obtained by substituting carrier for quartz. Adding Al carrier lowers the ^{26}Al/^{27}Al ratio, and should be avoided for young, low-altitude, or heavily shielded samples. (ii) Conversely, the ^{10}Be/^{9}Be ratio increases with sample size, so using larger amounts of quartz will improve ^{10}Be results from low-level samples. (iii) Note, however, that processing samples larger than 30 - 35 g is tedious, expensive, and best avoided. (iv) If you know the approximate age of your samples, you can predict ^{26}Al/^{27}Al and ^{10}Be/^{9}Be ratios for different quartz and carrier weights below. Aim for ^{10}Be/^{9}Be ratios > 10^{-13}, and ^{26}Al/^{27}Al ratios > 10^{-12}.
- Note: conversation with Perry Spector (UW), old bedrock samples weighed out ~5g, and post lgm (LGM=~25kya) was 10-20g

Weighing:

- For a batch of standard samples (weights ~10-20 g):
- Make a copy of the “CC-XXXX-Worksheet” file via the UNDCosmo shared drive on the Lab PC and rename it appropriately. Enter user information and the sample IDs. Under the “Carrier Required” tab, add information from Al checks, and use the sheet to estimate how much sample to digest and/or how much carrier to add to achieve at least 1.5 mg of AL (typically 10-20 g clean quartz may be required) Print the batch worksheet and add it to the lab logbook.
- For each sample:
- Weigh a clean 100 mL or 250 mL FEP Teflon (bottle + solid lid) using the deionizer and analytical scale. Record the bottle number and its tare weight on your worksheet.
- Transfer the sample to the bottle with a clean, non-reagent spatula, with weighing paper or by cutting a corner off the Zip-Lock bag (if planning on using the entire sample). If possible, move the sample grains all the way into the bottle and tip them directly onto the base. Try to minimize static build-up on the bottle rim and prevent grains from jumping to the neck, especially onto the outer screw thread. Don't pour directly from a plastic sample bag. Inevitably, some grains will charge and cling to the bottle walls. No problem, as long as they are inside. Cap the bottle.
- Re-weigh the bottle and record the combined weight. Subtract the tare to determine the sample weight (automatically calculated once entered into spreadsheet).
- Using 1% HNO_3 from the wash bottle, wash sample grains down and away from the bottle mouth. Add just enough acid to fully wet the sample grains in the bottom of the bottle. Take care not to touch the spout on the sample container.

Carrier addition:

Be & Al Carrier precautions: Causes burns. Causes severe skin burns and eye damage. Causes serious eye damage. Do not breathe dust/fume/gas/mist/vapors/spray. IF ON SKIN (or hair): Remove/Take off immediately all contaminated clothing. Rinse skin with water/shower. IF IN EYES: Rinse cautiously with water for several minutes. Remove contact lenses, if present and easy to do. Continue rinsing. IF SWALLOWED: Rinse mouth. Do NOT induce vomiting. Store locked up. Dispose of contents/container in accordance with local/regional/national/international regulations. In case of contact with eyes, rinse immediately with plenty of water and seek medical advice. Wear suitable protective clothing, gloves and eye/face protection. In case of accident or if you feel unwell, seek medical advice immediately (show the label where possible). Chemical formulas: $Be_4O(C_2H_3O_2)_6$ in 5% HNO_3, $Al(NO_3)_3$ in 5% HNO_3

- Take the current Be carrier bottle and invert it a few times to homogenize the solution. Be sure drops of condensation around the lid are taken up and mixed in. Weigh it. Record the initial weight (and confirm that it equals the final weight from the previous use).
- In the fume hood, places a beaker lined with a labeled plastic Zip-Lock bag to use for anything contaminated with Beryllium (i.e. pipette tips or ChemWipes for spills)
- Load the Fischer (100-1000ul) pipette with a clean tip and adjust it to deliver ~250ug of Be carrier to each sample bottle. Note, carrier concentration is 1000ppm (1ug/ml = 1ppm), so this will usually require ~ 0.25 ml. You can verify using lab scale.
- Note: If carrier concentration is anything else then we'll have to calculate how much to add to get 250ug. This function most likely happens on the lab spreadsheet. If this is the case, don't make the mistake of adding 0.25 mL in this case, which will usually contain a lot less Be than you need. Be sure the tip does not touch anything while handling the pipette. If it does, discard it and take another. DON'T RISK CONTAMINATING THE CARRIER.
- In the fume hood, open the 100ml or 250ml sample bottle.
- Tare the balance to zero. Remove the carrier bottle from scale, open it and pipette carrier solution into the sample bottle. Eject the carrier smoothly, being sure not to leave a drop in the tip. Don't allow the tip to touch the sample bottle. Recap the carrier bottle and re-weigh it. The balance will read the weight removed. Record the weight. Calculate the Be added. Work deftly, but not hurriedly, while the carrier bottle is open. Everyone's work depends on the integrity of the carrier. Don't leave it open to evaporate any longer than necessary. Don't contaminate it with lab-ware that has come into contact with sample material. Mix it well before use. Store it properly after use in a Zip-Lock bag in the lab refrigerator.
- At the end of each session, record the final weight of the carrier bottle for cross-comparison next time it is used. Check the cap is screwed on firmly.
- Repeat with Al carrier for samples that contain less than 1.5 mg Al. Use enough carrier to bring the total Al in each bottle up to 1.5 mg. Usually you will need to adjust the pipette for each sample.
- Enter all of the data (bottle numbers, tare, sample and carrier weights) in the log-book and spreadsheet via google docs.

Dissolution:

- This is done in the fume hood, wearing all required HF safety clothing.
- Fill a beaker or wash bucket with cold tap water and place in hood.
- For each sample, uncap the sample bottle and store the solid cap in a clean plastic bag.
- Using a plastic measuring cylinder or the 50 ml Teflon beaker marked for clean acids, add 5 mL of AR grade HF for each gram of quartz The computer spreadsheet lists the amount of HF required for each sample.
- Re-cap the bottle tightly with a vented (drilled) cap. Match each bottle with its corresponding drilled cap. Check that the bottle is not sealed, so that fumes can escape and pressure won't build up (squeeze it gently). Beware if the sample is fine-grained - the reaction may proceed fast and the bottle may get quite hot. If it does, be prepared to cool it down by sitting it in a large beaker of cold water. Don't swirl the bottle at first - the initial reaction doesn't need any encouragement. Never shake the bottle.
- Once the reaction has subsided (usually a few hours), the bottles can be placed around the edges of a hotplate set to its lowest setting "warm" and gradually increase the temperature to 200 °F over the next 24 hours. Samples should dissolve in ~24-48 hrs. The bottles can be gently swirled occasionally to mix up the dense layer of H_2SiF_6 which forms over the quartz grains. Wear full protective gear when handling the bottles, and beware of droplets of acid condensed on the lid, which can be pushed through the vent hole if you squeeze the bottle while handling it. Handle the bottles only from the cap.
- Note: If a salt precipitates on the side of the bottle, try to dissolve it by tilting the bottle on its side and letting the salt sit in the HF solution.

Splitting for Al determination (2^{nd} ICP):

- Once the samples have dissolved completely...
- Turn off the hotplate and allow the bottles to cool to room temperature. This may take a few hours.
- Tilt the bottles to recover droplets of condensation from the walls and lid, being very careful to retrieve all drops around the lid but not allowing any drops to squeeze through the vent hole.
- Exchange the drilled lid on each bottle for its corresponding solid lid and tighten firmly. Check that the bottle is safely sealed (squeeze it gently). Keep a plastic beaker of DI water on hand, and submerge the lids with holes as you remove them then set aside to be cleaned.
- Homogenize the solutions by swirling and inverting the bottles, mixing dense H_2SiF_6 up off the floor of the bottles and droplets condensed on the walls. Splits of these solutions will be used to measure total Al concentrations, so they must be well mixed.
- Weigh the bottles on the balance (up to 110 g). Record the weights. Subtract the bottle tare weights to calculate solution weights. These weights will be used to calculate ppm Al for the 2nd ICP measurement.
- For each sample, take 2 round-bottomed, 22 mL, Savillex screw-top vials (marked with "AB" numbers). Record the sample ID, the bottle it was dissolved in and the corresponding two vial numbers. Tare each vial with its lid and record the weights.
- Return the samples to the fume hood, along with the Savillex vials for aliquoting.

- Open the 22ml Savillex vials. Open the sample bottle. Use a disposable pipette to transfer an amount equal to ~4% of the solution into each Savillex vial (usually 4 mL, [this is also calculated on the lab spreadsheet]). Add 3 ml to one and 4 ml to the other jar.
- Re-cap the Savillex vials, tightening the lids gently. Re-cap the sample bottle. Rinse out the pipette in a plastic beaker of water. Leave it in the beaker of water and get a clean pipette for the next sample. Take care with this step - the solutions you are handling are strong HF/H_2SiF_6. It is important to aliquot at least 4 ml to ensure we measure above minimum Al detection allowable by the FAAS.
- Carefully transfer the remaining solution to a large vessel (180 ml Savillex or FEP beaker) for drying. Rinse the original sample bottle with a few mL of DI water and add the rinse to the dry-down vessel. Take care not to let any sample solution splash back onto the DI wash bottle. Record each vessel number against its corresponding sample on the tracking sheet.
- Place each vessel on the hotplate as you go, and then set the hotplate to 275 °F.
- Continue to chloride conversion.

Preparing the splits for 2nd ICP analysis

- Weigh the Savillex vial splits and record the weights. Calculate the weight of each split. Take care not to splash droplets of the split solutions onto the lids of their vials when moving them in and out of the balance.
- After weighing each split sample, the aliquots can be dried down to remove HF in preparation for ICP analysis.
- Uncap each vial on the hotplate and add 1 mL 8% H_2SO_4 to each and set the hotplate to ~275 °F. HF / SiF_4 will evaporate overnight, leaving a small pool of H_2SO_4 in the base of each vial.
- Cool the Savillex vials. Ensure that the vials have sufficiently cooled
- Using a disposable pipette, add 2 mL DI water to each 22ml Savillex vial. Turn the hotplate to 275 °F and evaporate again. This removes the last of the HF/ H_2SiF_6 from the beakers. Residual H_2SiF_6 will lead to low Be and Al totals in the ICP analysis and must be thoroughly removed.
- Cool the vials again. Add 8 mL 1% HNO_3 to each using a graduated cylinder or repeat pipettor. Again, 8 ml is our lucky number to ensure or concentrations are within range of the FAAS for Al and Be.
- Add 0.32ml 5% Potassium ionization buffer in 1% nitric to each vial. Re-cap them and let them stand (preferably overnight) to equilibrate.
- The final acid strength (1% HNO_3 / 1% H_2SO_4) is matched to the FAAS standards to avoid matrix effects.
- Weigh the vials immediately prior to FAAS analysis. Record the solution and vial weights in the database.
- Analyze for Al and Be by FAAS in EARL lab on the third floor of Leonard Hall. It's usually efficient to have at least 5-10 samples to analyze.
- Upload the results to the database, which will report back the total amount of Al and Be in each sample. You should expect to get duplicate analyses of the two splits (i.e. 4 analyses) for each element which is consistent to within ~1-2%. Total Be results should closely match the amount of carrier added (98% - 102%). Total Al results less carrier,

divided by sample weight, should match the value of your initial Al check within ~ 10-20%.

- Note: Multiply the results by the weight of 1% HNO_3, divide by the aliquot weight and multiply by the total weight of the sample solution to determine the total amount of Al in each sample (dividing by the weight of quartz dissolved gives the Al concentration of the quartz. You should expect to get a value within 10% of your initial test result).

Dry-down and chloride conversion:

- Place the vessels on the hotplate and evaporate at ~275 °F. Small vessels that contain < 100 mL will dry down overnight. Larger volumes may take 48 hours or more. When dry, there will be a thin covering of fluoride salts on the floor of the vessel, usually white but occasionally ranging in color to orange-brown or grey-green. You may also notice tiny insoluble grains (ilmenite, zircon, etc.). Take care when handling the vessels, the dry fluorides are often flaky and prone to static build-up. Wear nitrile gloves; samples have jumped their Teflon beakers when handled with vinyl gloves, which are more prone to static charging.
- To convert the residue to chloride form:
- Carefully take the vessels off the hotplate and cool them. Using a disposable pipette, add ~2 mL of 6M HCl (the amount is not critical; samples with a very large fluoride cake may require a little more). The cake should re-dissolve almost entirely; any residual solid will usually go back into solution after a little warming on the hotplate.
- Return the vessels to the hotplate and dry again. Cool and repeat the HCl addition.
- Heat the samples again, taking them down to a few drops. Try to avoid complete dry-down, making it easier to get the samples back into solution for anion exchange. Don't worry if the samples dry completely, however.
- Cool and repeat the HCl addition. The samples dissolved in 2-3 mL of 6M HCl are ready for anion exchange. They can be capped or covered with parafilm at this stage. Al and Be are stable in this form almost indefinitely; if the solutions are left for a long time however, they may precipitate TiO_2. This can be removed by centrifuging, see below.

The succession of evaporations and re-dissolutions should have eliminated fluoride (as HF) almost entirely. Fe, Ti, Al, Be, alkalis and other metals present should now be in the form of chloride salts, ready for clean-up by anion exchange. The remaining solution is usually deep yellow-green, due to $FeCl_3$. By the end of this procedure, however, some samples may have thrown a fine, powdery white precipitate that will not re-dissolve. This is TiO_2. Little or no Al or Be co-precipitates with the Ti, which can be removed by centrifuging before anion exchange. If this is necessary, use a clean disposable pipette to transfer the HCl solution to a clean (1% nitric soaked overnight) 15 mL centrifuge tube. Add 1 mL 6M HCl to the beaker as rinse (use a separate, clean pipette). Swirl to pick up any last droplets of sample solution. Transfer the rinse to the centrifuge tube using the sample pipette. Spin at 2500 RPM for 3 minutes to sink the precipitate. The supernatant is ready for anion exchange.

Column Chemistry

This chemistry isolates the Be atoms and Al atoms from the other elements in the quartz. The Be and Al fractions are packed in "targets" which are analyzed by AMS (Finkel and Suter, 1993). The accelerator doesn't consume the full sample, rather a portion is used and a ratio of cosmogenic to non-cosmogenic isotopes is given. Therefore, the total concentration of target

element in the sample must be measured during the sample preparation in order to calculate the concentration of cosmogenic isotopes: $^{Total}Al(^{26}Al/^{27}Al) = {}^{26}Al$ mg/g quartz

- Note: We are using Dowex 1 and Dowex 50 for our ion exchange resins.

Fe, Ti clean-up (anion exchange columns):1-2 hrs

- Load a column rack with a set of 10 mL Pierce centrifuge anion exchange columns. Place a plastic tray under the columns.
- Squirt a few ml of isopropanol into each column to wet the frit. Let the columns drain.
- For each column either:
- Run a few mL of DI water smoothly down the wall of the column, and before it drains, pipette in a loose slurry (2 mL) of anion exchange resin (AG-1 X8 200-400#) from the stock soaking in dilute HCl (use a disposable pipette). The aim is to block the column and back up a head of dilute acid so that the resin bed can be built up from suspension. This avoids trapping air bubbles in the resin bed. Now continue slurrying resin into the columns to build the resin beds up to 2 mL (more, e.g. 3 mL will only be required for very Fe-rich samples). If too much resin has been added, a long disposable pipette can be used to adjust the volume.

Or:

- Run a dense slurry of resin slowly down the wall of the column, gradually building up the resin bed so as to avoid trapping bubbles. In either case, if bubbles get trapped in the bed, the resin must be re-suspended and re-packed (bubbles will channel flow through the column and ruin the separation). Once the resin has settled and compacted to the correct height, allow the supernatant to drain through.
- Wash the resin bed with 5 times its volume of 0.3 M HCl (usually 10 mL). Allow the wash solution to drain through the resin bed.
- Condition the resin with 3 bed volumes of 6M HCl (usually 6 mL). This should be dispensed carefully, without disturbing the top of the resin bed. Don't squirt it forcefully from the wash bottle. The resin will darken and shrink as it adjusts to the higher acid strength.
- After the columns have been conditioned, remove the plastic tray and load the samples as follows:
- First, check the samples for any signs of smoky white insoluble material (this will be TiO2). If any is present, the solutions will have to be centrifuged before running them through the columns. To do this, transfer solutions to disposable 15 mL centrifuge tubes using a clean disposable pipette for each sample. Add a further 1 mL of 6M HCl to the sample containers as a rinse (use a separate, clean pipette). Pick the rinse solutions up and add them to their appropriate centrifuge tubes. Cap the tubes and spin at 2500 RPM for 3 minutes. The pipette used for each sample should be reserved (in the original sample container) for loading.
- Take a batch of 22 mL savillex vials (high-level samples) and record their numbers on the tracking sheet against the corresponding sample IDs. Place each vial under its appropriate column.
- Using a separate disposable pipette for each sample (those centrifuged will already have one), load the sample solutions onto the columns. Drip the solution down the column wall, reaching as far as possible into the column with the pipette. Do NOT pour the

sample into the column. Try not to disrupt the top surface of the resin. Transfer the entire sample. Return each pipette to its sample container.

- Add 1 mL of 6 M HCl to each sample container and swirl to pick up any remaining droplets of the original sample solution. (This step is not necessary for samples that were centrifuged, and have already been washed out of their containers).
- Sometimes there is some grey crud in the bottom of the test tubes. Try to avoid sucking this crud up so as not to run the crud through the columns and resins.
- Allow the loading solutions to drain fully into the resin. Now add the 1 mL wash solutions, taking care to load each into the correct column. Allow to drain into the resin.
- Elute Al + Be from the columns by adding 3 times the bed volume of 6M HCl (usually 6 mL). The first 2 mL should be added carefully from a disposable pipette so as not to disrupt the top of the resin bed. Keep the pipette tips clear of the column walls to prevent cross-contamination. In strong HCl, Fe(III) forms a range of anionic Cl^- complexes $FeCl_4^-$, $FeCl_5^{2-}$ and $FeCl_6^{3-}$, which bind tightly to the anion exchange resin. These will form a yellow-brown band at the top of the resin column. Al and Be do not form strong Cl^- complexes and elute from the column with the HCl. Some Ti in the form of $Ti^{(IV)}Cl_6^{2-}$ will bind, but most will drain through as cationic or neutral species, ending up with the Al + Be.
- Remove the vials containing the Al + Be and set them aside in the hood.
- Replace the plastic tray beneath the columns. Wash Fe (+ Ti) off the resin with a few bed volumes of dilute 1% HCl (HCl will drip yellow-green due to Fe after a few mL). Discard the resin in the trash or down the sink using an air hose.
- Wash the columns by running 2 volumes of DI through them then soaking in 5% Nitric overnight, rinse 3X with DI, and dry. Store in plastic bag labeled "Clean Columns". Rinse out and discard the sample and dispensing pipettes. Rinse out, scour and wash the sample transfer containers.

Conversion to sulfate: 1 day if diligent

- Once Al + Be have been eluted, add 1 mL of 0.5 M H_2SO_4 to each Savillex vial and dry on the hotplate at ~275 °F. Residues will range from a syrupy drop of H_2SO_4 (small samples, blanks) to a cake of sulfate salts (larger samples). The residue from this step may turn an alarming dark-brown to black color. This is due to charry reaction products formed from organics which bleed from the anion resin. Don't worry, this will disappear gradually over the next couple of steps.
- Cool the vials and add 2 drops of ~2% H_2O_2. Then add 2 mL of DI water. The cakes will begin to dissolve, taking on an amber/gold color ($TiO[H_2O_2])^{2+}$) if Ti is present. Reheat the vials. The black charry material will disperse and disappear after a while. Dry the samples down again.
- Cool, repeat the H_2O_2 /H_20 addition, and dry the samples a second time. At the end of this procedure, the samples should end up either as compact white cakes or small, syrupy droplets of involatile H_2SO_4. If they remain charry or discolored, repeat the peroxide/water addition and dry them down a third time.
- Take the samples up in 3-4 mL of DI water, containing a trace of 2% H_2O_2 (add 1 drop of 2% H_2O_2). Warm them a little if necessary to get them back in solution. Don't risk evaporating too much water - keeping the acid strength low for column loading gives a

sharper elution and cleaner Ti-Be cut. The samples are now in ~0.2 M H_2SO_4, ready for loading on the cation exchange columns. They can be stored indefinitely in this form.

Al-Be separation (cation exchange columns): only do 5 samples at a time

- Load a column rack with small 5 mL Pierce centrifuge columns. Place a plastic tray under the columns. Add a few drops of isopropanol to each to wet the frit. Allow it to drain through.
- Using a disposable pipette, add 2 mL of DOWEX-50 X8 200-400# cation exchange resin to each column. Load the columns either by suspending the resin in DI water, or by running a slurry down the column wall (see the notes above on loading anion columns). Take care not to trap air bubbles against the column wall. Allow any DI water or dilute acid from the loading procedure to drain.
- Strip the resin by filling each column headspace with 3 M HCl (i.e. ~9 mL, equal to 4-5 bed volumes). Allow it to drain completely.
- Make up a beaker of ~ 0.2 M H_2SO_4 containing a trace of 2% H_2O_2. This is 4 parts 0.5 M H_2SO_4 to 6 parts DI water. Accurate volumes are not important; the aim is to match roughly the acid strength of the sample solution. Mix well. Condition the columns by filling the headspace with this solution. Allow it to drain through.
- Discard any leftover conditioning acid in the waste container, and replace it with 0.5 M H2SO4 containing a dash of 2% H_2O_2. Check the volume of acid in the tray below the columns and, if necessary, discard it in the acid-waste container.
- *Tip: Before adding sample, add ~2 mL DI water to each sample and mix with the sample pipette. Cations adsorb to the resin better in weaker acids. When strong acids are added, the overwhelming number of protons bond to the adsorption sites, eluting the cations.*
- Load each sample onto its column using a clean disposable pipette. Ti will form a narrow brown band at the top of each resin bed. While the sample solutions run in, add 1 mL of 0.5 M H_2SO_4/trace of 2% H_2O_2 to each beaker as a rinse. Swirl the beakers to pick up any droplets of the original solution left over from the first load. Add the rinse solutions to their respective columns.
- Once the rinse solutions have drained into the columns, gradually add 10 mL (5 bed volumes) of 0.5 M H_2SO_4/trace H_2O_2 to each. Allow it to run to waste into the plastic tray. Watch the orange-brown Ti bands move down the resin and elute from the columns. For Ti-rich samples, it may be necessary to add a further 1-2 mL of 0.5 M H_2SO_4 to completely remove Ti. 12 mL of the sulfuric acid eluent can be run through the columns without risk of losing Be.
- Remove the plastic tray and replace it with medium, 22 mL savillex vials. Record the number of each vial against its corresponding sample on the tracking sheet.
- Elute Be from the columns with 10 mL (5 bed volumes) of 1.2 M HCl. Add the first few mL carefully to each column, to avoid disturbing the resin. You will need to add this in two stages. No need to allow the first to drain completely before adding the second.
- After the Be fraction has drained through, remove the vials and add 5 drops of 8 M HNO3 to each vial. Dry them on the hotplate at ~275 °F. Dry-down will take ~8 hours.
- Place a second medium 22 mL round base savillex vial under each column. Record the number of each vial against its corresponding sample.
- Elute Al from the columns with 6 mL (~3 bed volumes) of 3M HCl.

- After the Al fraction has drained through, remove the savillex vials, add 0.5 mL (~10-15 drops) of 8M HNO_3 to each and dry on the hotplate at ~275 °F. Dry-down will take ~4 - 6 hours.
- Note: Wash the columns by running 2 volumes of DI through them then soaking in 5% Nitric overnight. Do not heat. Heating will change the color of our columns. Rinse 3X with DI, and dry. Store in plastic bag labeled "Clean Columns". Rinse out and discard the sample and dispensing pipettes. Rinse out, scour and wash the sample transfer containers.

Al & Be recovery and storage

- For each sample, label TWO clean (1% nitric soaked overnight) 15 mL screw cap centrifuge tubes - one for the Be fraction, one for the Al fraction. Use the original sample ID, not a beaker or bottle number. Be sure to identify the "Be" and "Al" fractions separately. (It is useful to note the date to key the sample back to your workbook).
- Once the Be and Al fractions have dried, cool and remove them from the hotplate. The Be fractions should have contracted to a tiny, clear droplet of concentrated H_2SO_4. Occasionally they will form a small white cake. This may indicate residual Ti, an impurity, or, most commonly, Al cross-over. The Al fractions will vary in size from sample to sample, but they should dry to a small, dense white cake in the base of each vial.
- Pipette 2 mL of 1% HNO_3 into each vial. If pure, both Al and Be fractions will dissolve freely. Al samples can be slow to dissolve, so, if necessary, warm the vials for a few minutes on the edge of the hotplate to ensure complete dissolution.
- Carefully tip each solution into its correct centrifuge tube. Al fractions generally come away freely from the round bottom vials. Don't worry if a last drop clings to the floor of the Be beakers.
- Pipette a second 2 mL aliquot of 1% HNO_3 into each vial as a rinse. Warm it, run it around the beaker and add it to the correct centrifuge tube.
- Cap the centrifuge tubes and store for hydroxide precipitation.

Al, Be recovery and cathode preparation for AMS analysis

Precipitate, ignite, and pack Al and Be samples shortly before the accelerator run in which they will be measured. Superstition among practitioners hold that Al-and Be-oxides slowly rehydrate if left for weeks or months after baking and will produce lower beam currents. Cathodes packed in advance of a run (or cathodes which have to be stored after a cancelled run) should be stored in the desiccator cabinet in the Al-Be lab. Refresh the desiccant pack (3 hours in the oven at 80 °C) before doing so.

Precipitate Beryllium Hydroxide

- Using 15% ammonia hydroxide add ~5 drops to a sample, close the centrifuge tube, and use the vortex mixer to homogenize. Continue to add ~5 drops at a time and spin with the vortex mixer until a white, almost translucent precipitate forms. It is very difficult to see.
- Precipitated Be(OH)2 is easiest to see against a bright light immediately after removing the tube from the mixer. The pH should be ~7 for $Be(OH)_2$ to precipitate. If pH paper is used to test the pH, dispose of the strips in beryllium waste. Once the first sample has precipitated you will have an idea of how many drops are required to precipitate the sample (often ~20-25, but possibly more).

- Note: BeOH takes more base to neutralize because of the Sulfuric acid left over after elution (UVM).
- Maybe think about using methyl red? Indicates when pH =6.2

The reaction in this step is:

$$2Cl^- + Be^{2+} + 2(NH_4OH) \longleftrightarrow Be(OH)_2 + 2(NH_4Cl)$$

- After all samples have precipitated $Be(OH)_2$, wait 30 minutes for the precipitate to flocculate (this helps the solution separate better in the centrifuge). If possible, maybe allow the Beryllium to flocculate overnight. Centrifuge at 3,500 RPM for 10 minutes.
- Pour the supernatant into the sink, retaining the white hydroxide gel. Fill to 5 mL with DI water, spin again on the vortex mixer, wait for the precipitate to flocculate, centrifuge again, and pour off the liquid. (This helps to remove soluble ions such as Ca and Na)
- To dry the $Be(OH)_2$, place the centrifuge tubes in a rack laid on its side (tubes should be horizontal) (resting on the caps?) in the oven set to (temperature?). This allows any residual liquid to flow down onto the side of the tube, away from the $Be(OH)_2$, rather than accumulating in the base of the tube.
- Drying >65 degrees prevents the gels from forming small pellets. We want small pellets
- Note: Any water remaining in the test tube with the gels, prevents Be from drying into small pellets.

Alternate Method apart from test tube strategy:

- After Beryllium has flocculated, been washed, and centrifuged. Remove excess water while retaining flocculant. Ideally there would be less than 0.5ml (500 ul) of fluid/precipitate in the bottom of the test tube at this point. Use the 1000ul repeat pipettor with a clean tip and adjust it to 300ul (the avergae volume of our small quartz crucibles. Suck up the gel/precipitate and carefully pipette it into an HF cleaned quartz crucible. Place in a tube rack in the oven on it's side to dry. We place the vials on their side 1) because the crucibles are so small that the surface tension of the water keeps the fluid from flowing out and 2) because the crucibles usually have a small pit in the bottom which is hard to get our Beryllium pellet out of when it comes time for grinding.

Precipitate Aluminum Hydroxide

- Slowly add NH_4OH, 5 drops at a time to each tube to bring the pH to 6.5-7 or precipitate appears. Vortex between each NH4OH additions (previous tries used ~15 drops Ammonia Hydroxide). Centrifuge the tubes for 10 minutes at 4000 rpm.
- The precipitate should be a milky gel at the bottom of the tube. If the precipitate is present, carefully decant the liquid down the drain and continue to step 4. if the precipitate is not present, add more NH_4OH and repeat step 1.
- Add 10 mL ultrapure water to the centrifuge tubes. Vortex to re-suspend everything. Centrifuge for 10 minutes. Look for the precipitate. Decant the liquid and repeat rinse 2 more times.
- Sample is now rinsed and ready to convert to the oxide.

Note: Stone lab co-precipitates Ag in solution for better beam currents with Al. Their procedure for this is listed below.

- Add AgNo3 ~12 drops for samples with 1.5 mg Al (should be about 2 parts Ag to 1 part Al). Silver is used as a conductor in the cathode, and you want aluminum to be in a fine matrix of silver. LLNL doesn't want silver in the cathodes, but John still adds some,

dispersed among the sample because apparently it's really hard to grind a nugget of just Al2O3. John used to use just silver, and no niobium.

- Precipitate Al with NaCO3, a weaker base than Ammonia (~20 drops). Some CO2 bubbles off. Add ~13-16 drops of NaCO3 and vortex until it's an incipient cloudiness, opalescent. This is just starting to precipitate Al(OH)3. Then add another ~4-7 drops and vortex. Sample should look cloudy and milky. This is a co-precipitation of Al(OH)3 and a silver compound. Don't add too much NaCO3, otherwise, this will re-dissolve Al(OH)3.
- Centrifuge once the precipitate has started to settle a bit and the top of the solution is clear. Drain the supernatant, add a rinse of DI H2O, vortex, and centrifuge again. Do this twice. The precipitate at the base of the centrifuge can be quite difficult to break up during vortexing, but be persistent. After two rinses, drain the supernatant and dry down the sample in the oven. Once dry, the sample should be black flakes of Al(OH)3.
- Transfer the samples to quartz vials in same way as for Be. The Al(OH)3 flakes can stick to the tube walls tenaciously, so you may need to vigorously tap the tube to loosen the flakes.
- Bake samples (similar as for Be), converting Al(OH)3 to Al2O3. Once sample is red hot, bake for 1:30. Aluminum has a higher propensity of jumping out of the quartz vial than Be, so use the spatula to try to contain runaway flakes.
- Add niobium. Samples already contain some silver, so not quite as much niobium is needed as for Be samples.
- Crushing sample: Al2O3 is what they make sandpaper out of (also what corundum is (hardness 9)), so it is quite difficult to crush and disaggregate. Unlike for BeO, don’t get a chunk of sample under the drill bit and press until it disintegrates, for you greatly risk sending bits of sample flying out of the tube. Rather, place the drill bit over the sample and very lightly tap, or hammer the sample until it falls apart.

Conversion to Aluminum & Beryllium Oxide

Note: Have clean quartz crucibles before proceeding (see below)

$$Be(OH)_2 \rightarrow BeO + H_2O$$

- Clean workbench/glovebox with DI and ChemWipe. (Do this after every sample)
- Cut 4x4 in. weighing paper into four (2x2 in.) pieces until there is at least one for each sample.
- Place a ChemWipe down.
- Fold two adjacent edges the weighing paper towards the center and then grasp the corner between the two folds so that it points outward and the two folded pieces are roughly vertical. Place it on the ChemWipe. This will catch your dried hydroxide precipitate.
- Wave the test tube in front of the ionizer to reduce static before tipping it onto folded weighing paper. From here, transfer it to one of the clean HF etched glass vials. Label the vial with the sample name and cover it with parafilm. Repeat this process for each sample.
- Place the butane torch in the fume hood well away from the walls.
- Place a large ChemWipe on the lab bench with tweezers, a spatula and a cathode tube.
- Light the torch.
- After removing the parafilm from the vial, grasp the vial with the tweezers about halfway up (below the sample name so that the ink does not run from the heat). Hold the base of the vial with a spatula over the top (but not touching!) in case it should try to pop out of the vial. Once the sample begins to glow an incandescent red you may remove the spatula. After that happens, hold it in the flame for 30 to 40 seconds more. Remove it from the heat and place it in the cathode tube in the hood to cool.
- Once the sample has cooled sufficiently, remove it from the hood and cover with parafilm.

Niobium Addition

- Clean the niobium scoop with a ChemWipe and alcohol.
- Set up a large ChemWipe, along with the sample vial rack and the niobium box with scoop.
- For each sample…
- Add 1:1 niobium powder to sample, being careful not to touch the vials with the scoop. If you do touch it, wash the scoop. Each sample should end up with roughly equal amounts of niobium powder and sample.
- Add a clean drill bit to the tube, and then label a cathode and cathode container with the sample name. Record the cathode # in the logbook. Place the vial in the cathode and the cathode in the cathode container.
- Used drill bits go in a small beaker of isopropanol.
- Note: Drill bits are pre-cleaned with sand paper and isopropanol
- Note: Generally there is more Al than Be
- Note: It’s common to change gloves between every other sample to avoid sample cross talk (not really possible in glove box).

Quartz Crucibles:

- Our quartz crucibles are hand made from a scientific glassblower from Washington State. They are cheap, and disposable. Before using to convert Al and Be to oxides they must be cleaned. Sonicate the vials for a few hours in DI, inverting often to remove bubbles caught in the tube. Pour off DI water and clean with a quick 1% HF etch.
- Etch and sonicate the crucibles in 1% HF for 2-3 hours (enough time to frost them, but not enough to dissolve them completely). A hot bath is not needed.
- After 2-3 hours pour off HF in acid waste bucket (BEING VERY CAREFUL OF DRIBBLING HF). Consider finding a screen or making a hole in another lid to keep from losing crucibles.
- Rinse 2-3 times with DI water and Isopropanol.
- Sonicate for a few hours in DI and Isopropanol.
- Then rinse 1 more time in pure reagent grade isopropanol.
- Shake clean crucibles into a clean beaker and dry in the oven.

Cathode Packing

- Cleaning Cathodes: When you receive cathodes from PRIME lab, they may come either in a bag or in a #'s and labeled tray and the cathodes themselves may have metal clippings and oil/dirt on them. Remove the cathodes from whichever container and sonicate in isopropanol for 1hr or so. Pour off sonicated fluid and rinse with more isopropanol. Let dry on a ChemWipe or in the oven. Clean the cathode rack with soap and water and rinse with DI. Either put cathodes back in tray (face down, number up) or in a new baggie.
- First, prepare the glove box. Wipe out the floor of the box with DI water, which you should leave in the box. Make sure the Be waste container has a Zip-Lock bag with enough room for ChemWipes and vials. Place ChemWipes, ionizer, hammer, small beaker of isopropanol and the rack of cathodes inside of the box.
- Place materials in glove box and close side lid.
- Lay down a ChemWipe on the bottom of the box and place a cathode onto it. Remove a quartz vial and begin crushing the BeO pellet with the drill bit and mixing it with the niobium powder. Once it is completely crushed and roughly homogeneous, scrape down the inside of the vial with the drill bit to gather all of the powder into the very bottom.
- Note: Our crucibles are not perfectly rounded on the bottom, and it is easy to "jam" the oxide into the bottom. Try not to do this. We want homogenized oxide and silver/niobium.
- At this point, you can remove the drill bit and place it on the ChemWipe (remember which end is the business end) or hold it between two of your fingers while you do the next step.
- Position yourself holding the cathode in one hand and the vial in the other so that you can upend the vial into the small cylinder and hole on top of the cathode. It may be helpful to hold the cathode like you are holding a dart (horizontally) and then press it onto the cathode in that position. Then bring them both together down onto the ChemWipe so that nothing will fall out.

- Holding the cathode and vial with one hand, gently tap any remaining sample onto the cathode using the side of the hammer. Place the empty vial on the ChemWipe. Continue to tap around the sides of the cathode until all the powder has made it into the hole.
- Place the business end of the cathode into the cathode hole and press down until it slides in. Holding the cathode and drill bit like a nail, firmly tap the bit until it you hear a solid, sturdy sound and are certain that it has been sufficiently packed down. Remove the drill bit.
- Gently upend cathode on the ChemWipe to remove any loose powder. Put the cathode into the cathode container (1 mL Nalgene screw top vial) with the barcode facing up and label written on the outside, and close the cap. Place the drill bit into the small beaker of alcohol with the business end in the liquid. Put the vial and ChemWipe into the beryllium waste bag.
- Between each sample be sure to wipe down the central floor of the box to prevent cross-contamination.
- You can check your cathode to see if they have been thoroughly crushed on the microscope in the main lab.

From Susan Ma @ Prime lab:

- Put the loaded holder into vial, with the laser marked side up, cover it with the lid
- Write on the holder number on the outside of vial
- record the holder number, sample PRIME Lab ID, sample name in Excel file and email to me with required sample information.
- Put the holder in micro-tube storage box or any contain with fitting material to reduce vibration and FedEx to me.
- Mail to Prime lab.

REFERENCES

Ackert, R.P., and Kurz, M.D., 2004, Age and uplift rates of Sirius Group sediments in the Dominion Range, Antarctica, from surface exposure dating and geomorphology: Global and Planetary Change, v. 42, no. 1-4, p. 207–225, doi: 10.1016/j.gloplacha.2004.02.001.

Balco, G., and Shuster, D.L., 2009a, 26Al–10Be–21Ne burial dating: Earth and Planetary Science Letters, v. 286, no. 3-4, p. 570–575, doi: 10.1016/j.epsl.2009.07.025.

Balco, G., and Shuster, D.L., 2009b, Production rate of cosmogenic 21Ne in quartz estimated from 10Be, 26Al, and 21Ne concentrations in slowly eroding Antarctic bedrock surfaces: Earth and Planetary Science Letters, v. 281, no. 1-2, p. 48–58, doi: 10.1016/j.epsl.2009.02.006.

Balco, G., and Stone, J.O., 2003, Measuring the density of rock, sand, till, etc. UW Cosmogenic Nuclide Laboratory, methods and procedures.:, http://depts.washington.edu/cosmolab/chem.html p.

Balco, G., Stone, J.O., and Mason, J. a., 2005, Numerical ages for Plio-Pleistocene glacial sediment sequences by 26Al/10Be dating of quartz in buried paleosols: Earth and Planetary Science Letters, v. 232, no. 1-2, p. 179–191, doi: 10.1016/j.epsl.2004.12.013.

Barrett, P.J., Lindsay, J.F., and Gunner, J., 1970, Reconnaissance Geologic Map of the Mount Rabot Quadrangle, Transantarctic Mountains, Antarctica [map] 1:250,000: Washington, DC: Department of the Interior, United States Geologic Survey.

Berg, T.E., and Black, R.F., 1966, Preliminary measurements of growth of nonsorted polygons, Victoria Land, Antarctica., *in* Tedrow, J.C.F. ed., Antarctic Soils and Soil-Forming Processes. American Geophysical Union, Washington, DC, p. 61–108.

Bliss, A.K., Cuffey, K.M., and Kavanaugh, J.L., 2011, Sublimation and surface energy budget of Taylor Glacier, Antarctica: Journal of Glaciology, v. 57, no. 204, p. 684–696, doi: 10.3189/002214311797409767.

Braucher, R., Del Castillo, P., Siame, L., Hidy, a. J., and Bourlés, D.L., 2009, Determination of both exposure time and denudation rate from an in situ-produced 10Be depth profile: A mathematical proof of uniqueness. Model sensitivity and applications to natural cases: Quaternary Geochronology, v. 4, no. 1, p. 56–67, doi: 10.1016/j.quageo.2008.06.001.

Van den Broeke, M.R., 1997, Spatial and temporal variation of sublimation on Antarctica: Results of a high-resolution general circulation model: Journal of Geophysical Research, v. 102, no. D25, p. 29765, doi: 10.1029/97JD01862.

Cardyn, R., Clark, I.D., Lacelle, D., Lauriol, B., Zdanowicz, C., and Calmels, F., 2007, Molar gas ratios of air entrapped in ice: A new tool to determine the origin of relict massive ground ice bodies in permafrost: Quaternary Research, v. 68, no. 2, p. 239–248, doi: 10.1016/j.yqres.2007.05.003.

Comiso, J.C., 2000, Variability and Trends in Antarctic Surface Temperatures from In Situ and Satellite Infrared Measurements: Journal of Climate, v. 13, no. 10, p. 1674–1696, doi: 10.1175/1520-0442(2000)013<1674:VATIAS>2.0.CO;2.

D'Erricco, J., 2012, fminsearchcon: Mathworks file exchange, http://www.mathworks.com/matlabcentral/fileexchange/8277-fminsearchbnd--fminsearchcon,.

Denton, G.H., Bockheim, J.G., Wilson, S.C., Leide, J.E., and Andersen, B.G., 1989, Late Quaternary ice-surface fluctuations of Beardmore Glacier, Transantarctic Mountains: Quaternary Research, v. 31, no. 2, p. 183–209, doi: 10.1016/0033-5894(89)90005-7.

Denton, G.H., Prentice, M.L., and Burkle, L.H., 1991, Cenozoic history of the Antarctic Ice Sheet, *in* Tingey, R.J. ed., Geology of Antarctica, Oxford University Press, p. 365–433.

Denton, G.H., Prentice, M.L., Kellogg, D.E., and Kellogg, T.B., 1984, Late Tertiary history of the Antarctic ice sheet: Evidence from the Dry Valleys: Geology, v. 12, no. 5, p. 263, doi: 10.1130/0091-7613(1984)12<263:LTHOTA>2.0.CO;2.

Ditchburn, R.G., Graham, I.J., and Zondervan, A., 2000, Analytical methods for measuring Be and U-Th isotopes in loess.: Institute of Geological and Nuclear Sciences science report 2000/09, p. 10.

Ditchburn, R.G., and Whitehead, N.E., 1994, The separation of 10Be from silicates.: 3D Workshop of the South Pacific Environmental Radioactivity Association, v. 4-7.

Dunai, T.J., 2000, Scaling factors for production rates of in situ produced cosmogenic nuclides: a critical reevaluation: Earth and Planetary Science Letters, v. 176, no. 1, p. 157–169, doi: 10.1016/S0012-821X(99)00310-6.

Dunne, J., Elmore, D., and Muzikar, P., 1999, Scaling factors for the rates of production of cosmogenic nuclides for geometric shielding and attenuation at depth on sloped surfaces: Geomorphology, v. 27, no. 1-2, p. 3–11, doi: 10.1016/S0169-555X(98)00086-5.

Edwards, K.L., Padilla, A.J., Evans, A., Morgan, D.J., Balco, G., Putkonen, J.K., and Bibby, T.C., 2014, Provenance of glacial tills in Ong Valley, Antarctica, inferred from quartz cathodoluminescence imaging, zircon U/Pb dating, and trace element geochemistry., *in* American Geophysical Union Fall Meeting,.

Fischer, H., Severinghaus, J., Brook, E., Wolff, E., Albert, M., Alemany, O., Arthern, R., Bentley, C., Blankenship, D., Chappellaz, J., Creyts, T., Dahl-Jensen, D., Dinn, M., Frezzotti, M., et al., 2013, Where to find 1.5 million yr old ice for the IPICS "Oldest-Ice" ice core: Climate of the Past, v. 9, no. 6, p. 2489–2505, doi: 10.5194/cp-9-2489-2013.

Gosse, J.C., and Phillips, F.M., 2001, Terrestrial in situ cosmogenic nuclides: theory and application: Quaternary Science Reviews, v. 20, no. 14, p. 1475–1560, doi: 10.1016/S0277-3791(00)00171-2.

Grindley, G.W., 1967, The geomorphology of the Miller Range, Transantarctic Mountains with notes on the glacial history and neotectonics of East Antarctica: New Zealand Journal of Geology and Geophysics, , no. 2, p. 557–598.

Grindley, G.W., and Laird, M.G., 1969, Geology of the Shackleton Coast, Geologic Map of Antarctica, Sheet 15 [map] 1:1,000,000: American Geographical Society,.

Hagedorn, B., Sletten, R.S., and Hallet, B., 2007, Sublimation and ice condensation in hyperarid soils: Modeling results using field data from Victoria Valley, Antarctica: Journal of Geophysical Research, v. 112, no. F3, p. F03017, doi: 10.1029/2006JF000580.

Hall, B.L., and Denton, G.H., 2005, Surficial geology and geomorphology of eastern and central Wright Valley, Antarctica: Geomorphology, v. 64, no. 1-2, p. 25–65, doi: 10.1016/j.geomorph.2004.05.002.

Hindmarsh, R.C.., Van der Wateren, F.M., and Verbers, A.L.L.M., 1998, Sublimation of Ice Through Sediment in Beacon Valley, Antarctica: Geografiska Annaler, v. 80(A), no. 3/4, p. 209–219.

Holt, J.W., Safaeinili, A., Plaut, J.J., Head, J.W., Phillips, R.J., Seu, R., Kempf, S.D., Choudhary, P., Young, D.A., Putzig, N.E., Biccari, D., and Gim, Y., 2008, Radar Sounding Evidence for Buried Glaciers in the Southern Mid-Latitudes of Mars: Science, v. 322, no. 5905, p. 1235–1238, doi: 10.1126/science.1164246.

Hooke, R.L.B., 2005, Principles of Glacier Mechanics: Cambridge University Press, Cambridge.

Hunt, A.L., Larsen, J., Bierman, P.R., and Petrucci, G.A., 2008, Investigation of factors that affect the sensitivity of accelerator mass spectrometry for cosmogenic 10Be and 26Al isotope analysis.: Analytical chemistry, v. 80, no. 5, p. 1656–63, doi: 10.1021/ac701742p.

Hunt, A.L., Petrucci, G. a., Bierman, P.R., and Finkel, R.C., 2007, Investigation of metal matrix systems for cosmogenic 26Al analysis by accelerator mass spectrometry: Nuclear Instruments and Methods in Physics Research Section B: Beam Interactions with Materials and Atoms, v. 260, no. 2, p. 633–636, doi: 10.1016/j.nimb.2007.03.101.

Hunt, A.L., Petrucci, G. a., Bierman, P.R., and Finkel, R.C., 2006, Metal matrices to optimize ion beam currents for accelerator mass spectrometry: Nuclear Instruments and Methods in Physics Research Section B: Beam Interactions with Materials and Atoms, v. 243, no. 1, p. 216–222, doi: 10.1016/j.nimb.2005.07.220.

International Partnerships in Ice Core Sciences The oldest ice core: A 1.5 million year record of climate and greenhouse gases from Antarctica: White Paper,.

Ivy-Ochs, S., Kober, F., Alfimov, V., Kubik, P.W., and Synal, H. -a., 2007, Cosmogenic 10Be, 21Ne and 36Cl in sanidine and quartz from Chilean ignimbrites: Nuclear Instruments and Methods in Physics Research Section B: Beam Interactions with Materials and Atoms, v. 259, no. 1, p. 588–594, doi: 10.1016/j.nimb.2007.03.001.

Jansen, E., Bleil, U., Henrich, R., Kringstad, L., and Slettemark, B., 1988, Paleoenvironmental changes in the Norwegian Sea and the northeast Atlantic during the last 2.8 m.y.: Deep Sea Drilling Project/Ocean Drilling Program Sites 610, 642, 643 and 644: Paleoceanography, v. 3, no. 5, p. 563–581, doi: 10.1029/PA003i005p00563.

Kohl, C.P., and Nishiizumi, K., 1992, Chemical isolation of quartz for measurement of in-situ -produced cosmogenic nuclides: Geochimica et Cosmochimica Acta, v. 56, p. 3583–3587.

Konrad, J.-M., 2005, Estimation of the segregation potential of fine-grained soils using the frost heave response of two reference soils: Canadian Geotechnical Journal, v. 42, no. 1, p. 38–50, doi: 10.1139/t04-080.

Kowalewski, D.E., Marchant, D.R., Levy, J.S., and Head, J.W., 2006, Quantifying low rates of summertime sublimation for buried glacier ice in Beacon Valley, Antarctica: Antarctic Science, v. 18, no. 3, p. 421–428, doi: 10.1017/S0954102006000460.

Kowalewski, D.E., Marchant, D.R., Swanger, K.M., and Head, J.W., 2011, Modeling vapor diffusion within cold and dry supraglacial tills of Antarctica: Implications for the preservation of ancient ice: Geomorphology, v. 126, no. 1-2, p. 159–173, doi: 10.1016/j.geomorph.2010.11.001.

Kwok, R., and Comiso, J.C., 2002, Spatial patterns of variability in Antarctic surface temperature: Connections to the Southern Hemisphere Annular Mode and the Southern Oscillation: Geophysical Research Letters, v. 29, no. 14, p. 1705, doi: 10.1029/2002GL015415.

Lacelle, D., Davila, A.F., Pollard, W.H., Andersen, D., Heldmann, J., Marinova, M., and McKay, C.P., 2011, Stability of massive ground ice bodies in University Valley, McMurdo Dry Valleys of Antarctica: Using stable O–H isotope as tracers of sublimation in hyper-arid regions: Earth and Planetary Science Letters, v. 301, no. 1-2, p. 403–411, doi: 10.1016/j.epsl.2010.11.028.

Lacelle, D., Lauriol, B., Clark, I.D., Cardyn, R., and Zdanowicz, C., 2007, Nature and origin of a Pleistocene-age massive ground-ice body exposed in the Chapman Lake moraine complex, central Yukon Territory, Canada: Quaternary Research, v. 68, no. 2, p. 249–260, doi: 10.1016/j.yqres.2007.05.002.

Lal, D., 1991, Cosmic ray labeling of erosion surfaces: in situ nuclide production rates and erosion models: Earth and Planetary Science Letters, v. 104, no. 2-4, p. 424–439, doi: http://dx.doi.org/10.1016/0012-821X(91)90220-C.

Lear, C.H., Elderfield, H., and Wilson, P.A., 2000, Cenozoic Deep-Sea Temperatures and Global Ice Volumes from Mg/Ca in Benthic Foraminiferal Calcite: Science , v. 287 , no. 5451 , p. 269–272, doi: 10.1126/science.287.5451.269.

Lenaerts, J.T.M., van den Broeke, M.R., Déry, S.J., König-Langlo, G., Ettema, J., and Munneke, P.K., 2010, Modelling snowdrift sublimation on an Antarctic ice shelf: The Cryosphere, v. 4, no. 2, p. 179–190, doi: 10.5194/tc-4-179-2010.

Leya, I., Lange, H.-J., Neumann, S., Wieler, R., and Michell, R., 2000, The production of cosmogenic nuclides in stony meteoroids by galactic cosmic-ray particles: Meteorites and Planetary Sciences, v. 35, p. 259–286.

Liu, L., Sletten, R.S., Hallet, B., Mischna, M.A., Vasavada, A.R., and Martin-Torres, F.J., 2014, Ground Ice Dynamics at Beacon Valley, Antarctica and its Application to the Potential Persistence of Ground Ice at Gale on Mars: Eighth International Conference on Mars,.

Luthi, D., Le Floch, M., Bereiter, B., Blunier, T., Barnola, J.-M., Siegenthaler, U., Raynaud, D., Jouzel, J., Fischer, H., Kawamura, K., and Stocker, T.F., 2008, High-resolution carbon dioxide concentration record 650,000-800,000 years before present: Nature, v. 453, no. 7193, p. 379–382.

Marchant, D.R., Denton, G.H., and Swisher III, C.C., 1993, Miocene-Pliocene-Pleistocene Glacial History of Arena Valley, Quartermain Mountains, Antarctica: Geografiska Annaler. Series A, Physical Geography, v. 75, no. 4, p. 269–302, doi: 10.2307/521204.

Marchant, D.R., Lewis, A.R., Phillips, W.M., Moore, E.J., Souchez, R.A., Denton, G.H., Sugden, D.E., Potter Jr., N., and Landis, G.P., 2002, Formation of patterned ground and sublimation till over Miocene glacier ice in Beacon Valley, southern Victoria Land, Antarctica: Geological Society of America Bulletin, v. 114, no. 6, p. 718–730, doi: 10.1130/0016-7606(2002)114<0718:FOPGAS>2.0.CO;2.

MATLAB and Statistics Toolbox Release 2013a, The MathWorks, Inc., Natick, Massachusetts, United States.

Mayewski, P.A., 1975, Glacial geology and late Cenozoic history of the Transantarctic Mountains, Antarctica: Institute of Polar Studies, The Ohio State University, v. Report 56, p. 168.

McDougall, I., and Grindley, G.W., 1965, Potassium-argon dates on micas from the Nimrod-Beardmore-Axel Heiberg Region, Ross Dependency, Antarctica: New Zealand Journal of Geology and Geophysics, v. 8, no. 2, p. 304–317.

McKay, C., Mellon, M.T., and Friedmann, E.I., 1998, Soil temperatures and stability of ice-cemented ground in the McMurdo Dry Valleys, Antarctica.: Antarctic science / Blackwell Scientific Publications, v. 10, no. 1, p. 31–8.

Morgan, D.J., Putkonen, J.K., Balco, G., and Stone, J.O., 2010a, Degradation of glacial deposits quantified with cosmogenic nuclides, Quartermain Mountains, Antarctica: Earth Surface Processes and Landforms, v. 36, no. 2, p. 217–228, doi: 10.1002/esp.2039.

Morgan, D.J., Putkonen, J.K., Balco, G., and Stone, J.O., 2010b, Quantifying regolith erosion rates with cosmogenic nuclides 10 Be and 26 Al in the McMurdo Dry Valleys, Antarctica: Journal of Geophysical Research, v. 115, no. F3, p. 1–17, doi: 10.1029/2009JF001443.

Ng, F., Hallet, B., Sletten, R.S., and Stone, J.O., 2005, Fast-growing till over ancient ice in Beacon Valley, Antarctica: Geology, v. 33, no. 2, p. 121, doi: 10.1130/G21064.1.

Di Nicola, L., Strasky, S., Schlüchter, C., Salvatore, M.C., Akçar, N., Kubik, P.W., Christl, M., Kasper, H.U., Wieler, R., and Baroni, C., 2009, Multiple cosmogenic nuclides document complex Pleistocene exposure history of glacial drifts in Terra Nova Bay (northern Victoria Land, Antarctica): Quaternary Research, v. 71, no. 1, p. 83–92, doi: 10.1016/j.yqres.2008.07.004.

Niedermann, S., 2002, Cosmic-Ray-Produced Noble Gases in Terrestrial Rocks: Dating Tools for Surface Processes: Reviews in Mineralogy and Geochemistry, v. 47, no. 1, p. 731–784, doi: 10.2138/rmg.2002.47.16.

Nishiizumi, K., 2004, Preparation of 26Al AMS standards: Nuclear Instruments and Methods in Physics Research Section B: Beam Interactions with Materials and Atoms, v. 223-224, p. 388–392, doi: 10.1016/j.nimb.2004.04.075.

Nishiizumi, K., Imamura, M., Caffee, M.W., Southon, J.R., Finkel, R.C., and McAninch, J., 2007, Absolute calibration of 10Be AMS standards: Nuclear Instruments and Methods in Physics Research Section B: Beam Interactions with Materials and Atoms, v. 258, no. 2, p. 403–413, doi: 10.1016/j.nimb.2007.01.297.

Oberholzer, P., Baroni, C., Schaefer, J.M., Orombelli, G., Ochs, S.I., Kubik, P.W., Baur, H., and Wieler, R., 2003, Limited Pliocene/Pleistocene glaciation in Deep Freeze Range, northern Victoria Land, Antarctica, derived from in situ cosmogenic nuclides: Antarctic Science, v. 15, no. 4, p. 493–502, doi: 10.1017/S0954102003001603.

Ochs, M., and Ivy-Ochs, S., 1997, The chemical behavior of Be, Al, Fe, Ca, and Mg during AMS target preparation from terrestrial silicates modeled with chemical speciation calculations.: Nuclear Instruments and Methods, v. B123, p. 235–240.

Ólafur Ingólfsson, 2004, Quaternary Glacial and Climate History of Antarctica, *in* Ehlers, J. and Gibbard, P.L. eds., Quaternary Glaciations - Extent and Chronology, Part III, Elsevier, p. 3–43.

Plaut, J.J., Safaeinili, A., Holt, J.W., Phillips, R.J., Head, J.W., Seu, R., Putzig, N.E., and Frigeri, A., 2009, Radar evidence for ice in lobate debris aprons in the mid-northern latitudes of Mars: Geophysical Research Letters, v. 36, no. 2, doi: 10.1029/2008GL036379.

Portenga, E.W., and Bierman, P.R., 2011, Understanding Earth's eroding surface with 10Be: GSA Today, v. 21, no. 8, p. 4–10, doi: 10.1130/G111A.1.

Putkonen, J.K., Balco, G., and Morgan, D.J., 2008a, Slow regolith degradation without creep determined by cosmogenic nuclide measurements in Arena Valley, Antarctica: Quaternary Research, v. 69, no. 2, p. 242–249, doi: 10.1016/j.yqres.2007.12.004.

Putkonen, J.K., Balco, G., and Morgan, D.J., 2008b, Slow regolith degradation without creep determined by cosmogenic nuclide measurements in Arena Valley, Antarctica: Quaternary Research, v. 69, no. 2, p. 242–249, doi: 10.1016/j.yqres.2007.12.004.

Rignot, E., Hallet, B., and Fountain, A.G., 2002, Rock glacier surface motion in Beacon Valley, Antarctica, from synthetic-aperture radar interferometry, *in* Geophysical Research Letters, p. 48–51.

Scarrow, J.W., Balks, M.R., and Almond, P.C., 2014, Three soil chronosequences in recessional glacial deposits near the polar plateau, in the Central Transantarctic Mountains, Antarctica: Antarctic Science, p. 1–11, doi: 10.1017/S0954102014000078.

Schaefer, J.M., Baur, H., Denton, G.H., Ivy-ochs, S., Marchant, D.R., Schlu, C., and Wieler, R., 2000, The oldest ice on Earth in Beacon Valley , Antarctica : new evidence from surface exposure dating: Earth and Planetary Science Letters, v. 179, p. 91–99.

Schäfer, J.M., Ivy-Ochs, S., Wieler, R., Leya, I., Baur, H., Denton, G.H., and Schlüchter, C., 1999, Cosmogenic noble gas studies in the oldest landscape on earth: surface exposure ages of the Dry Valleys, Antarctica: Earth and Planetary Science Letters, v. 167, no. 3-4, p. 215–226, doi: 10.1016/S0012-821X(99)00029-1.

Sletten, R.S., 2003, Resurfacing time of terrestrial surfaces by the formation and maturation of polygonal patterned ground: Journal of Geophysical Research, v. 108, no. E4, p. 1–10, doi: 10.1029/2002JE001914.

Staiger, J.W., Marchant, D.R., Schaefer, J.M., Oberholzer, P., Johnson, J.V., Lewis, a. R., and Swanger, K.M., 2006, Plio-Pleistocene history of Ferrar Glacier, Antarctica: Implications for climate and ice sheet stability: Earth and Planetary Science Letters, v. 243, no. 3-4, p. 489–503, doi: 10.1016/j.epsl.2006.01.037.

Stone, J.O., 2000, Air pressure and cosmogenic isotope production: JOURNAL OF GEOPHYSICAL RESEARCH, v. 105, no. B10, p. 753–759.

Stone, J.O., Sletten, R.S., and Hallet, B., 2000, Old Ice, Going Fast: Cosmogenic Isotope Measurements on Ice Beneath the Floor of Beacon Valley, Antarctica: Eos Trans. American Geophysical Union 81(48) Fall Meet. Suppl., Abstract H52C-21,.

Sugden, D.E., Marchant, D.R., Potter, N., Souchez, R.A., Denton, G.H., Swisher III, C.C., and Tison, J.-L., 1995, Preservation of Miocene glacier ice in East Antarctica: Nature, v. 376, no. 6539, p. 412–414, doi: 10.1038/376412a0.

Sugden, D.E., Summerfield, M.A., Denton, G.H., Wilch, T.I., McIntosh, W.C., Marchant, D.R., and Rutford, R.H., 1999, Landscape development in the Royal Society Range, southern Victoria Land, Antarctica: stability since the mid-Miocene: Geomorphology, v. 28, no. 3-4, p. 181–200, doi: 10.1016/S0169-555X(98)00108-1.

Summerfield, M.A., Stuart, F.M., Cockburn, H.A.P., Sugden, D.E., Denton, G.H., Dunai, T., and Marchant, D.R., 1999, Long-term rates of denudation in the Dry Valleys, Transantarctic Mountains, southern Victoria Land, Antarctica based on in-situ-produced cosmogenic: Geomorphology, v. 27, no. 1-2, p. 113–129, doi: 10.1016/S0169-555X(98)00093-2.

Swanger, K.M., and Marchant, D.R., 2007, Sensitivity of ice-cemented Antarctic soils to greenhouse-induced thawing: Are terrestrial archives at risk? Earth and Planetary Science Letters, v. 259, no. 3-4, p. 347–359, doi: 10.1016/j.epsl.2007.04.046.

Swanger, K.M., Marchant, D.R., Kowalewski, D.E., and Head, J.W., 2010, Viscous flow lobes in central Taylor Valley, Antarctica: Origin as remnant buried glacial ice: Geomorphology, v. 120, no. 3-4, p. 174–185, doi: 10.1016/j.geomorph.2010.03.024.

Todd, C.E., Stone, J.O., Conway, H., Hall, B.L., and Bromley, G., 2010, Late Quaternary evolution of Reedy Glacier, Antarctica: Quaternary Science Reviews, v. 29, no. 11-12, p. 1328–1341, doi: 10.1016/j.quascirev.2010.02.001.

Vermeesch, P., Balco, G., Blard, P.-H., Dunai, T.J., Kober, F., Niedermann, S., Shuster, D.L., Strasky, S., Stuart, F.M., Wieler, R., and Zimmermann, L., 2012, Interlaboratory comparison of cosmogenic 21Ne in quartz: Quaternary Geochronology, , no. 0, doi: http://dx.doi.org/10.1016/j.quageo.2012.11.009.

Wang, Y., and Hou, S., 2009, A new interpolation method for Antarctic surface temperature: Progress in Natural Science, v. 19, no. 12, p. 1843–1849, doi: 10.1016/j.pnsc.2009.07.012.

Van der Wateren, D., and Hindmarsh, R., 1995, Stabilists strike again: Nature, v. 376, no. 6539, p. 389–391, doi: 10.1038/376389a0.

Zachos, J.C., and Kump, L., 2005, Carbon cycle feedbacks and the initiation of Antarctic glaciation in the earliest Oligocene: Global and Planetary Change, v. 47, no. 1, p. 51–66, doi: 10.1016/j.gloplacha.2005.01.001.

Zachos, J.C., Quinn, T.M., and Salamy, K.A., 1996, High-resolution (104 years) deep-sea foraminiferal stable isotope records of the Eocene-Oligocene climate transition: Paleoceanography, v. 11, no. 3, p. 251–266, doi: 10.1029/96PA00571.